Structural Biology of Auxin Efflux Carrier PIN Proteins

by

Xinghao Zhou

Thesis

Submitted to the University of Warwick
For partial fulfilment of the requirements for the degree of

Doctor of Philosophy in Life Sciences

University of Warwick, School of Life Sciences
November 2021

Table of Contents

Table of Figures

Table of Tables

Abbreviation

Å	Angstrom (10^{-10} meters)
At/ A.thaliana	Arabidopsis Thaliana
ABCBs	ATP binding cassette transporters
ABP1	Auxin binding protein
Abt	Amborella trichopoda
AFB	Auxin F-Box
Ala	Alanine
ARF	Auxin response factor
Aux/IAA	Auxin-IAA proteins
AUX1/LAX	AUXIN1/LIKE AUX1
CHS	Cholesteryl Hemisuccinate Tris Salt
cryo-EM	cryo-Electron Microscopy
Cys	Cysteine
DDM	n-Dodecyl-B-D-Maltoside
DM	n-Decyl-β-D-Maltopyranoside
DMSO	Dimethyl sulfoxide
DTT	DL-Dithiothreitol
EDTA	Ethylenediaminetetraacetic acid
ER	Endoplasmic reticulum
FBS	Fetal Bovine Serum
FLAG	FLAG peptide DYKDDDDK
FSEC	Fluorescent size exclusoion chromatography
GFP	Green fluorescent protein
Gm	Clycine max
Gln	Glutamine
Glu	Glutamic acid
Gly	Glycine
HEPES	4-(2-hydroxyethyl)-1-piperazineethanesulfonic acid
His	Histidine
HPLC	High-performance liquid chromatography
HL	hydrophilic loop
IAA	Indole-3-acetic acid
IBA	Indole-3-butyric acid
IMAC	Immobilised metal affinity chromatography
IPTG	Isopropyl β-D-thiogalactoside
LMNG	Lauryl Maltose Neopentyl Glycol
MES	2-ethanesulfonic acid
min	Minute
mM	Millimolar
MOI	Multiplicity of Infection

MW	Molecular weight
NPA	Naphthylphthalamic acid
OD600	Optical Density at 600 nm
Os	Oryza sativa
OG	n-Octyl-β-D-Glucopyranoside
OGNG	Octyl Glucose Neopentyl Glycol
PM	Plasma memberane
PINs	PIN-FORMED proteins
PSI	pound per square inch
PVDF	Polyvinylidene fluoride
RCF	Relative Centrifugal Force
rpm	Rotations per minute
RFU	Response Fluorescent Units
S. cerevisiae	Saccharomyces cerevisiae
SDS	Sodium Dodecyl sulphate
SDS-PAGE	sodium dodecyl sulphate–polyacrylamide gel electrophoresis
SEC	size exclusoion chromatography
sec	Second
Ser	Serine
SPR	Surface Plasmon Resonance
TBS	Tris Buffered Saline
Thr	Threonine
TCEP	Tris(2-carboxyethyl)phosphine hydrochloride
TEV	Tobacco Etch Virus
TMD	transmembrane domain
TIBA	2,3,5-triiodobenzoic acid
TIR1	Transport Inhibitor Resistant 1
Tris	Tris(hydroxymethyl)aminomethane
Trp	Tryptophan
Tyr	Tyrosine
UV	Ultraviolet
YPD	yeast extract peptone dextrose
WT	Wild type
µM	Micromolar
µl	Microliter

Acknowledgement

I would like to thank my supervisor, Professor Richard Napier for his guidance and help, especially in this extraordinary Cov19 period, Richard's encouragement and optimistic to life made me inspired through all my PhD times. I would also like to thank my co-supervisor Professor Alex Cameron for his expertise instruction.

I also would like to thank my parents Yuqing Lan and Dr Jungang Zhou for their encouragement and support, my partner Scarlet's accompany in my daily life and lab work which drive me finish my studies.

It has been a great pleasure to work with all members and alumnus in Napier group, Lab C10 and C46. I'd like to thank my mentor post-docs Dr Justyna Prusinska for helping through the introduction training and cloning, Dr Veselina Uzunova for helping through my thesis. Thanks to my colleagues Siree Tungsirisurp and Chitra Joshi for my daily work and fun. Thanks to Dr Charo Del Gino who helping in tutoring and explanations of mathematical and most important, testing my first car in Kidlington. I would like to thank my advisory panel: Professor Corinne Smith and Professor Murry Grant for their guidance, encouragement and support. A big thanks to Professor David Roper for his reliable AKTA purifier and centrifuge in C10.

Thanks Dr Saskia Bakker for helping my TEM and cryo-EM prep.

Great thanks to our calibrator Dr Andrew Quigley and his lab members in Membrane Protein Lab, for helping me through my protein screening and crystallization trials.

Special thanks to my friend Dr Juntai Liu and Dr Jie Zhang for our everlasting friendship, joy and fun in summertime weekly tennis game, back yard BBQ, cards game and Mario Party.

Declaration

This thesis is submitted to the University of Warwick in support of my application for the degree of Doctor of Philosophy. It has been composed by myself under the supervision of Prof. Richard Napier. It has not been submitted in any previous application for any degree

Abstract

Auxin is an important hormone in plants which regulates plant growth and development. The plant-specific proteins named PIN-FORMED auxin efflux carriers (PINs) control the direction of auxin flow and thus play a necessary role in the local auxin distribution within plant tissues and organs, and consequently guide plant ontogenesis. PINs are membrane proteins with two hydrophobic regions consisting of five transmembrane helices linked with a hydrophilic loop. Normally plasma membrane-localized PINs have longer loops then endoplasmic reticulum PINs. The PIN1 secondary structure was published in 1999, but the three-dimensional structure of PIN has not been solved yet.

This project aimed to express and purify PIN proteins for structural studies. 8 different PINs from 5 plant species were expressed in insect Sf9 cells and in *Saccharomyces cerevisiae*. A series of purification optimizations for PIN proteins were applied and *Arabidopsis thaliana* PIN5 and *Oryza sativa* PIN8 were purified. However, high purity combined with the high yields necessary for crystallography trails were not achieved, due to the instability of PINs. Some negative stain electron microscopy suggested a unit structure of a dimer, but at very low resolution and Saposin A nanodisc lipid complexes were investigated to try and improve PIN electron microscopy studies.

A range of approaches in this project have allowed us to learn more about PIN structure and hopefully a more comprehensive understanding of the PIN mechanism of action will be obtained in the future

Chapter 1 Introduction

1.1 Plant hormones

Plant hormones are a group of small organic compounds that occur naturally and influence physiological processes at low concentration. Plant hormones or phytohormones include several classes: auxin, salicylic acid (SA), ethylene, jasmonic acid (JA), abscisic acid (ABA), gibberellic acid (GA) and cytokinin (Wani et al., 2016, Öpik et al., 2005). They are essential for growth and development of plants and they also determine plant responses under environmental stresses (Wolters and Jürgens, 2009).

Auxin participates in numerous complex responses, but some pathways are non-redundant and show up significant phenotypes in loss-of-function mutants (Frauenfeld et al., 2016). However, the whole signalling system is not yet fully understood. In particular, the key transporters of auxin do not yet have solved structures, which is a topical area in current phytohormone research (Zwiewka et al., 2019).

1.1.1 Auxin, indole-3-acetic acid (IAA)

Auxin is the first plant hormone discovered. It takes its name from the Greek 'αυξανω' [auksáno] which means 'I grow' in English. Today, auxin refers to an important group of phytohormones that has been identified in most of the plant organs, coordinating growth and development changes that occur during a plant's life cycle (Teale et al., 2006).

Experimental auxin research is well established. Charles Darwin performed experiments on coleoptiles and uncovered some signalling molecule that had positive effect on coleoptiles phototropism. Further study by Frits Warmolt Went in 1926 extracted the chemicals from coleoptile tips, and in 1934 Kögl identified the active low molecular weight molecule – IAA (Kögl et al., 1934). IAA has an indole ring with an acetic acid group at the C3 position (Figure 1.1). The acid group is deptrotonated at physiological pH.

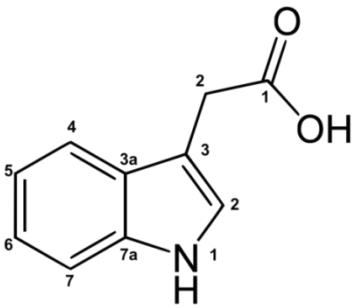

Figure 1.1 IAA structure with International Union of Pure and Applied Chemistry numbering convention

1.1.2 Other natural auxins

The major endogenous auxin in plants is IAA. It generates a response at a distance to its synthesis site and, therefore, fits the definition of a transported chemical messenger (Teale et al., 2006).

There are other natural small compounds with auxin-like activity in whole plants. Based on current research (Enders and Strader, 2015), there are four endogenous molecules with auxinic activity: IAA, indole-3-butyric acid (IBA), 4-chloro-indole-3-acetic acid (4-Cl-IAA) and phenyl acetic acid (PAA) (Figure 1.2). IBA is synthesized from IAA and can be converted back to IAA by the action of peroxisomal-oxidation enzymes. Therefore it is regarded as a storage precursor of IAA (Simon and Petrasek, 2011). 4-Cl-IAA has been identified as an endogenous auxin in several legumes and *Pinus sylvestris* (Reinecke, 1999). PAA has shown relatively weaker auxin effectiveness than IAA, although endogenous PAA was found in various plant species and in root symbiotic bacteria. PAA has some anti-microbial activity, therefore it may participate in plant root interactions with soil microorganisms (Simon and Petrasek, 2011).

In further chapter 1.2, auxin will be used synonymously with IAA.

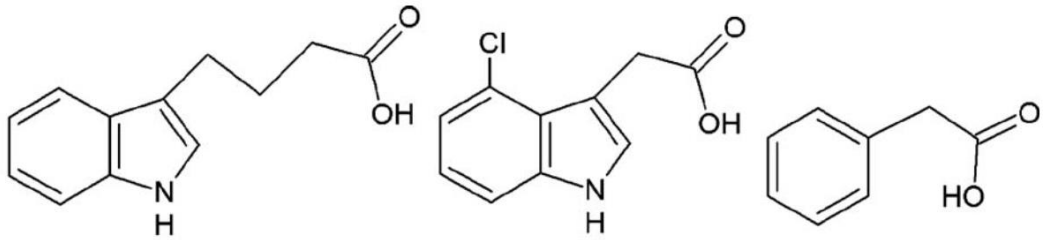

Indole-3-butyric acid (IBA) | 4-chloroindole-3-acetic acid (4-Cl-IAA) | Phenylacetic acid (PAA)

Figure 1.2 Structures of other endogenous auxins.

1.1.3 Synthetic auxins

Auxins and their synthetic cousins have been used to boost plant growth and kill weeds. Excessively high concentrations of auxins are deadly to plants. Synthetic auxins are designed to mimic IAA and are used as herbicides. They cause explosive growth in the weeds and thus kill them (Grossmann, 2007). Some of the commonly known synthetic auxins are for example, 2,4-dichlorophenoxyacetic acid (2,4-D), phenoxyacetic acid, 2-methyl-4-chlorophenoxyacetic acid (Methoxone), 1-naphthalene acetic acid (1-NAA), and 2-methoxy-3,6-dichlorobenzoic acid (Dicamba).

The most widely and heavily used synthetic auxins are dicamba and 2,4-D (Figure 1.3).

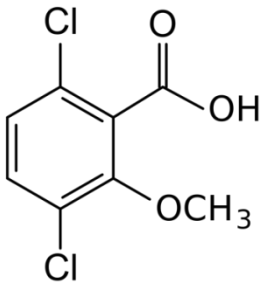

Dicamba
2-methoxy-3,6-dichlorobenzoic acid

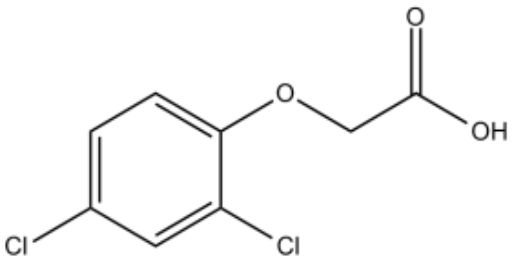

2,4-D
2,4-Dichlorophenoxyacetic acid

Figure 1.3 Structures of synthetic auxins Dicamba and 2,4-D.

1.2 Auxin metabolism

1.2.1 IAA synthesis

Auxin metabolism is centered on regulating the concentrations of the hormone via balancing synthesis and inactivation. For the model plant Arabidopsis thaliana, the main organs involved in auxin synthesis are young leaves, roots and cotyledons. Although the molecular pathways of the synthesis are not completely elucidated, the ones known are generally divided to tryptophan(Trp)-dependent and Trp-independent (Figure 1.4). Parallel Trp-dependent and Trp-independent pathways function in different organs, developmental stages, and environmental conditions (Wang et al., 2015).

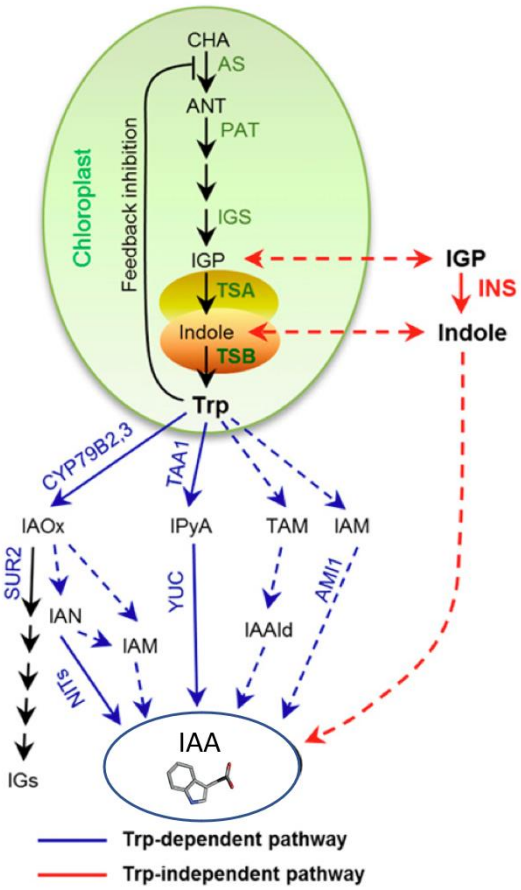

Figure 1.4 Tryptophan dependent and independent IAA biosynthesis (Wang et al., 2015).

Tryptophan (Trp) has been proposed as the primary precursor for IAA biosynthesis. Experimental evidence includes the use of radio-labelled Trp in plants, resulting in the formation of radio-labelled IAA (Sugawara et al., 2009). Several Trp-dependent auxin biosynthetic pathways contribute to IAA production, including the indole-3-acetaldoxime (IAOx) pathway, the indole-3-acetamide (IAM) pathway, the tryptamine TAM pathway and the the indole-3-pyruvic acid (IPA) pathway (Figure 1.4). The Trp-independant pathways are suspected to branch from indole or indole-3-glycerol phosphate (IGP) as shown on Figure 1.4.

1.2.2 IAA inactivation and storage

There are two forms of IAA in plants: free and conjugated. Free IAA is the active form of auxin, however, it only comprises up to about 25% of the total, depending on different plant species and tissues (Ludwig-Müller, 2011). Conjugated IAA is considered to be either a storage form or precursor for degradation. However the conjugated forms that accumulate after exposure to IAA and are meant for degradation generally differ from the forms for storage (Woodward and Bartel, 2005).

The main forms of auxin conjugates in higher plants include low molecular weight ester conjugates such as IAA-glucose and IAA-myo-inositol (Michalczuk and Bandurski, 1982), low molecular weight amide-linked amino acid conjugates such as IAA-Alanine, IAA-Leucine, IAA-Aspartic acid, IAA-Glutamic acid and IAA-Tryptophan (Kowalczyk and Sandberg, 2001, Ostin et al., 1998), and high molecular weight amide-linked peptide and protein conjugates (Walz et al., 2002).. Conjugation profile is species dependant (Woodward and Bartel, 2005). In Arabidopsis the main storage forms are IAA-conjugates to amino acids while in grasses mostly sugar conjugates take over. Ester-linked conjugates are found in endosperm tissues of monocots and dicots, whereas IAA-amino acid conjugates predominate in mature dicot seeds and vegetative tissues of most light-grown plants, including land plants, monocots and dicots (Tam et al., 2000, Sztein et al., 1995)

1.3 Auxin perception

Auxin performs its action by regulating transcription and it is perceived by a group of F-box proteins: the Transport Inhibitor Response 1 (TIR1)/Auxin-signalling F-Box (AFB) proteins (2009, PNAS Parry and Estelle). The best-studied of them is TIR1, which was discovered in 1998 (Ruegger et al., 1998).
Auxin F-Box (AFB) proteins as sites of auxin perception and the role of auxin as molecular glue in the assembly of co-receptor complexes has allowed the development of a definitive quantitative structure-activity relationship for TIR1 and (Lee et al., 2014). Auxin mediates a response through a Skp (Apoptosis signal-regulating kinase 1, ASK1), Cullin, F-box (SCF) complex which is a type of E3 ubiquitin ligase involving TIR1 the F-box protein (Figure 1.5) (Tromas et al., 2013, Skaar et al., 2013). Further research showed that TIR1 was the major auxin receptor (Dharmasiri et al., 2005a, Kepinski and Leyser, 2005), and by using pull down assays IAA was shown to bind to TIR1 and a member of the family of Aux/IAA transcriptional repressors (Dharmasiri et al., 2005b).
At low auxin concentrations, Aux/IAA proteins dimerise to repress transcriptional activators, the auxin response factors (ARFs). When auxin concentration rises, it binds to TIR1 and the Aux/IAA proteins complete the SCF-TIR1 co-receptor complex, resulting in the Aux/IAA proteins being marked for degradation by the E3 ubiquitin ligase and degraded by 26S proteasomes (Komander and Rape, 2012). In consequence, the ARFs are no longer repressed which allows transcription to start (Woodward and Bartel, 2005, dos Santos Maraschin et al., 2009, Stefanowicz et al., 2015).
The TIR1 receptor was crystalised in 2007 (Tan et al., 2007). The auxin-binding pocket become resolved and proved auxins can bind with TIR1 (Figure 1.5).
Auxin-binding protein1 (ABP1) has been discussed as an alternative receptor, but recent evidence suggest that this model is no longer convincing (Badescu and Napier, 2006).

A.

B.

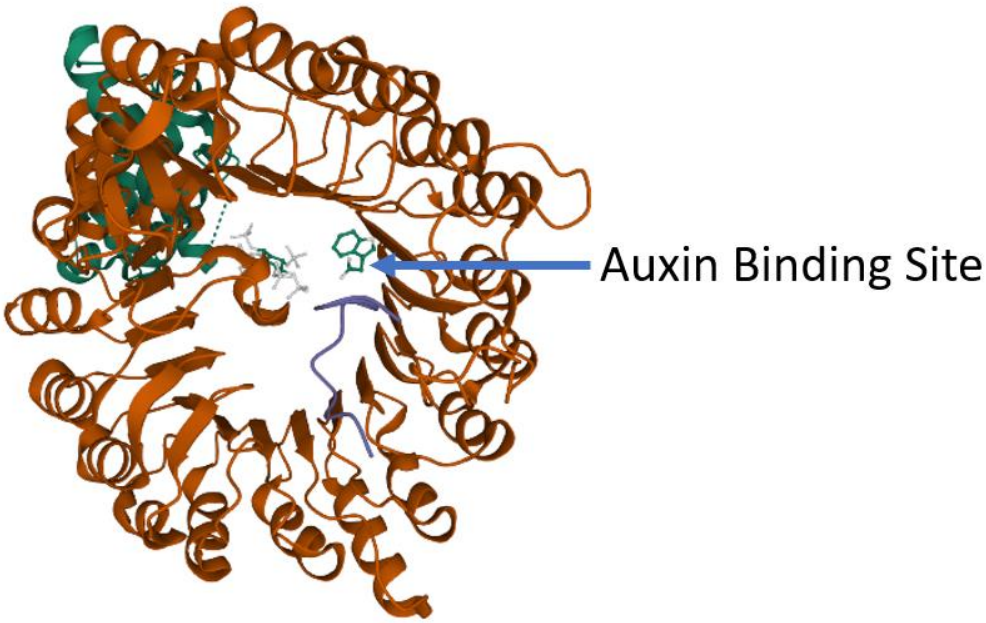

Figure 1.5 Structure of TIR1-ASK1 complex protein PDB: 2P1Q.

Structural model was generated by PDB 3D Canvas. TIR1 marked in red colour ASK1 marked in green colour

A. Side view of TIR1 and ASK1 complex

B. Top view of TIR1 and ASK1 complex, IAA as binding lignd in deep green colour.

1.4 Auxin transport

Net auxin uptake, accumulation and intercellular transport are driven by chemiosmosis, which is powered by the anion trap and the membrane potential across the plasma membrane (PM) (Rubery and Sheldrake, 1974). Except pH-dependent and ATP-dependent auxin transport, there moderated by the abundance and activity of combined actions of auxin transporters from at least three families: AUXIN1/LIKE AUX1 (AUX1/LAX), PIN-FORMED proteins (PINs), and members of the B subfamily of ATP binding cassette transporters (ABCBs) in the PM (Rubery and Sheldrake, 1974, Bennett et al., 1996, Geisler et al., 2014).

Cytoplasmic pH in plants is between pH 7.0 – 7.5, which is higher than the extracellular space, which is between pH 5.0 and 6.0 (Tominaga et al., 1998). This pH gradient helps create the anion trap, and in combination with AUX1-mediated uptake (Singh et al., 2018), and selective efflux allows auxin to accumulate inside cells to concentrations twenty times greater than in the apoplast (Rubery and Sheldrake, 1974, Delbarre et al., 1996). This concentration difference alone provides a chemiosmotic gradient which, in the presence of a suitable pore, would carry auxin out across the PM. However, once inside the cell at pH 7.0 – 7.5, IAA dissociates into an anionic IAA^- species which is membrane impermeant and is confined inside the cell by this anion trap.

Auxin uptake carriers:

The most studied influx carriers in Arabidopsis thaliana are members of the AUX1/LAX family, which includes the AUX1 and LAX1-3 proteins (Swarup and Peret, 2012). There are also two ABCB carriers and the nitrate transporter NRT1.1 shown to contribute to auxin uptake (Terasaka et al., 2005, Krouk et al., 2010, Kamimoto et al., 2012, Kubeš et al., 2012). ABCBs act as primary active auxin pumps that are able to transport against steep auxin gradients (Geisler et al., 2017).

Efflux proteins:

Auxin leaves the cell by efflux carrier PIN proteins, the PIN proteins acting as these pores, and auxin moving to lower chemical concentration gradient (Adamowski and Friml, 2015, Krecek et al., 2009)(Figure 1.6).

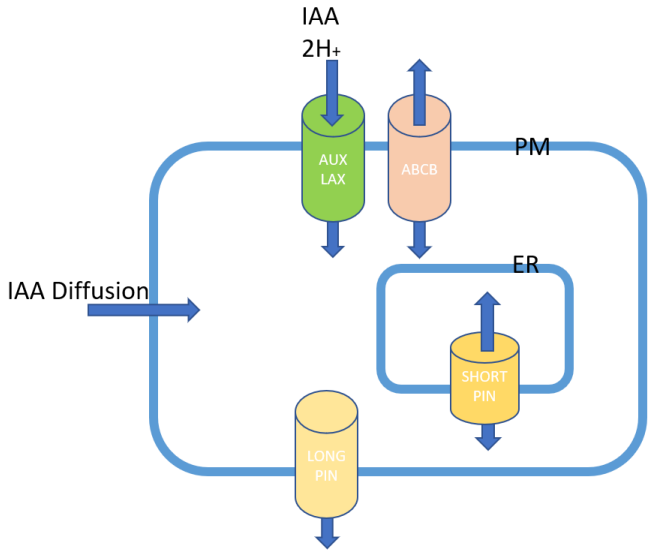

Figure 1.6 Schematic summary of the pathways of auxin transport in a plant cell

Blue arrows signify the direction of movement, PM: Plasma membrane, ER: endoplasmic reticulum.

The PINs are transporters involved in the efflux of the plant signal molecule auxin from cells. They are asymmetrically localized within cells and this polarity distribution determines the directionality of intercellular auxin flow (Krecek et al., 2009). ABCBs also efflux auxin in plants cells, as shown when PIN1 was co-expressed with ABCB1/ABCB19 the efflux rate of auxin was enhanced compared with PIN1 alone. (Blakeslee et al., 2007).

1.5 The PIN protein family

The first PIN protein family members identified and associated with auxin transport were described in *Arabidopsis thaliana*. The function of AtPIN1 was discovered through a loss-of-function mutation in the gene: mutant plants fail to develop floral organs properly and generate naked, pin-like inflorescences, which gave the name PINFORMED (PIN) to the family (Okada et al., 1991, Gälweiler et al., 1998).

PIN proteins are membrane-bound proteins, and the family has evolved into two major groupings referred to as the canonical PINs and non-canonical PINs (Bennett et al., 2014). In Arabidopsis, there are eight PIN proteins (table 1.1) of which AtPIN1-4, and 7 are canonical with long hydrophilic loops (also referred to as long PINs). These PINs are asymmetrically localized at the plasma membrane (PM) and this asymmetry confers polarity to the main long-distance polar auxin transport stream and to local morphometric gradients (Petrasek et al., 2006, Wisniewska et al., 2006). Of the others, PIN5 and PIN8 are non-canonical, have much shorter hydrophilic loops (short PINs) and show localization on the endoplasmic reticulum (ER) membrane to control auxin exchange between the cytosol and the ER lumen (Mravec et al., 2009, Ding et al., 2012). PIN6, also non-canonical has an intermediate length hydrophilic loop and shows dual PM and ER localization with (Simon et al., 2016, Ditengou et al., 2018). Additional clades have arisen in other some plant families, such as the PIN9 clade in the grasses (Poaceae; Bennett et al., 2014) and there are some discrete clades developed in more ancestral plant lineages such as the bryophytes.

Further, there is the PIN-LIKES (PILS) family of transporters involved in regulating auxin accumulation in ER and auxin availability for nuclear auxin signalling (Barbez et al., 2012).

AtPINs	Cellular location	Loop Amino Acids	Classification
AtPIN1	PM	330	canonical
AtPIN2	PM	355	canonical
AtPIN3	PM	348	canonical
AtPIN4	PM	324	canonical
AtPIN5	ER	57	non-canonical
AtPIN6	PM/ER	278	canonical
AtPIN7	PM	327	canonical
AtPIN8	ER	70	non-canonical

Table 1.1 Features of 8 PIN proteins in Arabidopsis thaliana

1.6 The PIN protein structural features

1.6.1 PIN proteins structural features

AtPIN1 secondary structural predication was first published in 1998 as a hydropathy plot, which showed a roughly 250 amino acids hydrophilic domain in the middle of the protein with two 170 amino acid, hydrophobic domains on N-terminal and C-terminal side of the protein (Gälweiler et al., 1998). Further topology studies confirmed the long PINs secondary structure by inserting GFP in the hydrophilic areas of PIN proteins (Nodzynski et al., 2016).

In general, tertiary structure predictions show that all PINs are likely to have ten transmembrane helices formed into two regions, each of five transmembrane helices, and linked by a central hydrophilic loop (HL)(Figure 1.7)(Ganguly et al., 2014, Krecek et al., 2009). There is a high level of sequence conservation across the 10 transmembrane domains about 280 amino acids, less in the loops (Figure 1.7A blue)(Bennett et al., 2014). A model of PIN2 has helped explain how two cysteine residues might contribute to redox regulation of this protein's localisation in the cell (Retzer et al., 2017), but otherwise there is little known about PIN protein structure or their mechanism of action.

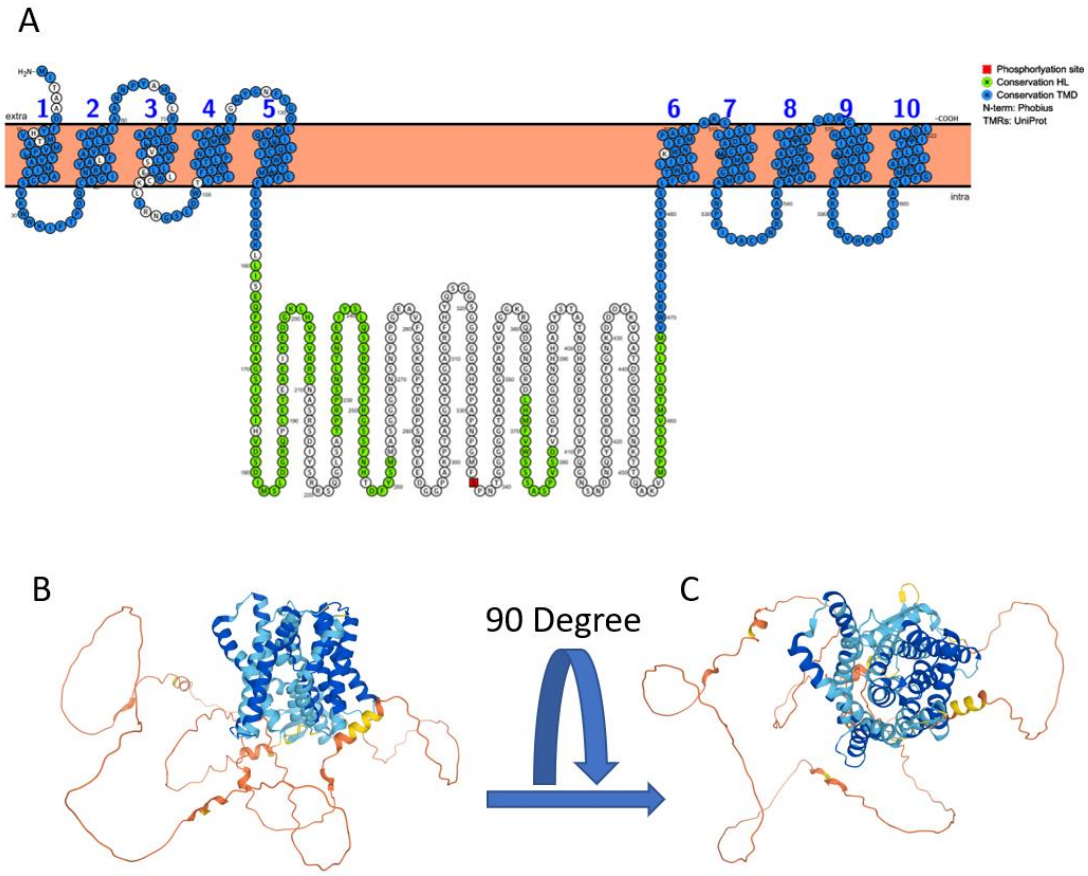

Figure 1.7 AtPIN1 Secondary Structure and AtPIN2 Tertiary Structure

A. AtPIN1 Secondary Structure, AtPIN1 amino acids FASTA sequence was downloaded from UniProt and uploaded into Protter open-source tool (http://wlab.ethz.ch/protter/start/) to generate the AtPIN1 secondary structural prediction. Blue: AtPIN1 conservation area of transmembrane domain. Green: AtPIN1 conservation of hydrophylic loop. Red: Ser337 phosphorlysation site.

B and C. AtPIN2 Tertiary Structure generated by alphafold2. Blue: High sataistic confidence of protein structural predication, Red and yellow: Low sataistic confidence of protein structural predication.

1.6.2 PIN proteins transmembrane domains

There are ten hydrophobic transmembrane domains in most of PIN proteins, in AlphaFold 2 predication, the hydrophobic area showed a brunch of helixes (Figure 1.7). Alignment of Arabidopsis PIN protein sequences showed high conservation of 280 amino acids in N and C terminal alpha helical region including the ER-localized short PINs (Petrášek et al., 2006). Some experimental evidence proved ER PINs have the capacity to transport the auxin (Mravec et al., 2009, Ding et al., 2012), which suggested auxin transport activity is highly related to the transmembrane domains rather than middle HL.

1.6.3 PIN proteins hydrophilic loop

PIN protein HLs are less conserved and much more divergent than the transmembrane domain (TMD), although multi-species sequence alignment identified some conserved features and flexible domains in the HL (Zažímalová et al., 2007). In another study about HL region of PIN proteins in multiple plant species, the alignment of PIN protein sequences has identified four conservative motifs on the HL (Figure 1.7A green) (Bennett et al., 2014). This helped to conclude that PIN proteins were canonical if they matched the consensus sequence of all four highly conserved motifs with at least 50% identity or 70% similarity. If PIN proteins did not fulfil these conditions they were named noncanonical, so, PIN1-4 and PIN7 are classified as canonical PINs, PIN5 and PIN8 are classified as noncanonical PINs. PIN6 is intermediate as semi-canonical.

To identify the functional part of canonical-PINs, experiment proved that the HL domain rather than TMDs contributed to PIN1 and PIN2 functional divergence (Zhang et al., 2020). They expressed AtPIN1 N-TMDs and C-TMDs with AtPIN2 HL and AtPIN2 N- and C-TMDs with AtPIN1 HL. The chimeric AtPIN2 TMDs with AtPIN1 HL showed ability to rescue the flower defects of the pin1 mutant, and the localization of these proteins was shifted from outer side of the root to the central stele cells to direct auxin flow towards the root tip (as AtPIN1 does), while chimeric AtPIN1 TMDs with AtPIN2 HL has no ability to maintain floral

organ development (Zhang et al., 2020), which proved the central hydrophilic loop contributes to their differential subcellular localizations and cellular polarity. PIN protein localization and activities are determined by phosphorylation of the HL (Barbosa et al., 2018). The Ser337 phosphorylation site on AtPIN1 (Figure 1.7A red) contributes to AtPIN1 functionality in plant development, and this site differs from AtPIN2 HL (Zhang et al., 2010).

Non-canonical PIN protein localization and functional are also related to the HL. Anindya et al expressed AtPIN5 TMDs as a chimera with the AtPIN2 HL. Some chimeric AtPIN5 localization was shifted to the PM and this appeared to correlate with inhibition of Arabidopsis root hair growth compared with WT, but the effect was not as strong as AtPIN2 overexpression (Ganguly et al., 2014).

1.7 Regulation of PINs

1.7.1 Regulation of PIN protein localization and expression

PIN proteins have specific developmental roles in specific plant tissues. Control of PIN gene expression is based on the diversification of PIN gene promoters. Arabidopsis PIN gene promoters give specific and partially overlapping expression patterns, which causes expression of PINs in different development processes with functional redundancy.

AtPIN1 is the major non-redundant member of the family involved in aerial development, and AtPIN1 expression is identified in apical parts of early embryos, throughout the vascular tissues, in the shoot apical meristem and in developing organs (Figure 1.8)(Gälweiler et al., 1998, Scarpella et al., 2006, Benková et al., 2003). AtPIN2, AtPIN3 and AtPIN4 act in the root tip, mediating the auxin maximum and auxin redistribution for root gravitropism (Müller et al., 1998, Friml et al., 2002b, Friml et al., 2002a). Among the short PINs, AtPIN5 is relatively weakly and ubiquitously expressed in the ER (Mravec et al., 2009), and AtPIN8 is also in the ER. AtPIN8 shows a very specific expression pattern in the pollen gametophyte. PIN promoter activity can be flexibly regulated, which accounts for a compensatory type of functional redundancy.

Several PIN knockout mutants in Arabidopsis show ectopic activity of other PIN proteins compensating for the lost PIN activity (Vieten et al., 2005a). This phenomenon seems to account for the high degree of functional redundancy among PIN genes, masking most of the phenotypic manifestations expected to result from single, and some double, PIN gene inactivation (Vieten et al., 2005b, Blilou et al., 2005, Friml et al., 2003).

A.

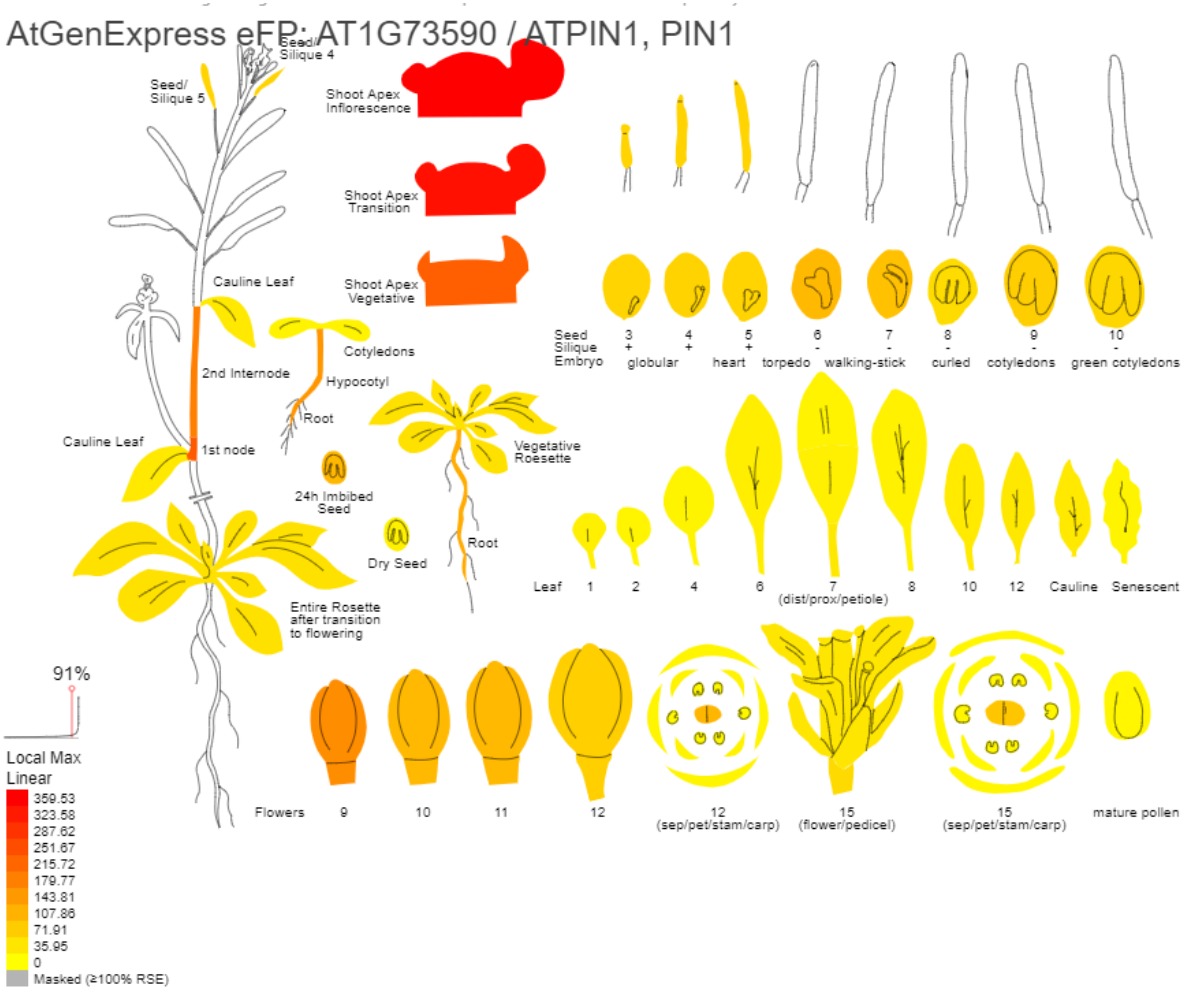
AtGenExpress eFP: AT1G73590 / ATPIN1, PIN1
Seed/ Silique 4
Seed/ Silique 5
Shoot Apex Inflorescence
Shoot Apex Transition
Shoot Apex Vegetative
Cauline Leaf
Cotyledons
2nd Internode
Hypocotyl
Root
Cauline Leaf
1st node
24h Imbibed Seed
Dry Seed
Vegetative Rosette
Root
Entire Rosette after transition to flowering
Seed Silique Embryo
3 + globular
4 + 5 + heart
6 - torpedo
7 - walking-stick
8 - curled
9 - cotyledons
10 - green cotyledons
Leaf 1 2 4 6 7 (dist/prox/petiole) 8 10 12 Cauline Senescent
Flowers 9 10 11 12
12 (sep/pet/stam/carp)
15 (flower/pedicel)
15 (sep/pet/stam/carp)
mature pollen
91%
Local Max
Linear
359.53
323.58
287.62
251.67
215.72
179.77
143.81
107.86
71.91
35.95
0
Masked (≥100% RSE)

B.

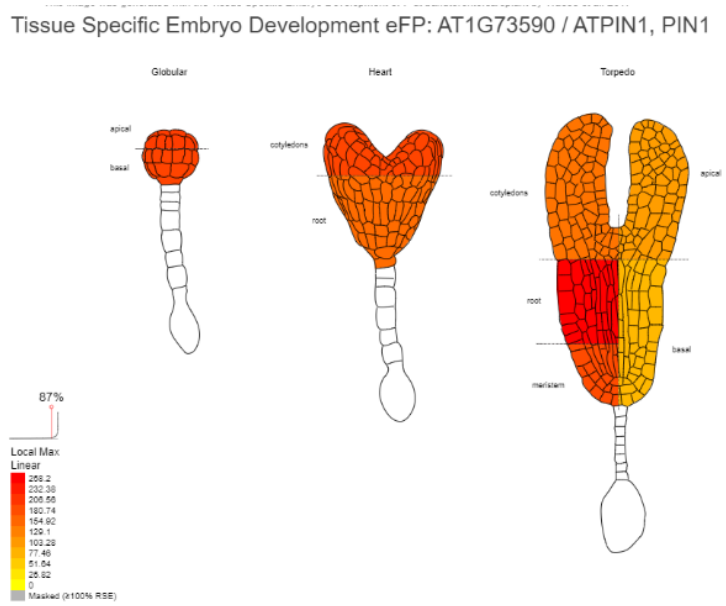

Figure 1.8 AtPIN1 expression in plant development as shown by ePLANT.

Heat map was generated by ePLANT (https://bar.utoronto.ca/eplant/), AT1G73590 gene distributaion (Fucile et al., 2011).

The Plant eFP viewer is an electronic flurorescent pictograph that displays gene expression patterns on the tissues as a cartoon plant. Stronger colours denote a higher level of expression.

A. AtPIN1 expression in plant tissues.

B. AtPIN1 expression in embryo development

1.7.2 PIN protein interactions

Cellular auxin efflux is the rate-limiting step of intercellular flow, and it is dependent on canonical-PIN protein polarization, phosphorylation and interactions with PGP transporters. Effective PIN-mediated auxin transport and polarity are controlled via phosphorylation by different kinds of protein kinases, such as D6PK, PINOID (PID) and WAGs (Barbosa et al., 2018).

PID mutants have similar phonotypes to pin1 mutants (Christensen et al., 2000, Benjamins et al., 2001), and PINOID also has a relationship with WAG1/WAG2 to regulate Arabidopsis root growth direction (Santner and Watson, 2006), apical hook opening (Willige et al., 2012), and phototropism (Haga et al., 2014). PID and WAGs are uniformly distributed at the plasma membrane of epidermal cells (Dhonukshe et al., 2015). Three conserved serine (S) residues on canonical PIN HLs, Ser231, Ser252, Ser290 (S1–S3), can be directly phosphorylated by PID/WAGs (Huang et al., 2010). In *Atpid* and *wag* mutants, accumulated PIN2 at the basal PM in root epidermal cells, PIN1 was accumulated at the basal PM in shoot cells, while overexpression of PID or WAG shifted PIN polarity from basal to apical PM. The authors concluded that PIN phosphorylation on S1-S3 controlled PIN polarity (Dhonukshe et al., 2015). To test this further, PIN1 HL S1–S3 phosphorylation sites were deleted, after which PID overexpression had no effects on PIN polarity and S1-S3 phosphorylation mimics induced apical targeting of PIN1 in the shoot apical meristem. These S1–S3 phosphosite mutations also disabled the ability of PIN1 to rescue the *pin1* inflorescence phenotype (Huang et al., 2010, Dhonukshe, 2011).

D6PKs share the same S1–S3 phosphorylation sites as PID/WAGs, although *d6pk* mutants have defects in lateral root initiation, root gravitropism, and shoot differentiation in axillary shoots, with a reduction in auxin transport. They do not show any ability to control PIN polarity (Zourelidou et al., 2009).

Other kinases

Arabidopsis has 20 MPKs and 10 MPK KINASES (MKKs) (Cristina et al., 2010). MKK7 has positive affect on auxin transport, and it has downstream activity

regulating MPK3 and MPK6. MKK7 controls shoot branching by phosphorylating PIN1 Ser377 (Dai et al., 2006, Jia et al., 2016). Ser337 and another close phosphosite Thr340 are essential for PIN1 polarization, and phosphomimic mutations of S337 and T340 display non-polar localization in embryo cells (Zhang et al., 2010). On PIN1, HL threonine residues, Thr227, Thr248, and Thr286, can be phosphorylated by MPK4 and MPK6 which affect PIN1 localisation in protoplasts (Dory et al., 2018).

Control of kinases

Ca^{2+} was recognised to impact on auxin transport. Higher Ca^{2+} levels suppressed the PIN1 gain-of-function phenotypes and caused defects in basal PIN localization, auxin transport and auxin-mediated development (Zhang et al., 2011). Experiments with a yeast two-hybrid system confirmed that PID interacts with Ca^{2+} binding protein TOUCH3 and ABCB1, which regulate the activity of PID in response to changes in calcium levels (Benjamins et al., 2003). Calmodulin-dependent kinase-related kinase (CRK5) mutants inhibit primary root elongation, delay gravitropic bending of shoots and roots and PIN2 shows basal to apical re-localisation in the root cortex. CRK5 also phosphorylates the hydrophilic loop of PIN2 in vitro (Rigó et al., 2013).

WRKY DNA-BINDING Protein 23 transcription factor regulates auxin-mediated PIN repolarization (Prat et al., 2018) by controlling auxin-regulated receptor CAMEL (Canalization-related Auxin-regulated Malectin-type RLK) together with CANAR (Canalization-related Receptor-like kinase) which interact with and phosphorylate PIN auxin transporters (Hajný et al., 2020). CAMEL can phosphorylate PIN1 HL T192, T234, T240, T257 and S408. In this work the phosphomimic mutants of PIN1 show apolar localization and no polarity changes after auxin treatment, the mutant displays pin-like inflorescences similar to the pin1 loss of function phonotype (Hajný et al., 2020).

Other auxin efflux proteins and NPA interact with PINs

ABCBs are also plants cell auxin efflux proteins, which use ATP to power auxin transport. When PIN1 was co-expressed with ABCB1/ABCB19, the efflux rate of auxin was enhanced compared with PIN1 alone. Substrate specificity was

also enhanced (Blakeslee et al., 2007). The shoot and leaf phenotypes observed in *abcb19 pin1* double mutant, were stronger than for the *pin1* mutant (Blakeslee et al., 2007) as was sensitivity to NPA. The *pin2 abcb1 abcb19* triple mutant had enhanced defects in gravitropism compared with *pin2* single (Blakeslee et al., 2007) which suggest that PINs and ABCBs characterize coordinated, independent auxin transport mechanisms but also function interactively in a tissue-specific manner.

NPA is known to inhibit auxin transport efficiently and quickly in plants. It was experimentally proved NPA binding to an intracellular allosteric site distinct from IAA substrate-binding sites, possibly involving membrane-proximal conserved Cys residues and an interface between monomers (Abas et al., 2021). Teale et al found PIN core transport unit was a homodimer and heteromers assembled from PIN1-4 and PIN7 subunits. These PIN dimers were stabilized by NPA as well as by endogenous flavonols (Teale et al., 2021).

1.8 Project objective and hypothesis

In this project, it was hypothesed that PIN proteins can be expressed in heterologous expression systems and purified for structural biology studies. Additionally, expressed PINs will retain activity for substrate binding assays.

The project aimed to express recombinant PIN proteins in insect cells and *Saccharomyces cerevisiae* for milligram scale PIN protein production. Expressed PIN proteins will be purified by IMAC and anti-FLAG resins, and purified PINs will be used for structural studies using crystallization and Cryo-EM.

This thesis will show that PIN proteins were expressed in *Spodoptera frugiperda* Sf9 cells and *Saccharomyces cerevisiae* FGY217. The PIN proteins were purified by nickel, cobalt IMAC beads and anti-FLAG beads. The purified OsPIN5:GFP fusion proteins were tested for activity with NPA, TIBA and amino acids conjugated IAA. The purified AtPIN5 and OsPIN8 proteins were used for crystallography trails, but these were not successful. AtPIN5:GFP fusion protein was detected under TEM after negative staining at a good particle distribution, and a 1.2nm resolution model was generated by Relion 3D classification. AtPIN5:GFP can be reconstituted into saposin A nanodisc proteins which may allow for further Cryo-EM studies.

Chapter 2 Materials and methods

2.1 Insect cell culture-based protein expression system

2.1.1 Insect cell culture

Spodoptera frugiperda (Sf9 and Sf21) cells adapted to serum free media were used throughout as the host cell line. Sf9 cells stored in liquid nitrogen were set up in T75 adherent culture flasks with 9 ml of Insect Xpress media with 1ml Fetal Bovine Serum (FBS), heated in water bath at 56℃ for 30min. The cells were grown at 28℃ as suggested by Oxford Expression Technology guidelines, for all insect suspension and adherent cultures, for 48 hours. The cells formed a monolayer with 90%-100% surface coverage and were passed into 100ml sterilized conical flasks stopped with a foam bung and covered with foil for suspension culture. The total culture volume was adjusted to 25 ml by Insect Express media and the flasks were incubated at 115 rpm for 48 hours.

Cells were counted on haemocytometer at 25x magnification under a light microscope. The cells were diluted to a density of $1x10^6$ cells/ml into a 500ml conical flask and counted daily, incubated until they reached a density of $6x10^6$ cells/ml ready for large scale expression. Cells were also passaged at $1x10^6$ cells/ml to maintain suspension culture stocks.

2.1.2 Generation of recombinant baculovirus

Recombinant baculovirus was generated by Dr Justyna Prusinska.

The transfer vector was codon-optimized for Sf9 cell line expression, A.thaliana PIN5 was engineered to given fusion protein AtPIN5-TEV-GFP-FLAG-His10 (Table 2.8).

2.1.2.1 PIN5 fusion protein expression vector

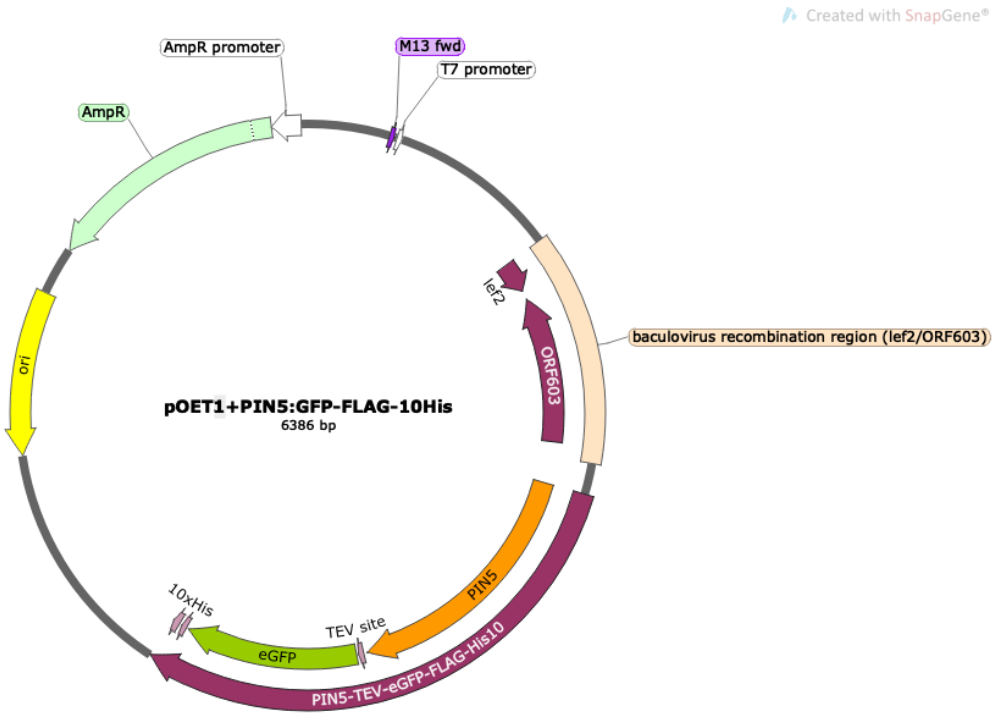

Figure 2.1 AtPIN5:GFP expression vector plasmid map

2.1.2.2 PIN5 fusion protein amino acid sequence

MINCGDVYKVIEAMVPLYVALILGYGSVKWWHIFTRDQCDAINRLVCYFTLPL
FTIEFTAHVDPFNMNYRFIAADVLSKVIIVTVLALWAKYSNKGSYCWSITSFSL
CTLTNSLVVGVPLAKAMYGQQAVDLVVQSSVFQAIVWLTLLLFVLEFRKAGF
SSNNISDVQVDNINIESGKRETVVVGEASKSFLEVMSLVWLKLATNPNCYSCI
LGIAWAFISNRWHLELPGILEGSILIMSKAGTGTAMFNMGIFMALQEKLIVCGT
SLTVMGMVLKFIAGPAAMAIGSIVLGLHGDVLRVAIIQAALPQSITSFIFAKEYG
LHADVLSTAVIFGMLVSLPVLVAYYAALEFIHSSGLEENLYFQGGGSVSKGEE
LFTGVVPILVELDGDVNGHKFSVSGEGEGDATYGKLTLKFICTTGKLPVPWP
TLVTTLTYGVQCFSRYPDHMKQHDFFKSAMPEGYVQERTIFFKDDGNYKTR
AEVKFEGDTLVNRIELKGIDFKEDGNILGHKLEYNYNSHNVYIMADKQKNGIK
VNFKIRHNIEDGSVQLADHYQQNTPIGDGPVLLPDNHYLSTQSALSKDPNEK
RDHMVLLEFVTAAGITLGMDELYKGSSDYKDDDDKGGSHHHHHHHHHH

A.thaliana PIN5-TEV-GFP-FLAG-His10

2.1.3 Titration of Recombinant Virus by Plaque-assay

Recombinant baculovirus pOET1-AtPIN5:GFP was quantified by titration. One virus stock required a 12-well culture plate for the test. 12-well plates were seeded with a sub-confluent monolayer of healthy Sf9 or Sf21 cells, about 4 x 10^5 cells/well and allowed to settle for at least one hour. Logarithmic dilutions of the virus stock were made from 1 in 10 (10^{-1}) to 1 in 10^7 (10^{-7}), in Insect Xpress cell culture medium. Medium was removed by aseptic technique from the 12-well plates, and 100 µl of diluted virus was added drop wise, gently to the centre of each dish.

Dilutions from 10^{-4} to 10^{-7} were plated and three wells per dilution in total 12 wells. The virus was allowed to adsorb at room temperature for an hour. Inoculum was removed and 0.5 ml of 2% agarose at 50-55℃ mixed with an equal volume of Insect Xpress cell culture medium at 28℃ were added per well of cells, and incubated at 28℃ for 4 days.

Neutral red stain (0.25 mg/ml dissolved into 0.5 ml PBS) was added to each well and incubated for 3-4 hours. Remaining liquid was decanted, virus plaques appeared clearly in a sea of red healthy cells and counted on a light box. Average plaque counts from the triplicate wells and virus titer were calculated.

Average number plaques x dilution factor x 10 = plaques/ml in the original virus stock.

2.1.4 MOI ratio and harvest time optimization for protein expression

Protein was expressed in Sf9 cells by shaking culture. Before large scale protein expression, a small-scale Multiplicity of Infection (MOI) and infection time test was undertaken.

To find the best MOI and time for cell harvest, Sf9 cells at $1x10^6$ cells/ml in 50ml were infected with recombinant baculovirus in qpfu/ml (Quantitative Plaque Forming Units / Millilitre) relating to 0.1x, 0.5x and 1.0x times the number of Sf9 cells in the given volume (MOI of 0.1, 0.5 and 1.0 respectively). Samples of 1 ml were collected at each time point respectively (24h, 48h, 72h centrifuged at 1,500xg for 3 minutes to collect pellets, and lysed into 1ml PBS by 3 sec sonication, 3x100 µl supernatant was collected for the eGFP fluorescence record.

Some P2 AtPIN5 virus stock was kept at 4℃ over 12 months. However, the virus titre started to drop thereby reducing the AtPIN5 protein expression. Fresh AtPIN5 P2 virus was amplified and used to compare with old P2 virus stock virulence. Three cell harvest points were set (24h, 48h, 72h), three different MOI (0.1, 0.5, 1.0), and two cell densities were applied (1 million/ml, 2 million/ml). All sample harvests were measured by whole cell GFP fluorescence as above.

2.1.5 Large scale protein expression in Sf9

500ml cells in 2L sterilized conical flasks were infected at a density of $1x10^6$ cells/mL in suspension cultures, with the optimized harvest time and multiplicity of infection (chapter 3.2), and incubated at 28℃,115 rpm. The cell pellet was harvested 48 hours after infection, Sf9 cell pellets were collected into 1 L centrifuge bottles by centrifugation at 10,000xg for 10 minutes, then washed in PBS and transferred into 50 ml centrifuge tubes to be re-pelleted at 4,000xg for 10 minutes at 4℃. The supernatant was discarded and the pellets were weighed, fast frozen in liquid nitrogen then stored at -80℃.

2.1.6 Large scale Sf9 cell lysis for membrane preparation

5 ml Tris lysis buffer (Table 2.1) was used per 1 g of cell pellet and incubated at 4℃ for 20 min. This extract was loaded twice into cell disrupter at 15 kPSI, and samples were pelleted by centrifugation at 200,000xg. The supernatant was discarded and the pellets were weighed, fast frozen in liquid nitrogen and stored at -80℃.

2.2 Saccharomyces cerevisiae GFP-based membrane protein expression system

2.2.1. *Saccharomyces cerevisiae* expression of PIN proteins with GFP

Saccharomyces cerevisiae was cultured and amplified in yeast extract peptone dextrose (YPD) medium for competent cell preparation. Four short PIN genes (OsPIN5a, PtrPIN12, GmPIN5a, AbtPIN5) were selected from 34 published genomes. Codon-optimized cDNA sequences of for *S. cerevisiae* expression, were synthesised as gBlocks by Twist Biosciences. gBlocks were amplified by primer extension PCR with overhangs required for homologous recombination. The cloning site in the GFP-fusion vector pDDGFP-2 (harbors a GAL1 promoter and URA selection marker) provided TEV, yEGFP, FLAG peptide and poly-Histidine affinity tags. *SmaI*-linerized vector and short-PIN PCR products were transformed into competent *S. cerevisiae* cells respectively, and cells were plated onto selective medium without URA. The plates were incubated at 30℃ for 2-3 days. Transformant colonies were inoculated into 10ml -URA medium with 2% glucose in 50ml aeration-capped tubes for overnight culture at 30℃ and 280 rpm. The overnight culture was diluted to optical density measured at a wavelength of 600 nm (OD600) to 0.12 with -URA medium with 0.1% glucose in 50ml aeration-capped tubes, incubated and at an OD600 of 0.6 (after 7 h), expression of membrane protein-GFP fusions were induced by adding 20% (wt/vol) galactose (final 2%). Twenty two hours after induction, cells were harvested by centrifugation at 3,000xg for 5min. The supernatant was discarded and cell pellets were resuspended into 200 µl PLB for whole cell GFP-fluorescent measurement.

2.2.2 *Saccharomyces cerevisiae* small scale lysis and short-PIN GFP fusion screening

The cell suspension obtained as described above was transferred into 1.5ml Eppendorf tubes and glass beads were added so that the final volume with suspension was 500µl. An additional 500µl of PLB was added. Yeast cells were lysed using a mixer-mill disruptor set at 25 Hz for 7 min at 4℃. Unbroken cells were pelleted by centrifugation at 22,000 xg in a desktop centrifuge for 5 s at 4℃ and 500 µl of the supernatant was transferred into a new tube. 500 µl of lysis buffer was added to the unbroken cell pellet and glass beads. Yeast lysis steps were repeated and the supernatant was transferred to the 500 µl batch obtained from the first round of cell breakage. Samples were analysed by GFP-fluorescence measurement and SDS-PAGE. Short-PIN GFP fusion cells were made into glycerol stocks and frozen at -80℃ for storage.

2.2.3 *Saccharomyces cerevisiae* large scale culture and lysis

Yeast glycerol stocks were inoculated by inoculation loop, and swabbed across the -URA plate. The plates were incubated at 30C for 2-3 days, and single colonies were inoculated into 10ml -URA medium with 2% glucose in 50ml aeration-capped tubes for overnight culture at 30C 280 rpm. The culture was diluted into 100ml -URA with 2% glucose in 250ml sterilized conical flask for another overnight culture, and diluted the overnight culture to OD600 of 0.12 by 1000ml -URA medium with 0.1% glucose in 2.5L sterilized polycarbonate baffled culture flasks, while at an OD600 of 0.6 (after 7 h), expression of membrane protein-GFP fusions were induced by adding 20% (wt/vol) galactose (final 2%). 22 hours after induction, short PINs-GFP fusion overexpression yeast cell pellets were collected into 1 L centrifuge bottles by centrifugation at 5,000 xg for 20 minutes. Yeast pellets were resuspended into yeast lysis buffer then broken by cell disrupter at 25, 30, 32, 35 psi respectively at 4C, cell debris was removed by centrifugation at 10,000 xg 4C for 10 minutes, and supernatant was pelleted by spinning at 200,000 xg 4C for 90 minutes, pellets were collected fast freeze by liquid nitrogen and kept in -80 for further usage.

2.3 TEV and 3C protease expression and purification

2.3.1 TEV protease Expression and purification

A plasmid of Super TEV protease with a C terminal poly-histidine tag was kindly provided by MPL (Table 2.8), a was transformed into Rosetta2 (DE3) strain cells cultured with 50 mg/ml kanamycin selection on LB plates. Colonies were selected and sequenced, glycerol stocks were created and stored at -80 C. Transformed expression strain was grown in LB with 34mg/ml chloramphenicol shaking culture at 37 C. While OD600 reached 0.5, temperature was reduced to 25 C and 0.4 mM IPTG was induced for overnight culture.

TEV protease purification buffers
Lysis buffer: 1 x PBS, 70 mM imidazole pH 7.5, 1 mM MgCl2, 10 % glycerol, 10 µg/ml DNase I, 0.3 mM TCEP
Wash buffer 1: 1 x PBS, 70 mM imidazole pH 7.5, 10 % glycerol, 0.3 mM TCEP
Wash buffer 2: 1 x PBS, 100 mM imidazole pH 7.5, 10 % glycerol, 0.3 mM TCEP
Elution buffer: 20 mM Tris pH 7.5, 300 mM NaCl, 250 mM imidazole, 20 % glycerol, 0.3 mM TCEP
Storage buffer: 20 mM Tris pH 7.5, 300 mM NaCl, 50 % glycerol, 0.3 mM TCEP

Cells were harvested and resuspended in lysis buffer (3ml/g cell pellet), then broken by cell disrupter at 20psi, 4C. Cell debris was removed by 200,000 xg centrifugation for 1 hour, supernatant was collected. A 5ml His trap column was prepared and equilibrated with 5 column volumes wash buffer 1. Sample was loaded onto the column and flow speed was set at 2ml/min. The column was washed by 10 column volumes wash buffer 1 and wash buffer 2 respectively at 4ml/min. Sample was eluted by 5 column volumes elution buffer and dialysed against storage buffer. Single-use aliquots(1ml) were transferred into 1.5ml Eppendorf tubes and stored at -80C.

2.3.2 3C protease expression and purification

3C protease plasmid (Table 2.8) transformation and expression was same as TEV in 2.3.1.

3C protease purification Buffers
Lysis buffer: 50 mM Tris pH 7.5, 150 mM NaCl, 20 mM Imidazole, 1 mM TCEP, 1 mM MgCl2, ~10 µg/ml DNase I. No protease inhibitors!
Wash buffer 1: 50 mM Tris pH 7.5, 500 mM NaCl, 20 mM Imidazole, 1 mM TCEP
Wash buffer 2: 50 mM Tris pH 7.5, 500 mM NaCl, 30 mM Imidazole, 1 mM TCEP
Elution buffer: 50 mM Tris pH 7.5, 500 mM NaCl, 150 mM Imidazole, 1 mM TCEP, 10 % glycerol
Storage buffer: 50 mM Tris pH 7.5, 150 mM NaCl, 10 mM EDTA, 1 mM TCEP, 20 % glycerol

Cells were harvested and resuspended in lysis buffer (3ml/g cell pellet), then broken by cell disrupter at 20psi, 4C. Cell debris was removed by 200,000 xg centrifugation for 1 hour, supernatant was collected. A 5ml His trap column was prepared and equilibrated with 5 column volumes wash buffer 1. Sample was loaded onto the column and flow speed was set at 2ml/min. The column was washed by 10 column volumes wash buffer 1 and wash buffer 2 respectively at 4ml/min. Sample was eluted by 5 column volumes elution buffer and dialysed against storage buffer. Single-use aliquots (1ml) were transferred into 1.5ml Eppendorf tubes and stored at -80C.

2.4 Affinity chromatography protein purification – PIN proteins

The AtPIN5 fusion protein was designed with a C terminal 10x Histine tag for purification. The IMAC resin is an affinity chromatography support for the purification of recombinant His-tagged proteins. Small scale purification used 100 µl IMAC resin packed into Bio-Rad 1.2ml mini spin columns.

Table 2.1 Tris buffer reagent composition

pH=8	Tris-HCl	NaCl	Glycerol	Imidazole	Protease inhibitor	DNAse	Detergent DDM
Tris Lysis Buffer (TLB)	50mM	150mM	5%	0	1 tablet/ 50ml buffer	2000 units	1%
Tris Column Buffer (TCB)	50mM	150mM	5%	10	1 tablet/ 50ml buffer	0	0.1%
Tris Washing Buffer (TWB)	50mM	500mM	5%	15	1 tablet/ 50ml buffer	0	0.1%
Tris Elution Buffer (TEB)	50mM	500mM	5%	250	0	0	0.05%
Tris HPLC Buffer	50mM	500mM	5%	0	0	0	0.05%

Table 2.2 Phosphate buffer reagent content.

pH=8	diSodium Phosphate	NaCl	Glycerol	Imidazole	Protease inhibitor	DNAse	Detergent DDM
Phosphate Lysis Buffer: (PLB)	50mM	150mM	5%	0	1 tablet/ 50ml buffer	2000 units	1%
Phosphate Column Buffer: (PCB)	50mM	150mM	5%	10	0	0	0.1%
Phosphate Washing Buffer: (PWB)	50mM	500mM	5%	15	1 tablet/ 50ml buffer	0	0.1%
Phosphate Elution Buffer: (PEB)	50mM	500mM	5%	250	0	0	0.05%

Table 2.3 MES buffer reagent content

pH=6.5	MES	NaCl	Glycerol	Imidazole	Protease inhibitor	DNAse	Detergent DDM
MES Lysis Buffer: (MLB)	50mM	150mM	5%	0	1 tablet/ 50ml buffer	2000 units	1%
MES Column Buffer: (MCB)	50mM	150mM	5%	10	0	0	0.1%
MES Washing Buffer: (MWB)	50mM	500mM	5%	15	1 tablet/ 50ml buffer	0	0.1%
MES Elution Buffer: (MEB)	50mM	500mM	5%	250	0	0	0.05%

Table 2.4 HEPES buffer A& B reagent content

pH=7.0(A), 7.5(B)	HEPES	NaCl	Glycerol	Imidazole	Protease inhibitor	DNAse	Detergent DDM
HEPES Lysis Buffer:	50mM	150mM	5%	0	1 tablet/ 50ml buffer	2000 units	1%
HEPES Column Buffer:	50mM	150mM	5%	10	0	0	0.1%
HEPES Washing Buffer:	50mM	500mM	5%	15	0	0	0.1%
HEPES Elution Buffer:	50mM	500mM	5%	250	0	0	0.05%

2.4.1 AtPIN5 Purification by nickel IMAC Resin

5 ml of Tris lysis buffer (TLB, without n-Dodecyl-B-D-Maltoside, DDM) was added for each gram of Sf9 cell pellets, and the extract was sonicated on ice for 20 seconds repeated three times with 10 seconds gap between each repeat. Samples were centrifuged at 6,000 xg for 10 minutes and the supernatant was collected, centrifuged at 180,000 xg for 90 minutes, the new supernatant discarded and the membranes in the pellet collected and stored at -80 C if necessary. The pellet was homogenized into 6ml TLB, 1 ml aliquot transfered to six (1.5ml) bench top ultracentrifugation tubes respectively, 10% of DDM was added to final 0.5% concentration and incubated into cold room for 0.5/ 1/ 2 hours. Finally, bench top ultracentrifugation applied 130,000 xg for 45 minutes, and the supernatant was collected as it contained solubilized AtPIN5:GFP protein for fluorescence reading.

The nickel spin column purification as follows, 100μl nickel resin was loaded on the mini spin column, washed with PBS and 2ml TCB, 5.5ml protein sample was loaded through spin column and repeated 3 times. Flow through was collected, column was washed twice by 600 μl TWB, wash through was collected, and the samples were eluted with 600 μl TEB and 4 elution fractions were collected.

2.4.2 AtPIN5 Purification by TALON IMAC Resin

Protein membrane stock was resuspended into PLB (15-30 mg/ml) and 10% DDM/0.5% CHS stock added to give a final 1% DDM /0.05% CHS. After incubation with rolling at 4 C for 2 hours, samples are centrifuged in a 45Ti rotor for 60 min at 160,000x g and the supernatant was filtered by 0.45 um PVDF filter. The sample was rolled with TALON beads (1 ml TALON resin for 1 L cell culture) at 4C for 2 hours, then the mixture was loaded into a glass column, a peristaltic pump is connected to the bottom of the column, flow speed 0.5 ml/min for 1 hour. The column was washed by 20 column volumes PWB (Table 2.2) and eluted by 5 column volumes of PEB (Table 2.2). Fractions were collected and analysed by SDS-PAGE, in-gel fluorescence, SEC A280 and FSEC.

2.4.3 AtPIN5 Purification by Anti FLAG

Protein membrane stock was resuspended into lysis buffer (15-30 mg/ml) and 10% DDM/0.5% CHS stock added to give a final 1% DDM /0.05% CHS. After incubation with rolling at 4 C for 2 hours, samples are centrifuged in a 45Ti rotor for 60 min at 160,000x g and the supernatant was filtered by 0.45 um PVDF filter. 2.5ml FLAG resin was added into the supernatant and incubated for at least 3 hours and loaded mixed sample with resin on the column, before the mix was loaded into a column. The flow through was collected, and the column washed by 10 column volumes TLB, samples were eluted by 10ml TLB (dissolved 0.1mg/ml 3x FLAG peptide), collect in 1ml factions, and analysed by GFP fluorescence reading, SDS-PAGE, in-gel fluorescence.

2.4.4 AtPIN5 Purification by Anti-GFP

Protein membrane stock was resuspended into TLB (15-30 mg/ml) and 10% DDM/0.5% CHS stock added to give a final 1% DDM /0.05% CHS. After incubation with rolling at 4 C for 2 hours, samples are centrifuged in a 45Ti rotor for 60 min at 160,000x g and the supernatant was filtered by 0.45 um PVDF filter. 2.5ml Anti-GFP resin was added into the supernatant and incubated for at least 3 hours and loaded mixed sample with resin on the column, before the mix was loaded into a column. The flow through was collected, and the column washed by 10 column volumns TLB, samples were eluted by 10ml TLB (dissolved 0.2mg/ml TEV protease), collect in 1ml factions, SDS-PAGE, in-gel fluorescence.

2.5 High Performance Liquid Chromatography system

The Speax SRT-C SEC-300 HPLC column was connected to the 1260 Infinity II SFC System HPLC kept into a 4C cold room. The column was pre-washed by two column volume mobile phase (30ml Tris HPLC Buffer). 30µl sample was loaded into an HPLC sample vial (0.5 ml). The HPLC was programmed for a sample injection volume 10 ul, flow speed 1.0 ml/min and total running volume 15ml. The HPLC UV detection sensor was set as UV 280 nm and fluorescence sensor excitation at 488 nm emission at 512 nm. One column volume (15 ml) of mobile phase data was collected.

2.6 Detergent and lipids screening

In order to optimize the solubilization for PIN proteins and on TALON resin purification, 12 different detergent and lipid combinations were tested. The TALON column detergent screening process was as follows; cell pellet was collected into 1 L centrifuge bottles by centrifugation at 10,000x g for 10 minutes, then suspended for washing by TBS and transferred into 50 ml centrifuge tubes, pelleted at 5,000xg for 10 minutes at 4℃. The supernatant was discarded, the pellet was weighted. 5 ml Tris Lysis Buffer was used for resuspending each 1 g of cells and incubated in cold room for 20 min. This extract was run through a cell disrupter at 15 kPSI. The lysate was collected and separated into 12 tubes with 12 different detergent mixes (DDM, DDM/CHS, DM, DM/CHS, OG, LMNG, OGNG/CHS, LDAO, C12E8, C12E9, Cymal-5, Fos choline-12) and incubated at 4°C for two hours. Samples were centrifuged by 70.1Ti rotor for 30 min at 160,000x g and 4°C. The supernatant was collected and loaded on mini spin columns which were pre-packed with 0.05 ml TALON beads. The sample was spun for 1 sec at 8,000x g. The columns were washed with 2ml Tris Wash Buffer (Table 2.1), 1ml each washing, before the sample was eluted with 0.2ml Tris Elution Buffer (Table 2.1). Samples were taken from each elution for evaluation by SDS-PAGE and in-gel fluorescence, and the rest of each elution run on HPLC to collect FSEC data.

2.7 Buffer and lipids screening

Cell pellets were collected into 1 L centrifuge bottles by centrifugation at 10,000x g for 10 minutes, then washed by TBS and transferred into 50 ml centrifuge tubes, pelleted at 5,000x g for 10 minutes at 4℃. Supernatant was discarded and the cell pellet was weighed by balance. 5 ml Tris Lysis Buffer was used for 1 g of cell lysis. The pellet was dissolved into lysis buffer and incubated in cold room for 20 min before loading into a cell disrupter at 15 KPSI. The lysate was collected and 10% DDM added to give a final 1%DDM. After incubation at 4℃ for 2 hours Samples were centrifuged by 45Ti rotor for 60 min at 160,000x g and 50ml supernatant was collected and aliquoted 500µlper well into the 96 well filter plate. 96 well filter plate was placed on 96 well deep plate for flow through collection, centrifuged for 2 minutes at 700g and flow through samples collected in the deep plate. TALON resin was washed with 2x 1ml Washing Buffer (96 conditions with different buffer base/ pH/ NaCl/ DDM/ lipids ratio; Table 2.5). A brief 1,000x g spin was applied to remove residual Washing Buffer before elution. 60µlelution buffers (96 conditions, ref as Table 2.5) were added into filter plate, the plate was sealed and incubated on a platform shaker at 4℃ for 20 min. Eluates were collected by centrifugation at 1,000x g. 10 µlof each eluate was kept on ice for 10 minutes and another 10µlwas heated at 40 C for 10 minutes and both samples were run on SDS-PAGE, using in-gel fluorescence as a measure of protein yield and protein integrity.

Table 2.5 TALON column purification buffer and lipids screening buffer and lipids composition

	150mM NaCl				300mM NaCl				500mM NaCl			
	MES pH6.5	HEPES pH7.0	HEPES pH7.5	TRIS pH8.0	MES pH6.5	HEPES pH7.0	HEPES pH7.5	TRIS pH8.0	MES pH6.5	HEPES pH7.0	HEPES pH7.5	TRIS pH8.0
Liver lipids (50:1)												
E.coli lipids (50:1)												
POPG (50:1)												
POPS (50:1)												
PC:PE:PG 2:1:1 (50:1)												
PC:PE 3:1 (50:1)												
CHS (10:1)												
Sodium cholate (10:1)												

2.8 Microscale Fluorescent Thermal Stability Assay

7-diethylamino-3-(4′-maleimidylphenyl)-4-methylcoumarin (CPM) dye was obtained from Invitrogen and dissolved in DMSO (Sigma) at 4 mg/ml. This stock solution was kept at −80°C. Prior to use the dye stock is diluted 1:40 in dye dilution buffer (50 mM Tris, pH 7.5, 150 mM NaCl, 5% glycerol, 0.025% DDM), and incubated for 5 min at room temperature. The thermal denaturation assay was performed in a total volume of 60 µl. The FLAG-SEC purified OsPIN5a:GFP was diluted in the appropriate buffer to a final concentration 10 µg/ml. After an incubation period (usually 5 min at 4℃), included to 49 µl of the protein with the buffer components, 10 µl of the diluted dye and 1µlof the binding ligand (50 nM IAA, NPA, TIBA, IAA-GLU, IAA-ASP dissolved into DMSO, DMSO as control) was thoroughly mixed with the protein. Same RFU of purified 10Histidine and FLAG tagged yeGFP was mixed with DMSO and used as control. The reaction mixture was transferred within a 5 min period to a qPCR machine and heated in a controlled way with a ramp rate of 1°C/min, the excitation wavelength was set at 387 nm, while the emission wavelength was 463 nm, the CPM dye fluorescence data was collected at every minute. Assays were performed over a temperature range starting from 25°C and ending at 90°C.

All data were processed with GraphPad Prism program (GraphPadPrism v.9.00 for MAC OS). yeGFP control data was subtracted from the OsPIN5:GFP melting fluorescence data to account for the effect of yeGFP in melting curves. In order to determine the inflection point of the melting curves, which was assumed to equal the melting temperature (Tm), a Bolzmann sigmoidal equation was fitted to the raw data

2.9 Negative Staining

Membrane protein was purified and polished by AKTA-FPLC SEC (method refer to 3.11 Figure 3.18), peak fractions were collected and diluted by gel-filtration buffer to 0.08mg/ml and 0.05ml for negative staining preparation.
Carbon-coated copper grids (300 mesh) were placed on top of a slide in a Quorum Q300 vacuum chamber, vacuum pump was turned on and glow discharge was applied for 1 minute. After that chamber was vented, the slide was placed on a bench, a Parafilm was prepared with 2% uranyl acetate droplets (20µl, 4 droplets per sample) and dH_2O droplets (20µl, 3 droplets per sample). A glow discharged grid was held in a clamping forceps, 5µl of diluted AtPIN5:GFP sample was pipetted onto grid and blotted off onto a Whatman filter paper after 30 seconds. The first uranyl acetate droplet was applied and blotted off immediately, the second uranyl acetate droplet was applied for 2 minutes, then blotted off and washed by applying a droplet of water and the excess was blotted off (repeat 3 times). The grid was dried in air for a few minutes and kept in a grid box for later TEM screening.

2.10 GFP confocal microscopy

pOET1-PIN5:GFP was expressed in Sf9 cells for 24 hours. 1ml of infected cells were harvested by 700xg spin for 2 min and resuspended in 1 ml of Insect Xpress medium containing 50% glycerol. 5 µl of cell suspension was added to a microscope slide and a coverslip placed on top. A Leica LSM 880 imaging system with a x25 oil objective was used with argon laser excitation at 488 nm and emission at 505-535 nm. Cell images were taken at different deeps of focus point.

2.11 Fluorescence based protein quantification

GFP fluorescence was measured in a SpectraMax M2e Microplate Reader by excitation at 488 nm, emission at 512 nm with bottom read and auto focus options.

Whole cell GFP fluorescence was measured follows. 1ml samples were collected into 1.5 ml Eppendorf tubes, and centrifuged at 1,500x g for 3 min. The pellets were washed by 1ml PBS and pelleted again. Pelleted cells were resuspended into 1ml PBS and 100 µl of the cell suspension was transferred into a black Nunc 96-well optical bottom plate for GFP Fluorescence measurement.

For protein samples, 100 µl of protein solution was transferred into a black Nunc 96-well optical bottom plate for GFP fluorescence measurement.

2.12 SDS-PAGE protocol

A total sample loading of 20µl per well was prepared with:
5µL of NuPAGE® LDS Sample Buffer (4X) (ThermoFisher Catalogue number: NP0007)
2µL of NuPAGE® Sample Reducing Agent (10X) (ThermoFisher Catalogue number: NP0009)
Up to 13µL of a sample - lysate/protein etc.
Should the sample volume be less than 13µL, Di-ionised water was used to make up the volume giving an overall total of 20µL.

15-well precast Tris-Glycine, 10 to 20% Novex™ WedgeWell™ gels were used in accordance with the manufacturers specifications with running conditions: – 215V for 50 minutes in a Novex® Tris-Glycine SDS Running Buffer in XCell SureLock Mini-Cell Electrophoresis System. Once run, gels were removed from their cassettes, visualised in a Syngene GBOX under UV trans-illumination. In gel fluorescence was scanned by GE Typhoon gel scanner and images recorded. These gels were suitable to be progressed onto Western blotting development.

2.13 Saposin A Nanodisc protein purification

Protein expression was carried out using a vector with the coding region for Saposin A inserted into a pNIC-Bsa4 plasmid which was obtained from Salipro Biotech. The cloning vector pNIC28-Bsa4 adds an N-terminal 6x histidine tag with an integrated TEV protease cleavage site. The protein was expressed using *E. coli* Rosetta gami-2 (DE3) (Novagen). Cells were grown at 37°C in TB medium supplemented with Tetracycline, Chloramphenicol and Kanamycin and induced with 0.7 mM IPTG. Sixteen hours after induction the cells were collected by centrifugation at 12.000×g for 15 min and the supernatant discarded. The cell pellet was resuspended in lysis buffer (20 mM Hepes pH 7.5, 150 mM NaCl, 20 mM Imidazole pH=8.0) and disrupted by sonication for 10 min. Lysates were subjected to centrifugation at 26,000×g for 30 min, the supernatant heated to 85°C for 10 min, followed by an additional centrifugation step at 26.000×g for 30 min. Preparative IMAC purification was performed by batch-adsorption of the supernatant by end-over-end rotation with 5 ml Ni Complete His resin for 60 min. After binding of Saposin A to the IMAC resin, the chromatography medium was packed in a 10-mm-(i.d.) open gravity flow column and unbound proteins were removed by washing with 15 bed volumes of lysis buffer. The resin was washed with 15 bed volumes of wash buffer WB2 (20 mM HEPES pH 7.5, 150 mM NaCl, 40 mM Imidazole pH=8.0). Saposin A was eluted by addition of five bed volumes of elution buffer EB (20 mM HEPES pH 7.5, 150 mM NaCl, 200 mM Imidazole pH=8.0). The eluate was dialyzed overnight against gel filtration buffer GF (20 mM HEPES pH 7.5, 150 mM NaCl pH=8.0) supplemented with recombinant TEV protease. TEV protease containing an un-cleavable His-tag was removed from the eluate by passing it over 2 ml IMAC resin. Cleaved target protein was concentrated to a volume of 5 ml using centrifugal filter units and loaded onto a HiLoad Superdex 75 16/600 GL column for polishing by using an AKTA chromatography system. Peak fractions were pooled and concentrated to 1.2 mg/ml by 3000 MWCO PES membrane concentrator, flash frozen in liquid nitrogen and stored at -80℃, all samples from the purification steps were loaded into SDS-PAGE for analysis.

2.14 Western blot protocol

Gels from 2.8 were transferred onto a PVDF (polyvinylidene difluoride) membrane using a transfer unit such as shown on Fig. 2.2.
The PVDF membrane was soaked in methanol for 15 seconds, then washed in water for 2 minutes. Filter paper, PVDF membrane and filter pad were soaked in 1xNuPAGE® Transfer Buffer supplemented with 10% methanol. The transfer units were loaded into a Bio-Rad Mini Trans-Blot® Cell, topped up with Transfer Buffer and run at 120V for 1 hour.

The membrane was then removed and blocked in TBS/Tween with 10% (w/v) skimmed milk or BSA powder for 1 hour on a platform shaker. This was followed by 3x 10 minutes TBS/Tween washes and incubation with primary antibody at 1:5000 (v/v) dilution in TBS/Tween with 5% (w/v) skimmed milk or BSA powder for 1 hour on a shaker, the membrane was washed by 3x 10 minutes TBS/Tween and processed secondary antibody and similar washing. The next step was incubation with 4ml Immobilon Western Chemiluminescent HRP Substrate (2mL of Luminol + 2mL of peroxide solution) in a clean container for 5 minutes, then imaging by ImageQuant LAS 4000 with Auto Exposure program under Chemiluminescence mode.

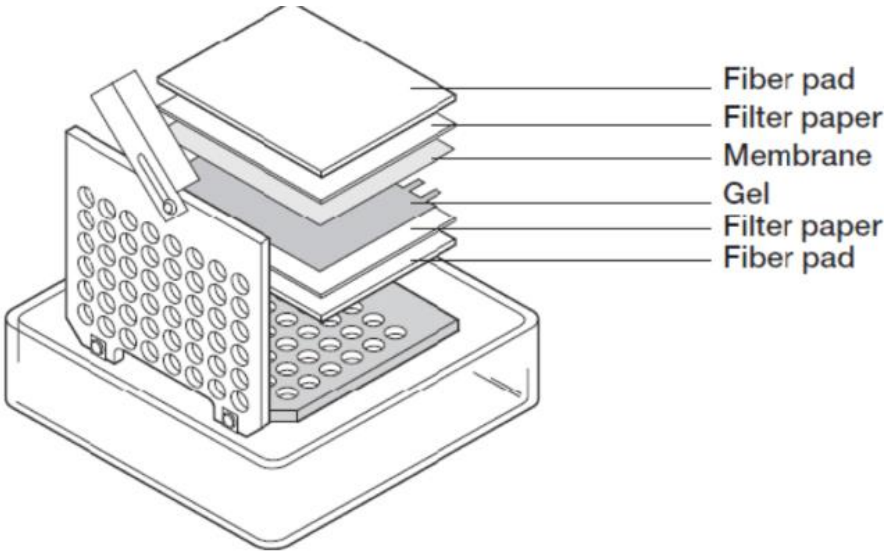

Figure 2.2 Diagram of western blot set-up

2.15 Size exclusion chromatography system

A Superose 6 10/300 GL column was connected to the AKTA purifier FPLC in a 4C cold cabinet. The Superose 6 10/300 GL Column was pre-washed by two column volume AKTA running buffer (50ml). 500 µl sample was loaded into the sample loop. The AKTA program was set for flow speed 0.30 ml/min, 200 µl fractions were collected by Nunc 96-well black optical bottom plate. Total running volume was 25ml. The UV detection sensor was set at 280 nm. The Nunc 96-well black optical bottom plate was removed from fraction collector to measure GFP fluorescence by plate reader, and fluorescent size exclusion chromatography (FSEC) data was analysed by Prism 9.

2.16 Lists of materials and equipment

All reagents and equipment and their manufacturers are listed below.

2.16.1 Chemical and Biological Materials

	Reagents	Provider
1	3xFLAG Peptide	Sigma-Aldrich
2	Anti-GFP Nanobody Affinity Gel	Biolegend
3	BenchMark Fluorescent Protein Standard 11-155 KDa	ThermoFisher SCIENTIFIC
4	Bolt LDS Sample Buffer (4X)	NuPAGE
5	Bolt Sample Reducing Agent (10X)	NuPAGE
6	C12E8 (Octaethylene glycol monododecyl ether)	Genero
7	C12E9 (Dodecyl nonaethylene glycol ether)	Genero
8	Cholesteryl hemisuccinate	Sigma-Aldrich
9	Colored Protein Ladder 11-245 KDa	New England BioLabs
10	Cymal-5 (5-Cyclohexyl-1-Pentyl-β-D-Maltoside)	Genero
11	DDM (Dodecyl Maltoside)	Genero

12	Deoxyribonuclease I, from bovine pancreas	Genero
13	Disodium phosphate	Sigma-Aldrich
14	Dithiothreitol	Genero
15	DM (Decyl Maltoside)	Genero
16	DMSO (Dimethyl sulfoxide)	Genero
17	E.coil Lipids	Sigma-Aldrich
18	Fos Chline-12 (n-Dodecylphosphocholine)	Genero
19	Glycerol	ThermoFisher SCIENTIFIC
20	Glycine	Sigma-Aldrich
21	Heat-Inactivated Fetal Bovine Serum	Labtech
22	HEPES (4-(2-hydroxyethyl)-1-piperazineethanesulfonic acid)	Sigma-Aldrich
23	IAA (Indole-3-acetic acid)	Genero
24	Imidizole	Sigma-Aldrich
25	Insext Xpress Cell Culture Medium	Lonza
26	Instant Blue Coomassie Stain	ThermoFisher SCIENTIFIC
27	LDAO (Lauryldimethylamine oxide)	Genero
28	Liver Lipids	Sigma-Aldrich
29	LMNG (Lauryl Maltose Neopentyl Glycol)	Genero
30	M2 Anti-FLAG Argose Beads	Sigma-Aldrich
31	Magnesium chloride	Sigma-Aldrich
32	MES (2-ethanesulfonic acid)	Sigma-Aldrich
33	OG (Octyl-beta-Glucoside)	Genero
34	OGNG (Octyl Glucose Neopentyl Glycol)	Genero
35	PBS buffer	Sigma-Aldrich
36	Phosphatidic acid (phosphatidate) (PA)	Sigma-Aldrich
37	Phosphatidylcholine (lecithin) (PC)	Sigma-Aldrich
38	Phosphatidylethanolamine (cephalin) (PE)	Sigma-Aldrich
39	Phosphatidylserine (PS)	Sigma-Aldrich
40	Phosphoinositides (PO)	Sigma-Aldrich
41	Pre-cast Gel	Bio-Rad
42	Protease Inhibitor tablets, EDTA-FREE	Roche

43	SDS	Sigma-Aldrich
44	Sf9 Cell	Oxford Expression
45	Sodium chloride	Sigma-Aldrich
46	Sodium cholate	Sigma-Aldrich
47	TALON CellThru Argose Beads	TAKARA
48	TALON Cobalt Argose Beads	TAKARA
49	TBS buffer	Sigma-Aldrich
50	TCEP (tris(2-carboxyethyl)phosphine)	Genero
51	TEV protease	Sigma-Aldrich
52	Tris (Trisaminomethane)	Self-Expressed
53	HPLC Sample Vial	VWR

Table 2.6 List of chemicals and biological materials

2.16.2 Equipment

	Equipment	Provider
1	Ultracentrifuge	Beckman Coulter
2	45Ti Ultracentrifuge Routor	Beckman Coulter
3	Balance	VWR
4	Cell Culture Shacking Incbator	Innova 44
5	Cell Culture Flask	Fisher
6	Bath Soniciate	ThemoFisher
7	Filteration Units	VWR
8	0.22um Filteration Membrane	VWR
9	0.45um Syringe Filter	VWR
10	0.22um Syringe Filter	VWR
11	1ml/2ml/5ml/10ml/20ml Syringe	VWR
12	Glass Bottle	Fisher
13	Borosilicate glass measuring cylinders, 50, 100, 250, 500 and 1,000 ml	VWR
14	Centrifuge tube, 15 ml, 50 ml	VWR
15	High-speed centrifuge	Beckman Coulter
16	Microfuge	Eppendof

17	Liquid chromatography system	GE Healthcare, ÄKTA explorer
18	Magnetic stirrer	VWR
19	SpectraMax M2e microplate reader	BMG Labtach
20	pH Meter	VWR
21	Ultracentrifuge Tubes 70ml	Beckman Coulter
22	Viva Spain 6, 20	GE Healthcare
23	Eppendof Tube 0.5 ml, 1.5 ml, 2 ml	Eppendof
24	HPLC UltiMate 3000 Standard	ThemoFisher
25	Superose 6 SEC Column	GE Healthcare
26	Nunc 96-well black optical bottom plate	Nunc
27	96 Well Deep Plate	VWR
28	Bio-Rad Gel Running Tank	Bio-Rad
29	Typhoon Gel Reader	GE Healthcare
30	PowerPac HC power supply	Bio-Rad
31	Confocal Microscope Zeiss LSM 880	Zeiss
32	Prism8 Satistic Software	Prism
33	Excel	Microsoft
34	PD-10 Desalting Column	GE Healthcare
35	96 Well Filter Plate	VWR
36	SRT-C SEC-300 HPLC Column	Sepax
37	Mini-Spin Column, 1.2 ml	Bio-Rad
38	Vortex Shacker	Scientific Industries
39	CellThru 10-ml Disposable Columns	TAKARA
40	ImageQuant LAS 4000 series	GE Healthcare
41	Peristaltic Pump Miniplus 2	Gilson

Table 2.7 List of equipment

2.16.3 Protein expression constructs and plasminds

Table 2.8 List of recombinant protein expression vector, constructs, and cell line.

Protein expression	Plasmids	Constructs	Molecular weight	Expression cell line
AtPIN1	pOET1, pOET3	AtPIN1-TEV-GFP-FLAG-12His	90kDa	Insect cell Sf9
AtPIN1-Cut	pOET1	AtPIN1-Cut-TEV-GFP-FLAG-12His	70kDa	Insect cell Sf9
AtPIN5	pOET1	AtPIN5-TEV-GFP-FLAG-12His	70kDa	Insect cell Sf9, ExpiSf
OsPIN8	pOPIN	OsPIN8-3C-10His, OsPIN8-3C-GFP-FLAG-10His	35kDa, 65kDa	Insect cell Sf9
OsPIN5a	p414GAL1	OsPIN5a-TEV-GFP-FLAG-12His	75kDa	*Saccharomyces cerevisiae FGY217*
GmPIN5a	p414GAL1	GmPIN5a-TEV-GFP-FLAG-12His	75kDa	*Saccharomyces cerevisiae FGY217*
AmbPIN5-like	p414GAL1	AmbPIN5-like-TEV-GFP-FLAG-12His	76kDa	*Saccharomyces cerevisiae FGY217*
PtrPIN12	p414GAL1	PtrPIN12-TEV-GFP-FLAG-12His	74kDa	*Saccharomyces cerevisiae FGY217*
TEV protease	pRK793	TEVprotease-6His	29kDa	E.coli Rosetta2 (DE3)
HRV-3C	pRK793	HRV-3C-6His	21kDa	E.coli Rosetta2 (DE3)
Saposin A	pNIC28-Bsa4	6His-Saposin A	9kDa	E.coli Rosetta gami-2 (DE3)

Chapter 3 AtPIN5 Expression and Purification

In this chapter, it was hypothesised that AtPIN5:GFP can be overexpressed in the baculovirus expression system. Expressed fusion proteins can be solubilized into detergents and purified by IMAC and IAAC methods.

The AtPIN5:GFP protein was expressed using the baculovirus expression system. Baculovirus multiplicity of infection, virulence, cell culture medium, cell density and cell harvest time were all optimized to obtain the best yield of intact AtPIN5:GFP fusion proteins. AtPIN5:GFP extraction was optimized by screening lysis buffer, detergent and lipids, all quantified by HPLC-FSEC. AtPIN5:GFP purification was optimized by testing different affinity purification methods and conditions.

3.1 Baculovirus transfer plasmid evaluation

For AtPIN5:GFP expression, the flashBAC system was used for the production and isolation of two recombinant baculoviruses. The transfer plasmids pOET1 (Polyhedrin gene promoter) or pOET3 (p6.9 gene promoter) were used for transfection of Sf9 cells with flashBAC DNA to generate P0 virus. P1 virus was amplified from P0 and, later, P2 virus was generated and titrated by plaque assay, giving a final virus titration of 1.05×10^8 pfu/ml.

30ml Sf9 cells were cultured at density of 1×10^6 cells/ml in 50ml conical flasks, and 0.3ml P2 recombinant baculoviruses were used to infect the cells. After 48 hours, cells were harvested for confocal-microscopy observation (Figure 3.1 A and B). A SpectraMax M2e Microplate Reader was used to record the whole cell fluorescence intensity for protein quantification (Figure 3.1 C).

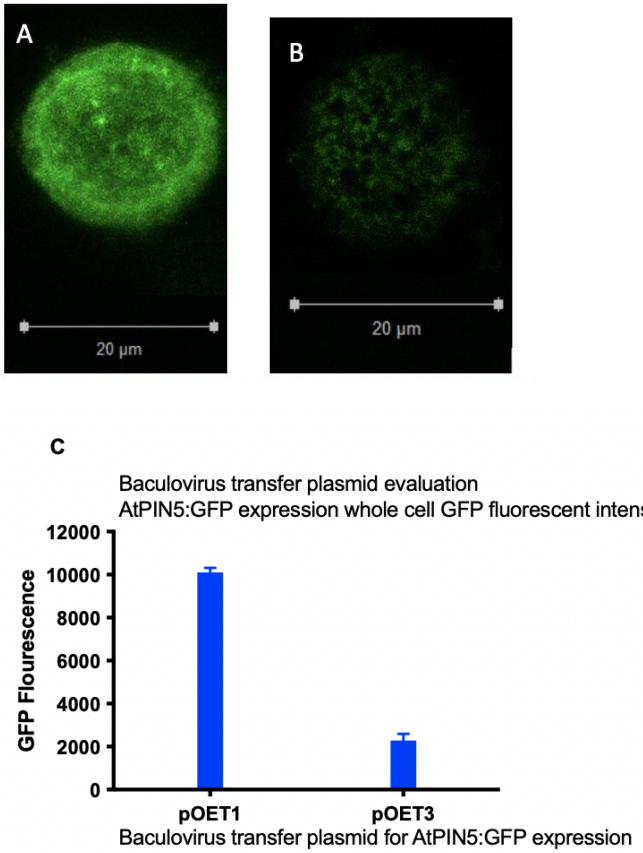

Figure 3.1 Baculovirus transfer plasmid evaluation for AtPIN5:GFP expression

pOET1 and pOET3 transfer plasmids were used for two types of AtPIN5:GFP recombinant baculoviruses. P2 viruses were used for AtPIN5:GFP expression, cells were harvested after 48 hours. confocal-microscopy and SpectraMax M2e Microplate Reader were used to analyse the expression of AtPIN5:GFP.

A: Confocal-microscopy photo of pOET1-AtPIN5:GFP fusion protein in Sf9 cell.

B: Confocal-microscopy photo of pOET3-AtPIN5:GFP fusion.

C: GFP fluorescence intensity of pOET1-AtPIN5:GFP fusion and pOET3-AtPIN5:GFP fusion, 100µlof 1x10^6 infected Sf9 cell suspension in PBS recorded by SpectraMax M2e Microplate Reader.

3.2 MOI, infection time and virus stock virulence optimization

The P2 AtPIN5:GFP virus stock was kept at 4 ℃ over 12 months. However, the virus titre can start to drop after a few weeks thereby reducing the AtPIN5:GFP protein expression. Before large scale purification, a small-scale Multiplicity of infection (MOI) and infection time test was undertaken. Three harvest points were set (24h, 48h, 72h), and each harvest point has three different MOI (0.1, 0.5, 1.0), and two cell densities applied (1 million/ ml, 2 million/ ml), in total 18 samples. All samples were measured by whole cell GFP fluorescence (Figure 3.2c & d).

Virulence of a 12-month-old virus stock was compared with fresh new P2 virus stock. Either 1 million/ ml and 2 million/ ml density of cells were infected at 3 different MOI (0.1, 0.5, 1) (Figure 3.2a & b). The GFP fluorescence reading at 1 million per ml cell density at infection gave more AtPIN5 protein expression only at 72 hours harvest time (Figure 3.2a). At a cell density of 2 million/ ml, new virus expressed more protein than old virus stock at all MOI when harvest after 48 and 72 hours (Figure 3.2b). New virus and old virus stock both expressed more protein at 2 million/ ml cell concentration (Figure 3.2c). The fresh virus stock to infect 2 million cells/ml at 0.1 MOI got the highest fluorescent intensity, however, the protein expression in Sf9 cell is not equally distributed. So, fresh virus stock was used to infect 2 million cells/ml at 0.5 MOI and harvest after 48 hours for the best protein yield.

0.1 MOI had higher fluorescent reading, however it generated more aggregated membrane proteins.

For each new virus stock generated, similar virus testing was applied to establish the best MOI for protein expression.

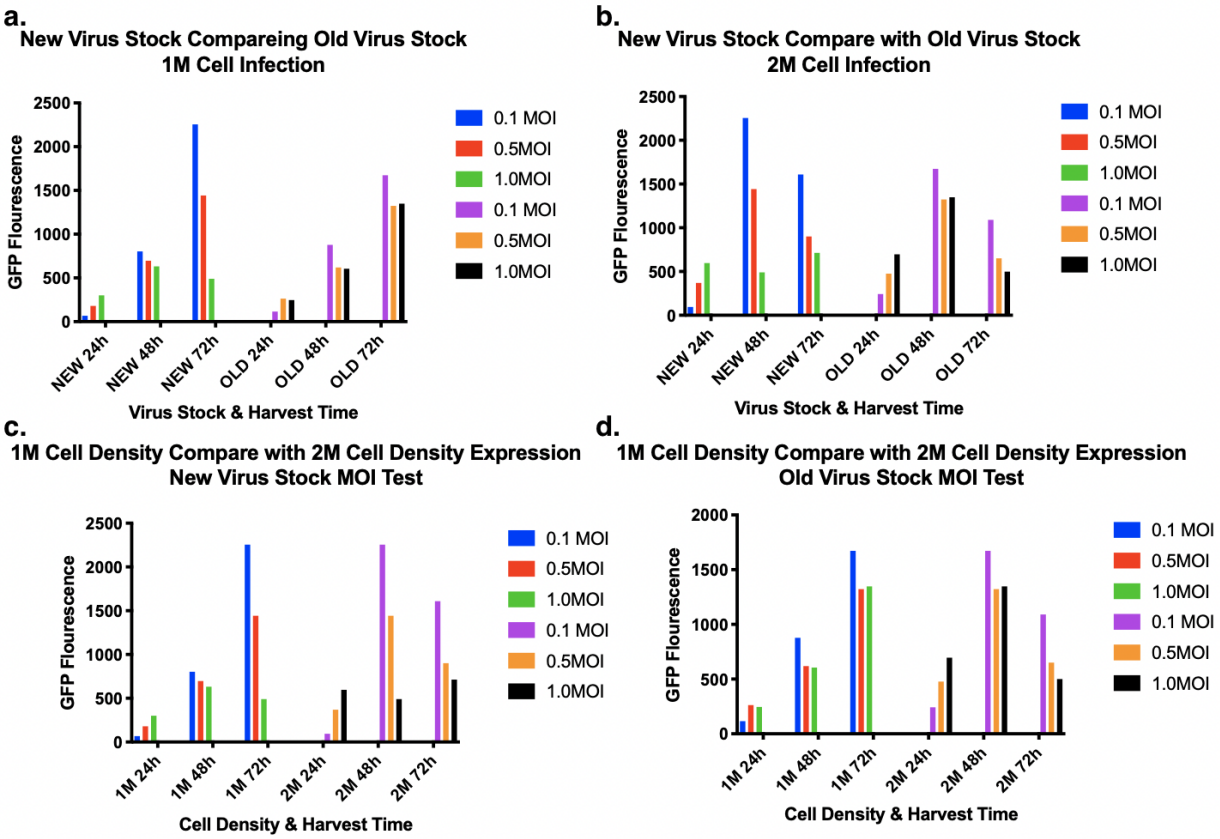

Figure 3.2 Optimizing expression of AtPIN5:GFP in Sf9 cells, by comparing virus stock, cell density and MOI.

AtPIN5 expression under different MOI and harvest times is measured by monitoring fluorescence of the fusion tag GFP over time.

a. New and old virus stock virulence comparation by infecting 1 million/ml density cells.

b. New and old virus stock virulence comparation by infecting 2 million/ml density cells.

c. 1 million/ ml density cell and 2 million/ ml density cell infected by new virus stock at different MOI

d. 1 million/ ml density cell and 2 million/ ml density cell infected by old virus stock at different MOI

3.3 Host cell evaluation between Sf9 and ExpiSf9

ExpiSf9 Cells are a new baculoviruses expression system host cell line which can be infected at a relatively high cell density ($8x10^6$) compared to conventional Sf9 cells ($2x10^6$).

ExpiSf9 cells were cultured in 100ml ExpiSf CD Medium. When cell density reached $1x10^6$, ExpiSf Enhancer was added (3.2ml/L cell culture) for extra 18 hours culture, and when the cell density reached $8x10^6$ the culture was infected by p2 pOET1-AtPIN5:GFP virus (what MOI is this?). Sf9 cells were cultured in 100ml Insect Xpress cell culture medium, and when the cell density reached $2x10^6$, cells were infected as above. 2ml cell samples were harvested from the ExpiSf9 and Sf9 cell cultures at certain times (24 hours, 44 hours, 50 hours, and 67 hours) and samples were loaded into 24 well plates and GFP fluorescence of live cells was screened by an EVOS cell imaging system (Figure 3.3).

AtPIN5:GFP expression level in high density ExpiSf9 cells was compared with Sf9 cells, in the GFP fluorescence cell images (Figure 3.3 A-H). Sf9 cells have relatively higher AtPIN5:GFP expression than ExpiSf9 cells. So, Sf9 cells will be used for further AtPIN5:GFP expression.

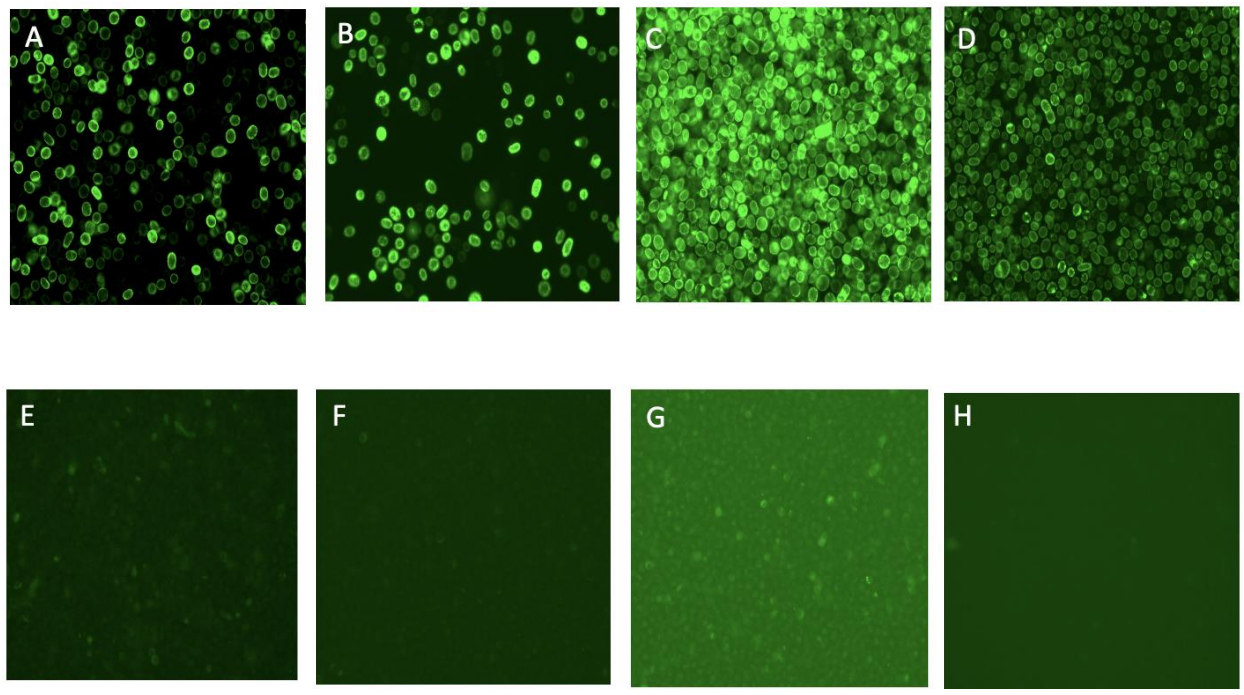

Figure 3.3 pOET1-AtPIN5:GFP expression overtime in Sf9 and EspiSf9 cells

Sf9 and EspiSf9 cells were infected by pOET1-AtPIN5:GFP baculovirus, samples were taken at four different time points for live cell GFP fluorescence screening by EVOS cell imaging system.

A-D: AtPIN5:GFP expression in Sf9 cells, fluorescence intensity in live cells at 24 hours, 44 hours, 50 hours, and 67 hours after infection.

E-F: AtPIN5:GFP expression in EspiSf9 cells, fluorescence intensity in live cells at 24 hours, 44 hours, 50 hours, and 67 hours after infection.

3.4 Insect cell culture medium evaluation

Sf9 cell culture media were evaluated for pOET1-AtPIN5:GFP expression optimization. Sf9 cells were cultured in 100ml Insect Xpress cell culture medium and SF-900 III cell culture medium respectively, and when the cell density reached $2x10^6$/ ml, cells were infected by p2 pOET1-AtPIN5:GFP virus (10ml virus stock/ L cell culture at 0.5 MOI). 2ml cell samples were harvested at four time points (24 hours, 44 hours, 50 hours, and 67 hours), and cells were lysed in 1ml Tris lysis buffer (Table 2.1) for SDS-PAGE and HPLC-FSEC screening (Figure 3.4).

The AtPIN5:GFP expression level in Sf9 cells cultured iin Insect Xpress medium was compared with SF-900 III cell culture medium. SDS-PAGE results were reviwed using in-gel fluorescence (Figure 3.4A) and showed a clean, intact AtPIN5:GFP had relative high expression at 44 h and 50 h in both cell culture medium. The HPLC-FSEC results (Figure 3.4 B) showed AtPIN5:GFP expression level in Insect Xpress cultured Sf9 cells was somewhat higher than in SF-900 III cell culture medium. 24 hours after infection in Insect Xpress the yield was 190,000 fluorescent units and in SF-900 III only 50,000 units. After infection in 50 hours Sf9 in Insect Xpress yield 240,000 fluorescent units and in SF-900 III only 220,000 units. So, Insect Xpress cell culture medium will be used for further AtPIN5:GFP expression in Sf9 cells.

AtPIN5 on SDS-PAGE

It is noted that the band visualised after SDS-PAGE ran at an apparent molecular weight of 50 kDa. The calculated molecular weight of AtPIN5:GFP fusion protein is 70 kDa. It is common for membrane proteins to appear smaller by around 20kDa on SDS-PAGE because of their hydrophobic structure, which results in them running faster than soluble proteins of the same molecular weight (Shirai et al., 2008).

In summary, we evaluated baculovirus plasmids, insect cell line and medium for AtPIN5:GFP expression, and optimized MOI, harvest time and cell density for AtPIN5:GFP yield. In further studies, Sf9 cells will be cultured in Insect Xpress medium and infected at 2 million cells/ml. We will use pOET1:AtPIN5:GFP baculovirus at 0.5 MOI and harvest at 48 hours after infection.

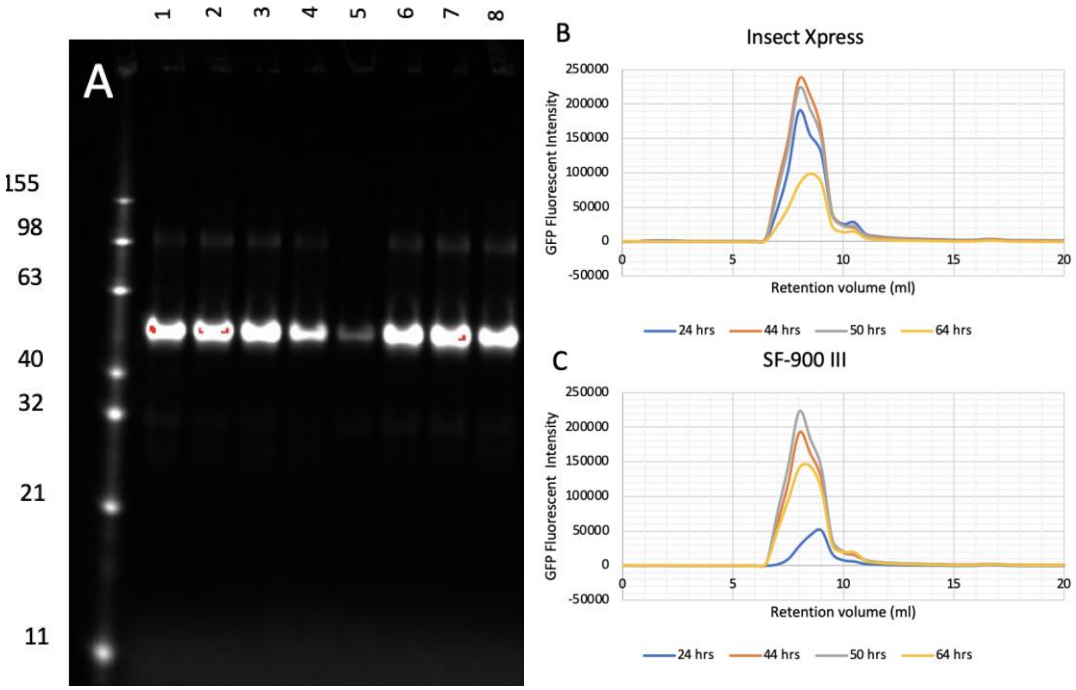

Figure 3.4 pOET1-AtPIN5:GFP expression over time in Sf9 cells with Insect Xpress and SF-900 III cell culture medium

Sf9 cells were infected by pOET1-AtPIN5:GFP baculovirus. Samples were taken at four different time points for SDS-PAGE for review using in-gel fluorescence and HPLC-FSEC screening.

A: In gel fluorescence of pOET1-AtPIN5:GFP overexpression in cells lysed at different time points, Lanes 1-4: Insect Xpress cell culture medium, cell samples at 24 hours, 44 hours, 50 hours, and 67 hours, 5-8: Sf-900 III cell culture medium, cell samples at 24 hours, 44 hours, 50 hours, and 67 hours.

B and C: HPLC-FSEC data of pOET1-AtPIN5:GFP overexpression in Insect Xpress and SF-900 III cell culture medium at four different time points.

3.5. Detergent and lipid screening

Introduction

Membrane protein (MP) purification condition is traditionally focused on identification of the most suitable detergent and buffer for purification before exchange into a shorter chain detergent prior to crystallisation. Although detergents have been an effective way to solubilise MPs, their use can lead to a loss of protein–protein and protein–lipid interactions, potentially destabilising the MP. Therefore, choice of detergent and lipids is a critical step when trying to purify an MP for crystallisation or cryo-EM.

A C-Terminal GFP as a fusion protein tag makes it easier to trace membrane proteins during purification. Analysis of the FSEC peak hight and shape will give information about MP:GFP size distribution, correct folding and quantify the yield.

3.5.1 Detergent

Selecting the best detergent for protein solubilization is important for maximising the protein yield and for crystallization. In order to optimize the solubilization for AtPIN5:GFP and its performance on TALON resin during purification, 12 different detergent and lipid combinations were tested (refer to methods, chapter 2.5 and 2.6).

The in-gel fluorescence screening and HPLC-FSEC traces showed Fos Choline-12 gave the best yield from solubilization (Figure 3.5 and 3.6). This detergent is as strong as SDS and gives a benchmark about total protein expression but is often not helpful for crystallography. Fos Choline-12 is used for proton nuclear magnetic resonance approaches, not for crystallization or cryo-EM. The LDAO also has strong fluorescent band, however, the FSEC peak was not as strong as the DDM peak. LDAO is a harsh detergent which might affect protein folding, especially of membrane proteins. Therefore, DDM/CHS which offers a good, gentler detergent mix will be used in further AtPIN5:GFP purification.

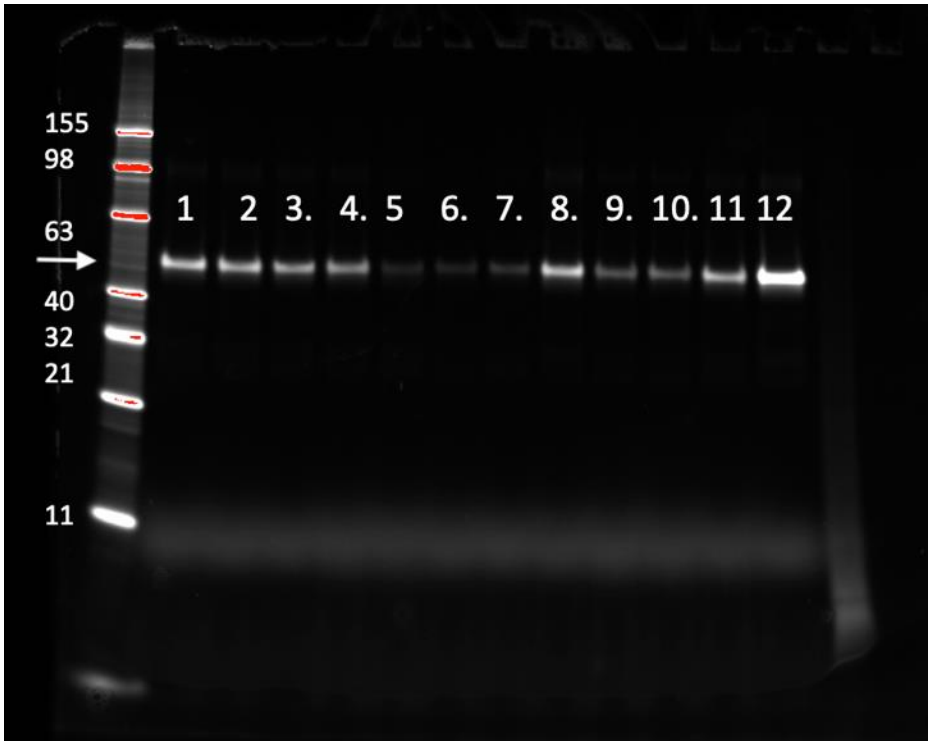

Figure 3.5 Optimizing detergents for TALON column protein purification.

SDS-PAGE was run on detergent-solubilized samples and the gel visualized under UV light to monitor in-gel fluorescence; 1: DDM solubilized sample, 2: DDM/CHS solubilized sample, 3: DM solubilized sample, 4 DM/CHS solubilized sample, 5: OG solubilized sample, 6: LMNG solubilized sample, 7: OGNG/CHS solubilized sample, 8: LDAO solubilized sample, 9: C12E8 solubilized sample, 10: C12E9 solubilized sample, 11: Cymal-5 solubilized sample, 12: Fos choline-12 solubilized sample. The ATPIN5-GFP runs at an apparent molecular weight of 55 kDa (arrow)

ATPIN5-GFP was solubilized into 12 different detergent and lipids and purified by TALON resin. Purified samples were loaded into HPLC for HPLC-FSEC data collection. The GFP fluorescence peak is positively correlated with the ATPIN5-GFP yield, Figure 3.5 and 3.6 and proved that the highest yield was solubilized by Fos choline-12, followed by DDM/CHS (Figure 3.6).

a.

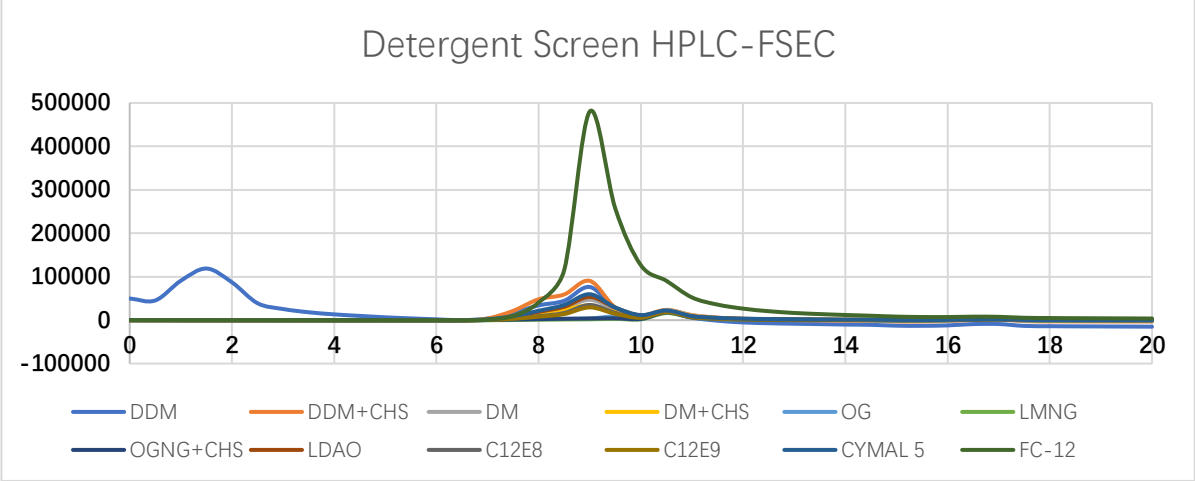

b.

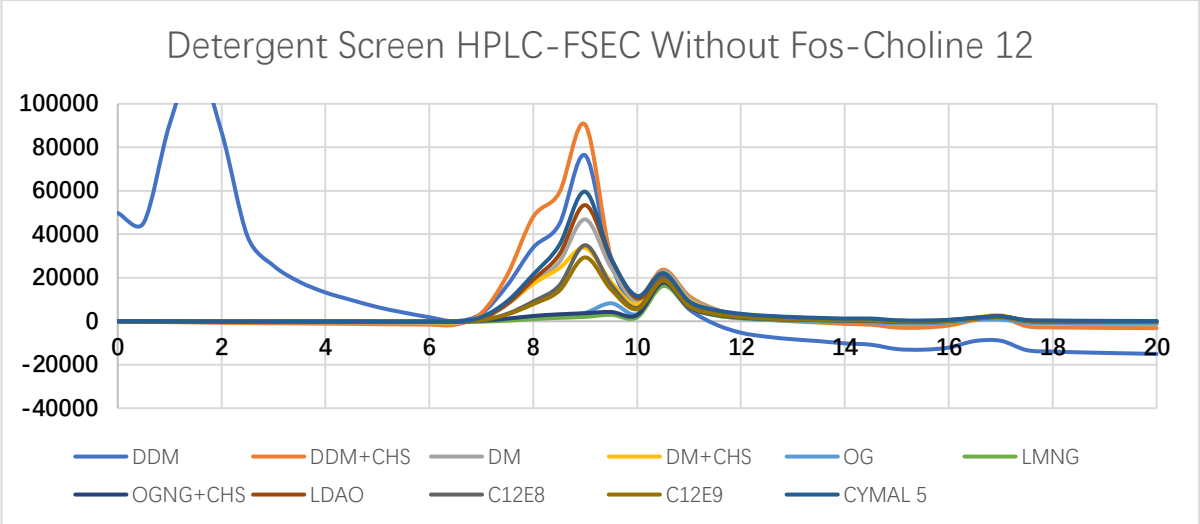

Figure 3.6 Optimizing detergent for TALON column purification, HPLC-FSEC results.

ATPIN5-GFP solubilized into 12 detergents and lipids and purified by TALON resin, 10 µlof each sample were loaded into HPLC for HPLC_FSEC data collection.

X axis: GFP RFU, Y axis: elution volume.

a, HPLC-FSEC data of 12 detergent solubilized ATPIN5-GFP.

b, HPLC-FSEC data rescaled without Fos Choline-12.

3.6 PIN protein purification buffer and extra lipid screening

The extraction conditions for ATPIN5-GFP TALON column purification were screened with different buffers and lipid combinations as follows; a 96 well filter plate was pre-packed with 50µl TALON resin. Each well was washed and equilibrated by the series of testing buffers with different lipids combinations (ref to Table 2.5).

Three ionic strengths were selected to test since ionic strength is important in controlling the charge screening in solutions and thus might affect formation of micelle and solubilization (Stigter et al., 1991). All standard buffers for protein purification were tested: MES, HEPES and Tris. Another important parameter for molecular interactions in solution is pH thus a range of pHs centered around physiological were asseyed. This as shown in Table 2.5 was combined with variation in added lipids. A critical step in any in vitro analysis of membrane proteins is the solubilization of the membrane in an active form to obtain an aqueous solution containing the membrane protein complexed with detergents and lipids in a form suitable for purification and further analysis (Duquesne and Sturgis, 2010).

The AtPIN5:GFP fusion protein buffer and lipids screening method is described in chapter 2.7. 96 elution samples were collected, 10 µl of each eluate was kept on ice for 10 minutes and another 10 µl was heated at 40 C for 10 minutes to give a heat treatment to test for protein thermal stability. Both samples were run on SDS-PAGE, using in-gel fluorescence as a measure of protein yield and integrity.

Unheated samples in Figure 4.3 Tris buffer (pH 8) with 500 mM NaCl (white box) were also run on HPLC to collect FSEC data (Figure 3.7b). The HPLC-FSEC profile double assessed AtPIN5:GFP yield and also quantified any free GFP. E.coli lipids and liver lipids showed high yield of AtPIN5:GFP (Figure 3.7b 8.5ml), however, they also had big free GFP peaks (Figure 3.7b 10.5ml) which suggested these conditions were not suitable to stabilize protein for further purification.Tris Buffer (pH 8.0) with 500mM NaCl plus DDM/CHS (10:1) proved the most promising set of conditions for stability as shown by less change in the

in gel fluorescence intensity and less free GFP(Figure 3.7). These will be adopted for further experimental optimisations.

a.

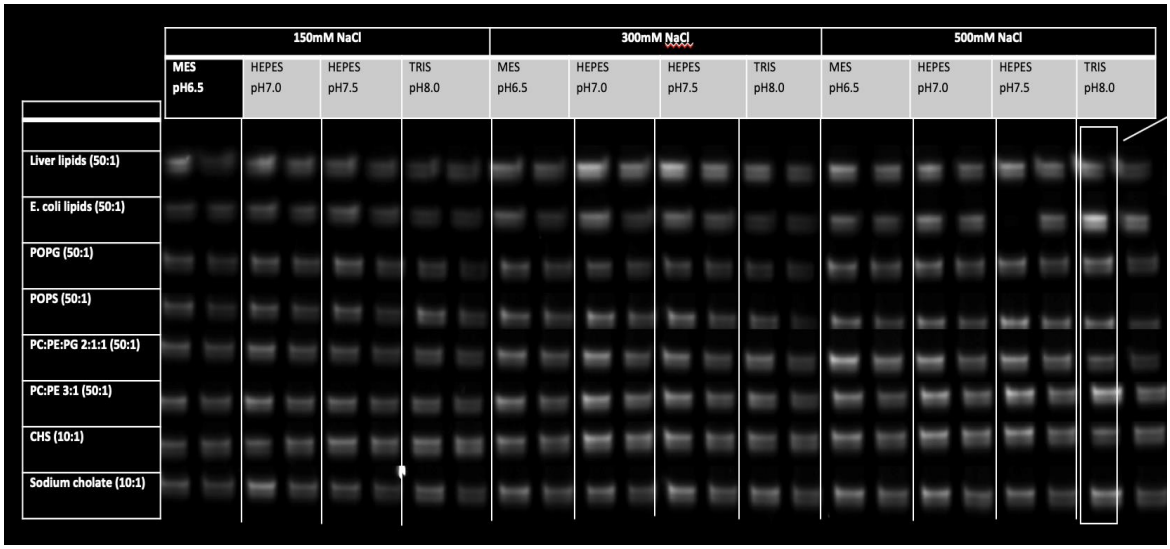

b.

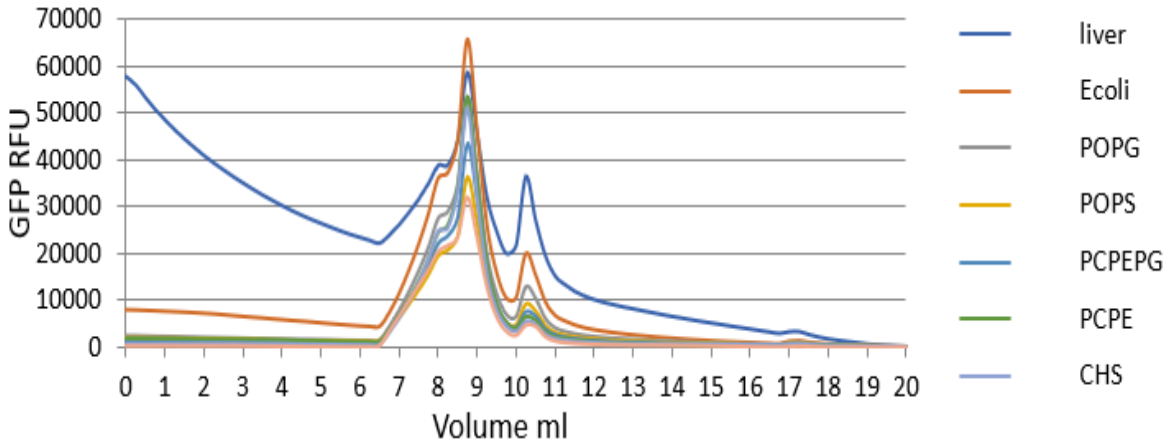

Figure 3.7 Optimizing buffer and lipids conditions for TALON column protein purification and protein stability. SDS-PAGE in gel fluorescence and HPLC-FSEC.

a. In-gel fluorescence photo was taken under same setting and all bands were aligned in one photo. In each condition, the left side column was TALON column elution kept on ice, the right side protein bands in each column were same heated at 40C for 10 min to give a heat treatment before running on the gel.

b. HPLC-FSEC profile of samples in figure 3.7 white box.

3.7 PIN protein purification based on antibody affinity chromatography systems

The solubilized protein needs affinity purification for further crystallization and biochemistry assays. M2 anti-FLAG resin was chosen because it is an easy and quick method to yield high purity and native proteins under mild conditions. The M2 Anti-FLAG column purification process was developed as follows: TLB was added to cell pellets, 1g pellet for 5ml TLB. This extract was sonicated on ice for 20 seconds repeated three times with 10 seconds gap between each repeat. Samples were incubated in the cold room for 10 minutes and sonication process repeated, before samples were centrifuged at 6,000 RCF for 10 minutes. The supernatant was collected and centrifugated at 180,000 RCF for 90 minutes, the new supernatant was discarded and membrane was collected. The membrane was homogenised into THB, 1g membrane with 5ml THB, 2% DDM/ 0.2% CHS and incubated more than 1 hour, before being centrifuged for 45 minutes to collect supernatant. GFP fluorescence was read and AtPIN5:GFP fusion protein yield calculated. The supernatant from last step was mixed with 2.5ml M2 Anti-FLAG beads and incubated for 3 hours after which the mixture was loaded on an Econo-Column. Waste flow was collected, the column washed with 25ml washing buffer and flow through was collected before the protein was eluted with 10ml THB + 0.1 mg/ml 3x FLAG Peptide, collecting 1ml fractions. The collected samples were analysed by GFP fluoresce screening and SDS-PAGE. 400 µl of elution was loaded into AKTA purifier, and FPLC-SEC and FPLC-FSEC data were collected (Figure 3.8).

a.

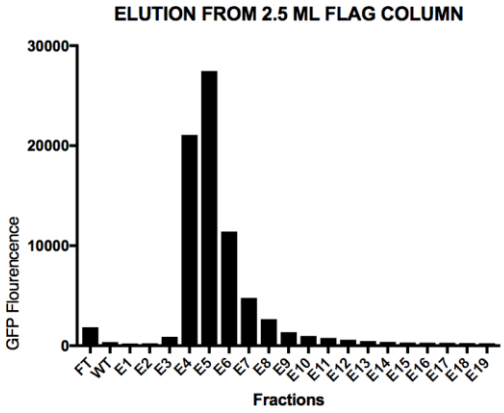

b.

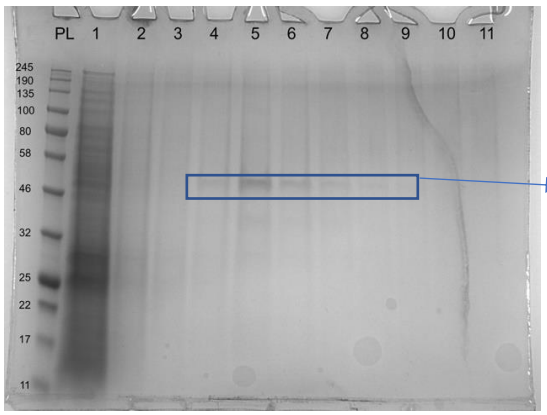

c.

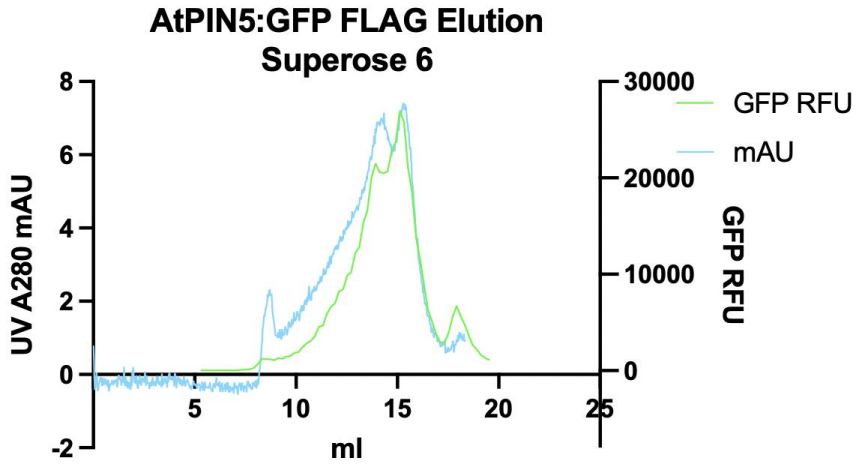

Figure 3.8 Sample collections from 2.5ml M2 Anti-FLAG beads AtPIN5:GFP purification process

All samples from AtPIN5:GFP M2 Anti-FLAG column purification were quantified using GFP fluorescence intensity by a SpectraMax M2e Microplate Reader and run on SDS-PAGE. 500µlpeak fraction of the FLAG elution was loaded onto an AKTA Superose 6 column for FPLC-SEC and FPLC-FSEC profile.

a. Samples of AtPIN5:GFP purification process, measured from each 1 ml fraction by GFP fluorescence. FT: Flow through, WT: Wash through, E1-E19 (Elution fraction 1 to fraction 19)

b. SDS-PAGE Coomassie stain of elution protein from 2.5ml M2 Anti-FLAG column, PL: Protein Ladder, 1: Flow Through; 2: Wash Through; 3- 11: Elution fractions 3- 11.

c. FPLC-SEC & FSEC profile of elution protein from 2.5ml M2 Anti-FLAG column

Single clear bands from SDS-PAGE (Fig 3.8, fraction 5) were cut and sent to proteomics for analysis to confirm the protein sequence. The peptide sequence results showed 33% covering of the full-length fusion protein. Importantly, the N-terminus is intact and the fusion protein was purified by C-terminal FLAG tag proving that the AtPIN5:GFP fusion protein is complete and intact (Figure 3.9).

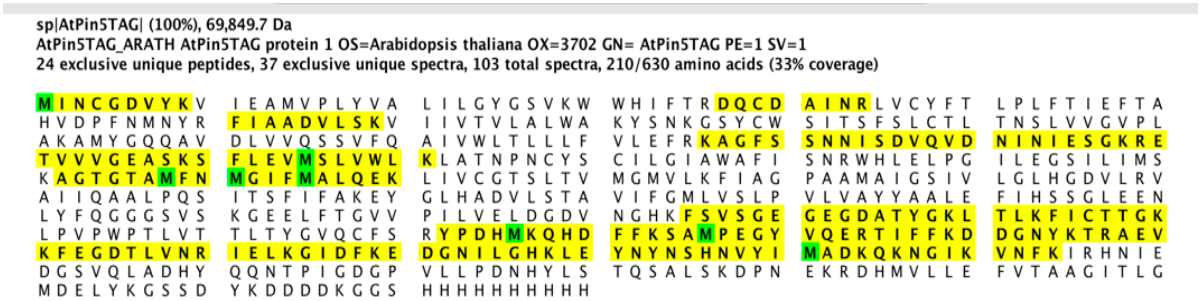

Figure 3.9 Proteomics Analysis results

Proteome Scaffold software was used to visualize proteomics results.
M marked in green was for methylation. Yellow highlight sequences were identified by Mass Spec, eGFP sequence start from G365.

High purity native AtPIN5:GFP fusion protein can be obtained by one step M2 anti-FLAG resin purification, and the FSEC results showed AtPN5:GFP fusion protein elution peak is around 15.5 ml in Superose 6 SEC column analysis. Because of high cost and low protein purification yield of FLAG resin (0.6mg protein yield per ml FLAG resin), scale up prep will need a higher yield and cheaper method for further structural studies. Immobilized metal affinity chromatography systems will be investigated for further purification.

3.8 PIN protein purification based on immobilized metal affinity chromatography system

3.8.1 AtPIN5:GFP purification based on TALON beads

The TALON purification uses the principle of binding of the polyhistidine tag to metal cations. However, in contrast to nickel based resins it uses cobalt. It is often better because TALON cobalt resin is particularly effective for MP purification and TALON has a lower affinity for polyhistidine and less non-specific binding compared to Ni-NTA; thus, the protein can be eluted at lower imidazole concentrations.
The general purification protocol is described in chapter 2.4.2.

3.8.1.1 Testing TCEP to optimize ATPIN5-GFP purification on TALON resin

When a protein contains cysteine residues, oxidation and intermolecular disulphide bridges could become a problem and cause protein aggregation. To prevent this, TCEP reducing agent was added in the lysis buffer. The samples from TALON column elution were collected and loaded into an AKTA Purifier, to collect FPLC-SEC and FPLC-FSEC data.

As SDS-PAGE in-gel fluorescence screening (Figure 3.10b fraction) shows, the AtPIN5:GFP protein is not more stable with TCEP in the lysis buffer, based on FPLC A280 and FSEC graphic (Figure 3.10a). Most of the protein purified was free GFP (Figure 3.11a fraction 5 compare with fraction 6). The gel showed a single band rather than double band with TCEP present. It appeared that the AtPIN5 fusion protein lost the GFP-FLAG-HIS tag during the overnight binding with TALON resin in both the reduced and non-reduced samples. In conclusion, further AtPIN5-GFP TALON binding time assays were run in the presence of TCEP.

a.

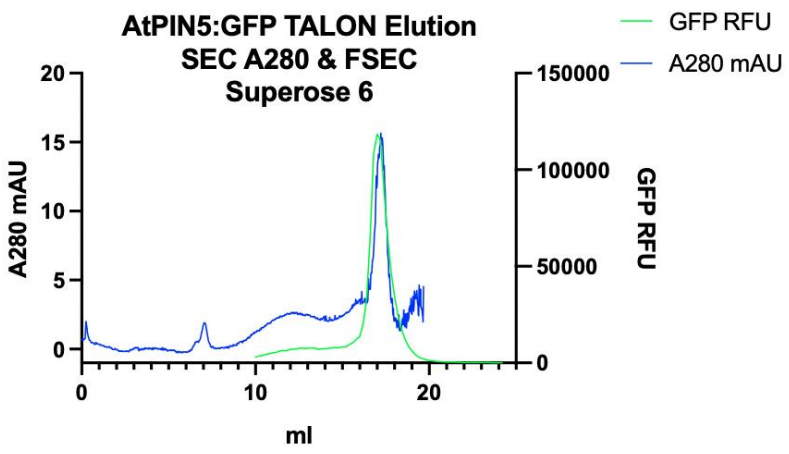

b.

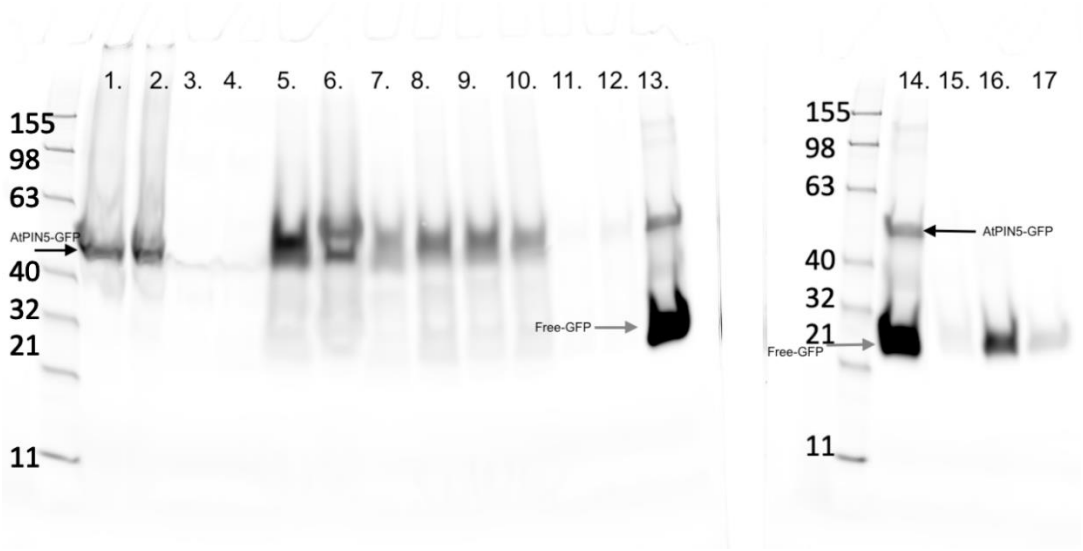

Figure 3.10 TCEP reducing agent assay for TALON purification.

AtPIN5-GFP: 55 kDa, black arrow; Free GFP: 28 kDa, grey arrow.

a. AKTA FPLC elution monitored by UV A280 and GFP FSEC traces.

b. SDS-PAGE in gel fluorescence, 24 fractions as follows: 1. +TCEP cell lysis, 2. -TCEP cell lysis, 3.+TCEP ultracentrifuge supernatant, 4. -TCEP ultracentrifuge supernatant, 5 +TCEP rolling with 1% DDM/CHS, 6. -TCEP rolling with 1% DDM/CHS, 7. +TCEP 2nd ultracentrifuge supernatant, 8. -TCEP 2nd ultracentrifuge supernatant, 9. +TCEP TALON unbinding flow through, 10 -TCEP TALON unbinding flow through, 11 +TCEP TALON washing through, 12 -TCEP TALON washing through, 13. +TCEP TALON Elution; 14. -TCEP TALON Elution, 15. AKTA Peak 11ml; 16: AKTA Peak 15ml; 17: AKTA Peak 17.5ml, 18: AKTA Peak 18.5ml.

3.8.1.2 Testing binding time on TALON resin

Protein solubilised and cleared (refer to 3.8.1.1), was separated into three tubes equally and binding with TALON tested for three different time periods (1h, 2h, 3h). Each TALON column was washed by 20 column volumes TWB and eluted by 5 column volumes of TEB. Three TALON column flow through fractions, washing through and elution were collected, and loaded on SDS-PAGE with in gel fluorescence screening. As Figure 3.11 shows, more free-GFP (28KDa) was generated when binding time increased. Further TALON purification will be limited to let protein bind for 2 hours, because the ratio of protein yield to tag loss seems the best (Figure 3.11).

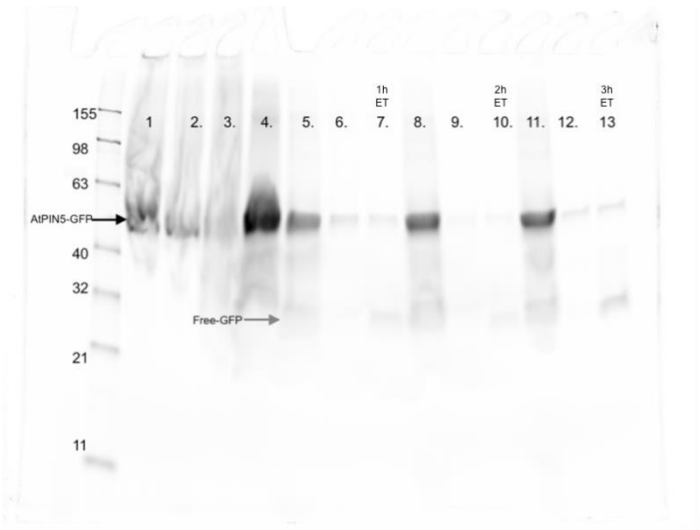

Figure 3.11 Optimizing TALON column purification protein binding time.

SDS-PAGE in gel fluorescence. AtPIN5-GFP: 55 kDa, black arrow; Free GFP: 28 kDa, gray arrow.

13 fractions loaded as follows, 1: Before cell lysis, 2: After cell lysis, 3: DDM sample mixture, 4: Solubilized AtPIN5 Ultracentrifugation supernatant, 5: unbinding flow through from 1 hour TALON column binding, 6: Washing through from 1 hour TALON column binding, 7: Elution from 1 hour TALON column binding, 8: unbinding flow through from 2 hours TALON column binding, 9: Washing through from 2 hours TALON column binding, 10: Elution from 2 hours TALON column binding, 11: unbinding flow through from 3 hours TALON column binding,12: Washing through from 3 hours TALON column binding, 13: Elution from 3 hours TALON column binding.

3.8.1.3 Rescreening buffer on TALON resin

Although buffer and lipids screening (as shown in section 4.2) showed that Tris buffer at pH8 with DDM/CHS detergent lipids provided the most stable conditions for AtPIN5 fusion protein, however, it also generated a lot of free-GFP and the binding efficiency was not high enough to trap most of the AtPIN5-GFP protein.

Buffer conditions for high protein binding with TALON column were tested (buffer composition ref to 2.4 Table 2.1-2.4), as gel Coomassie stain and in-gel fluorescence (Figure 3.12a, 3.12b) showed, phosphate buffer had highest clean yield with very low free-GFP generated in the TALON column purification.

Further TALON column AtPIN5 purification will only use phosphate buffer.

a. b.

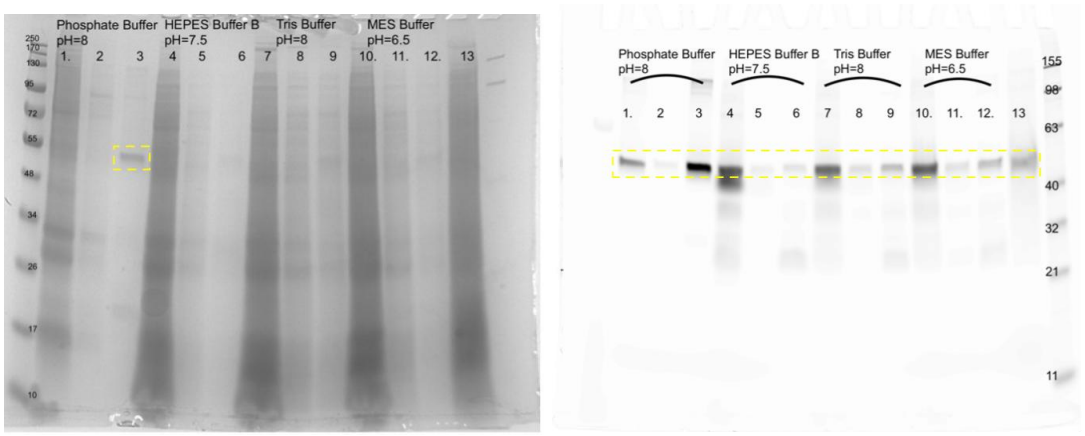

Figure 3.12 Optimizing buffer conditions for TALON column ATPIN5:GFP purification yields.

SDS-PAGE gel 13 loading fractions, yellow boxes: AtPIN5:GFP fusion protein. 1: Phosphate buffer condition TALON unbinding flow through, 2: Phosphate buffer condition TALON washing through, 3: Phosphate buffer condition TALON elution, 4: HEPES buffer condition TALON unbinding flow through, 5: HEPES buffer condition TALON washing through, 6: HEPES buffer condition, 7: Tris buffer condition TALON unbinding flow through, 8: Tris buffer condition TALON washing through, 9: Tris buffer condition TALON elution, 10: MES buffer condition TALON unbinding flow through, 11: MES buffer condition TALON washing through, 12: MES buffer condition TALON elution, 13 Cell lysis with DDM control.

a. SDS-PAGE gel Coomassie Stain

b. SDS-PAGE gel in gel fluorescence

3.8.1.4 Comparison of AtPIN5:GFP purification efficiency between two TALON purification resins

Two bead sizes of TALON resin (TALON CellThru diameter 300-500μm, TALON metal affinity diameter 45-165um) were compared for ATPIN5-GFP protein purification efficiency. Large beads allow quick flow speed, which shorten the time of purification.

Both TALON resins were pre-packed 1ml into specific column. The TALON gravity flow resin protein purification protocol was same as described in section 3.8.1.1.

The protein purification protocol was as above, except that after the 1% DDM/ 0.1% CHS was added and the sample incubated at 4℃ for 2 hours, it was centrifuged by high-speed centrifuge with JLA 25.5 rotor at 10,000 RCF for 10 minutes. The supernatant was collected and loaded directly onto a TALON CellThru column for one hour or a standard TALON column of the same dimensions. Samples were compared using SDS-PAGE gel, in-gel fluorescence, and FSEC.

As gel Coomassie stain and in-gel fluorescence (Figure 3.13a, 3.13b) show, small beads TALON metal affinity resin binding efficiency is better. FPLC-FSEC (Figure 3.13c, 3.13d) shows there are two fluorescent peaks from both resins, peak at 13ml is AtPIN5:GFP and peak at 18ml is free GFP.

The TALON metal affinity elution has slightly larger aggregation peak then TALON CellThru elution, in the FSEC peaks, TALON metal affinity elution has larger peak width but 13 times more fluorescent intensity then TALON CellThru elution. The TALON metal affinity resin clearly obtained more yield than TALON CellThru at the expense of only slight worsening of quality. Further purifications will use TALON metal affinity resin.

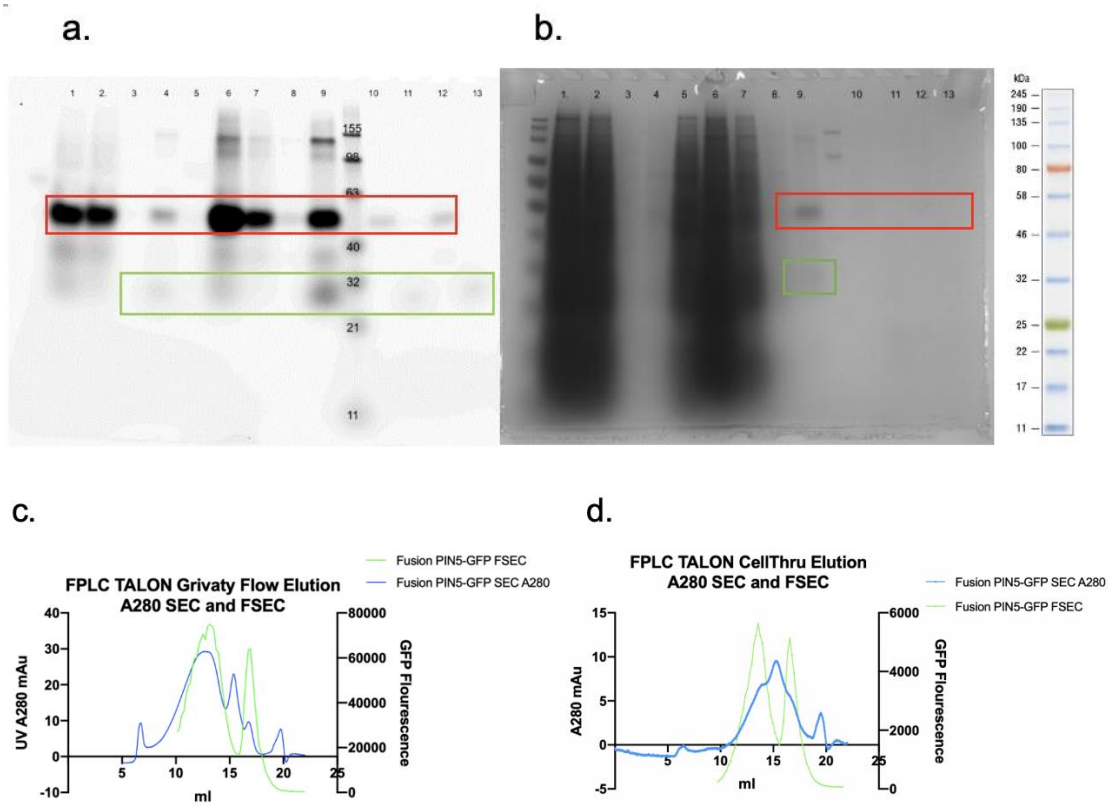

Figure 3.13 Comparing TALON gravity flow resin with TALON CellThru resin AtPIN5 protein purification efficiency.

SDS-PAGE 13 fractions loading, Red boxes AtPIN5:GFP, Green boxes free GFP, 1: Protein solubilized into DDM/CHS ultracentrifugation supernatant for CellThru purification, 2: CellThru column flow through, 3 CellThru column washing through, 4 CellThru column elution, 5: Membrane prep 1st ultracentrifugation supernatant, 6: Protein solubilized into DDM/CHS ultracentrifugation supernatant for gravity flow TALON purification, 7: TALON flow through, 8: TALON washing through, 9 TALON elution, 10 CellThru elution FPLC-SEC peak fraction 1, 11: CellThru elution FPLC-FSEC peak fraction 2, 12: TALON elution FPLC-FSEC peak fraction 1, 13: TALON elution FPLC-SEC peak fraction 2

a. In gel fluorescence

b. Coomassie staining

c. FPLC elution of TALON CellThru elution A280 SEC and FSEC

d. FPLC elution of TALON gravity flow elution A280 SEC and FSEC

3.8.2 AtPIN5:GFP Purification by Nickel IMAC Resin

TALON is a good IMAC resin for PIN purification, however, the protein binding efficiency is always affected by choice of detergent and reducing agent. Nickel resin has relatively stronger purification reagent tolerance compare with TALON resin, thus, to obtain better protein product, nickel resin was tested for PIN protein purification.

3.8.2.1 AtPIN5:GFP Purification by Nickel IMAC Resin in Small Scale

The nickel IMAC column purification process was as follows: AtPIN5:GFP cell membranes (from section 2.1.6) were collected and homogenised in PLB, 1g membrane with 5ml PLB and 10% DDM/ 1%CHS mixture added to give a final 1%DDM/0.1%CHS. After incubation at 4℃ for 2 hours, samples were centrifuged in 45Ti rotor for 60 min at 160,000x g and the supernatant was filtered by 0.45um PVDF filter.

25μl His resin was loaded onto mini spin columns and washed by PBS, then 2ml PCB was added to equilibrate the beads, after PCB flow out, the flow was stopped and 1ml filtered sample loaded into the spin column, covered and well mixed with the resin with sample by incubation into clod room for 1h. The flow through was collected, and the column washed by 2ml PWB, 1ml each washing, the wash through was collected. The samples was eluted with PEB, 500μl per elution fraction, with 5 fractions collected. All samples were run on SDS-PAGE and read using in-gel fluorescence (Figure. 3.14).

AtPIN5:GFP purification process on Ni^{2+} did not generated as much free GFP as TALON, although some optimization is required in further purification.

a. b.

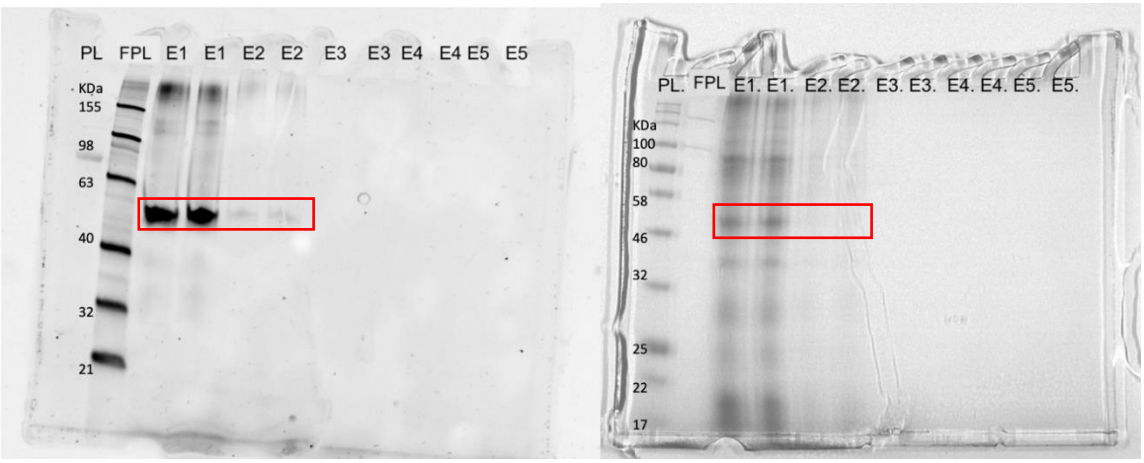

Figure 3.14 Histidine-tagged protein purification (HP) column elution

20µl sample+10µl SDS-PAGE buffer, Fraction: PL: Protein Ladder, FPL: Fluorescent protein ladder, E1-E5: Elution fraction collection from fractions 1 to 5. Red Boxes: AtPIN5:GFP.

a. In gel fluorescence

b. Coomassie of PIN5 elution

3.8.2.2 AtPIN5:GFP Purification by Nickel IMAC Resin in Large Scale

AtPIN5:GFP cell membranes (from 2.1.6) were collected and homogenised in PCB, 1g membrane with 5ml THB, 5mM TCEP and 10% DDM/ 1%CHS mixture added to give a final 1%DDM/ 0.1%CHS. After incubation at 4℃ for 2 hours, samples were centrifuged in 45Ti rotor for 60 min at 160,000x g and the supernatant was filtered through a 0.45µm PVDF filter. NaCl was added from a 5 M stock to give a final NaCl concentration to 500 mM, and the sample was loaded onto a glass column pre-packed with nickel resin (1 ml nickel resin for 1 L cell culture extraction). A peristaltic pump was connected to the bottom of the column, flow speed at 1 ml/min, and samples circulated for 2 hours. The IMAC column was washed by 10 column volumes PWB and eluted by 5 column volumes PEB. The IMAC column flow through, wash through and elution fractions were loaded and run on SDS-PAGE. 400µl IMAC elution was loaded onto an AKTA purifier Superose 6 column for FPLC-SEC and FPLC-FSEC (Fig. 3.15).

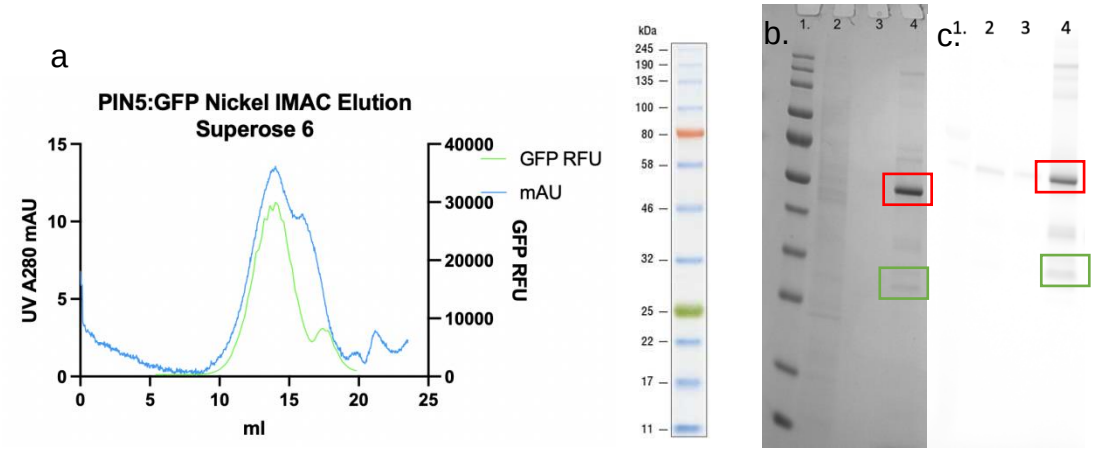

Figure 3.15 Elution of protein from nickel IMAC column.

AtPIN5:GFP purification by nickel IMAC column. 400µlIMAC elution was loaded onto Superose 6 for FPLC-SEC and FSEC profiles, SDS-PAGE 4 loading fractions, 1: protein ladder, 2: column flow through, 3: column washing through, 4: column elution

Red boxes: AtPIN5:GFP Green boxes: Free GFP

a. FPLC-SEC & FSEC profile of elution protein from nickel IMAC column

b. Coomassie staining

c. In gel fluorescence

The nickel IMAC elution FSEC profile showed sharp RFU and UV A280 absorption peaks at 14ml of Superose 6 column elution, the SDS-PAGE showed single clear band and very less free GFP generated during nickel IMAC AtPIN5:GFP purification, which was suitable for further assays.

3.9 TEV Protease Cleavage and Reverse IMAC results

The C-terminal GFP-FLAG-His tags which have been used for purification need to be removed before crystallization trails.

To ATPIN5:GFP protein collected from TALON column elution, and peak fractions from FPLC was added TEV-His protease (preparation refer to 2.3.1) for incubation overnight. Fusion protein concentrations were measured by Nanodrop microvolume spectrophotometer before a mole equivalents of TEV-His protease was added and mixed and incubated at 4℃ for 16 hours. The products were cleaned by reverse IMAC, and the flow through was collected and concentrated by Viva spin 20 (100kDa). The concentrated sample was applied to FPLC-SEC and peak fractions were run on SDS-PAGE.

FPLC-SEC (Fig. 3.16a) and SDS-PAGE Coomassie stained fractions (Fig. 3.16b and c) show that TEV protease cleaved AtPIN5 from the fusion protein, AtPIN5:GFP fusion protein in SEC and FSEC profile was around 12.5 ml (Figure 3.16a, blue and green curve), after TEV protease cleavage, the AtPIN5 peak was shifted to 14.5 ml (Figure 3.16a, red curve), the free GFP with was around 17.5 ml which reflective in fusion protein UV A280 and FSEC curves (Figure 3.16a).

The peak at 15.5 ml between AtPIN5:GFP fusion protein peak and free GFP peak might be contamination aggregated charged peptide and showed in both fusion protein SEC profile and cleaved protein SEC profile, in SDS-PAGE, it was between cleaved AtPIN5 and free GFP (Figure 3.16a, Figure 3.16c red box). The FSEC fusion

Further TEV protease cleavage substance will only be used the FPLC-FSEC peak fractions (fractions from 11.5ml to 13.5ml) from TALON column elution, which will avoid contamination from the intact AtPIN5:GFP fusion protein pool.

a.

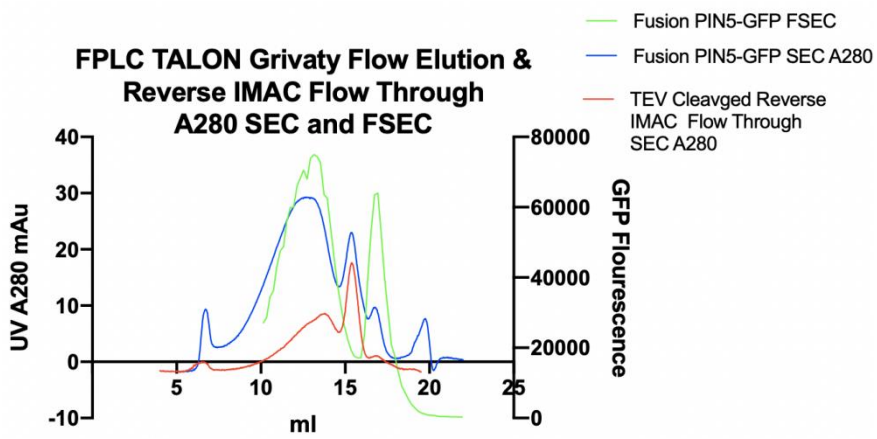

b.

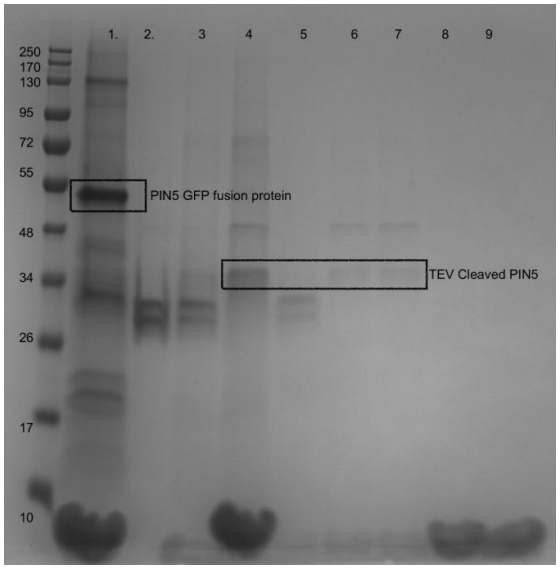

c.

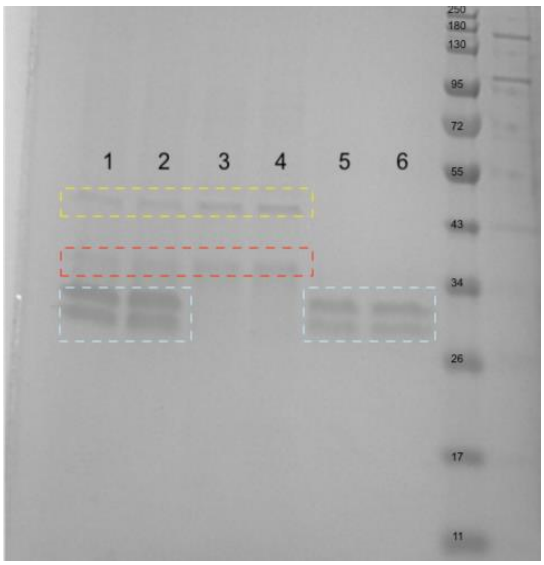

Figure 3.16 Testing TEV protease cleavage and reverse IMAC

a. FPLC TALON AtPIN5-GFP elution SEC-A280, FSEC and reverse IMAC flow through SEC-A280.

b. SDS-PAGE gel Coomassie Stain of TALON elution and TEV protease cleavage products. 1: Concentrated TALON elution, 2: TEV protease, 3: Reverse IMAC flow through, 4: Concentrated reverse IMAC flow through, 5: IMAC elution, 6& 7: reverse IMAC flow through applied to FPLC SEC, peak 1, 8& 9: reverse IMAC flow through FPLC peak 2.

c. FPLC fusion protein peak fraction TEV cleavage, SDS-PAGE gel Coomassie Stain, 6 fractions loading, 1& 2: Sample before reverse IMAC, 3& 4: Sample after reverse IMAC, 5& 6: IMAC elution. Yellow box: TEV protease contamination, red box: TEV cleaved AtPIN5, blue box: TEV protease and cleaved eGFP-FLAG-10x HIS tag.

3.10 Proteomics

Clear bands that were anticipated to be AtPIN5 (Fig 3.16b) at a size equivalent to around 35kDa, fractions 4, 6, 7) were cut out, combined and sent to proteomics for analysis. The results (Figure 3.17) showed only 5% of the AtPIN5 sequence was covered by the proteomics data, but fortunately, of the two peptides identified, one of 9 amino acids represented the N terminus of PIN5. Therefore, given that the presence of GFP during early purification shows that the C-terminus is intact, complete PIN5 has been expressed and purified.

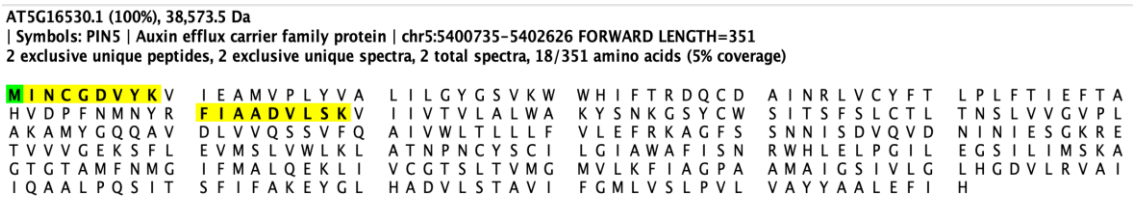

Figure 3.17 Proteomics Analysis results

Proteome Scaffold software was used to visualize proteomics results.

M marked in green was for methylation. Yellow highlight sequences were identified by Mass Spec

3.11 Optimized Protocol for Purifying AtPIN5:GFP

Table 3.1 Optimized conditions for AtPIN5-GFP TALON column purification

Cell density	2 million/ ml
Cell infection MOI	0.5
Cell pellet harvest time	48 hours
IMAC resin	Nickel resin
Cell Lysis buffer	Phosphate lysis buffer+1mM TCEP
Nickel Column buffer	Phosphate Column Buffer
Nickel Washing buffer	Phosphate Washing Buffer
Nickel Elution buffer	Phosphate Elution Buffer
AKTA Running buffer	Phosphate Elution Buffer -imidazole

Having evaluated all the variables tested above, the following describes the optimized protocol for AtPIN5 purification. Cell pellets were collected into 1 L centrifuge bottles by centrifugation at 10,000x g for 10 minutes, then washed in PBS and transferred into 50 ml centrifuge tubes to be re-pelleted at 5,000xg for 10 minutes at 4℃. The supernatant was discarded and the pellets were weighed. 5 ml PLB (Table 2.2) was used for 1 g of cells and incubate at 4℃ for 20 min. This extract was run through cell disrupter at 15 kPSI, and 10% DDM/0.5% CHS stock added to give a final 1%DDM/ 0.05%CHS. After incubation at 4℃ for 2 hours, samples are centrifuged in a 45Ti rotor for 60 min at 160,000x g and the supernatant was filtered at 0.45um. The sample was rolled with TALON beads (1 ml TALON resin for 1 L cell culture extraction) at 4℃ for 2 hours, then the mixture is loaded into a glass column, a peristaltic pump is connected to the bottom of the column, flow speed 0.5 ml/ min. The column was washed by 20 column volumes PWB (Table 2.2) and eluted by 5 column volumes of PEB (Table 2.2). Fractions are collected and analysed by SDS-PAGE, in-gel fluorescence, SEC A280 and FSEC (Figure 3.18a). Protein concentration from AKTA FPLC-SEC peak fractions were measured by Nanodrop. A mole equivalent of TEV protease is added and mixed with AtPIN5-GFP, incubated at 4℃ for 16 hours and analysed by SEC A280 and FSEC (Fig.

3.18b). Sample was loaded back to a fresh TALON column. Purified tag-free AtPIN5 was collected in the flow through.

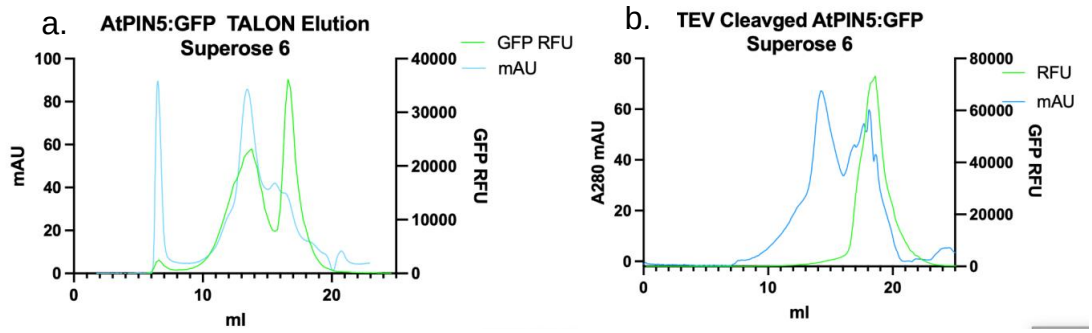

Figure 3.18 AtPIN5:GFP TALON purification, before and after TEV cleavage SEC and FSEC profile

AtPIN5:GFP was purified by TALON IMAC column, 500 µlTALON IMAC column elution was loaded onto Superose 6 for SEC & FSEC profile. TEV protease was added into TALON IMAC column elution, incubation in cold room overnight, 500 µlmixture sample was loaded onto Superose 6 for SEC & FSEC profile

a. SEC & FSEC profile of TALON IMAC column elution

b. SEC & FSEC profile of TALON IMAC column elution and TEV protease overnight incubation mixture

Ideally, the AtPIN5:GFP fusion SEC profile only has one or two peaks. In this experiment (Figure. 3.18a), the first peak at 6.5ml was aggregation, the second peak is at 13.5ml is AtPIN5:GFP fusion protein and the second at 17.5ml is free GFP. After TEV protease cleavage overnight (Figure. 3.18b), the SEC UV profile of the sample mixture ideally only has two peaks and FSEC only has one peak, the first peak at 14.5ml is AtPIN5 without GFP, the second peak at 17.5ml is the mixture of GFP and TEV protease. The only FSEC peak matched the 17.5ml GFP peak showing that the cleavage was complete.

Purified AtPIN5 samples were concentrated to 6 mg/ml in 25ul, and a Mosquito® crystal Nanolitre Protein Crystallization Robot was used to aliquot AtPIN5 to crystal screening plate MemGold, MemGold 2, MemMeso, MemStart+MemSys at 4℃. In conclusion AtPIN5 can be purified by IMAC to give a single peak in SEC. However, the protein band is not very clean in SDS-PAGE, especially after TEV cleavage, the protein tended to be unstable and did not crystallise in the crystallization screening. Other PINs will be used for crystallization study.

Chapter 4 Oryza sativa PIN8 (OsPIN8) expression and purification

The hydrophilic loop in PIN proteins is not conserved. As a flexible and disordered domain, the loop complicates protein crystallization. A bioinformatics search was done to select PIN variants with the shortest loop. Published works show that OsPIN8 is both a short loop PIN and is functional (Wang et al., 2009). The PIN protein sequence with the shortest central loop amongst all PIN proteins is OsPIN8 which has 15 amino acids (Figure. 4.1).
It was hyprothesised that OsPIN8 with this very short flexible domain would be an ideal subject for PIN protein crystallization.

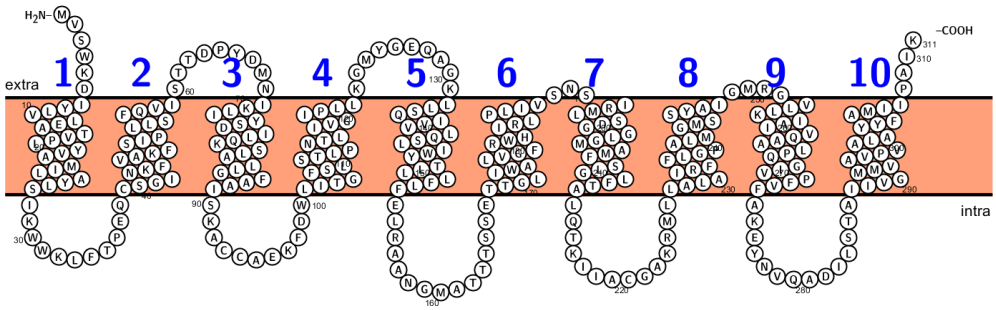

Figure 4.1 Predicted secondary structure of OsPIN8

The FASTA sequence of OsPIN8 was downloaded from UniProt and uploaded into Protter open-source tool (http://wlab.ethz.ch/protter/start/)(Omasits et al., 2014) to generate the OsPIN8 secondary structural prediction.

4.1 OsPIN8 Expression

OsPIN8 was codon-optimized for Sf9 cell line expression and an gBlock purchased from Integrated DNA Technologies. OsPIN8 transfer plasmids (Chapter 2 Table 2.8) were engineered to given a fusion protein as shown below in the Pop-In vector system. Recombinant baculovirus was generated by Chitra Joshi at the Membrane Protein Lab (MPL) in Diamond Light Source.

Three constructs listed below.
OsPIN8-TEV-GFP-His8 (referred to as OsPIN8:GFP)
OsPIN8-3C-FLAG-His8 ('3C' is human rhinovirus 3C protease cleavage site)
His8-3xFLAG-3C-OsPIN8.

a.

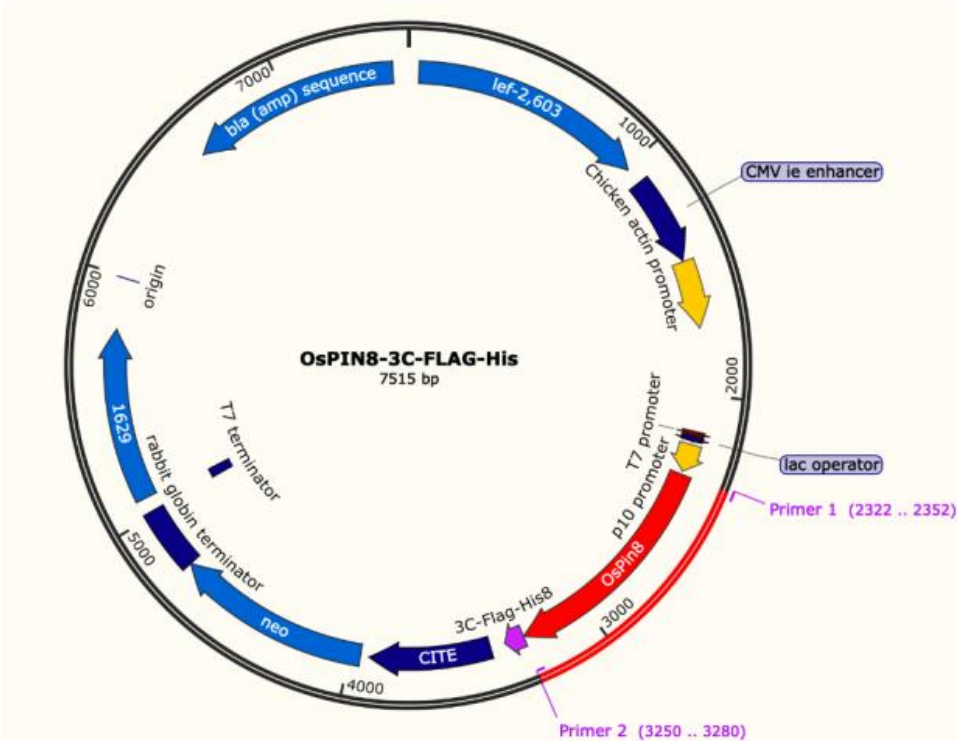

b.

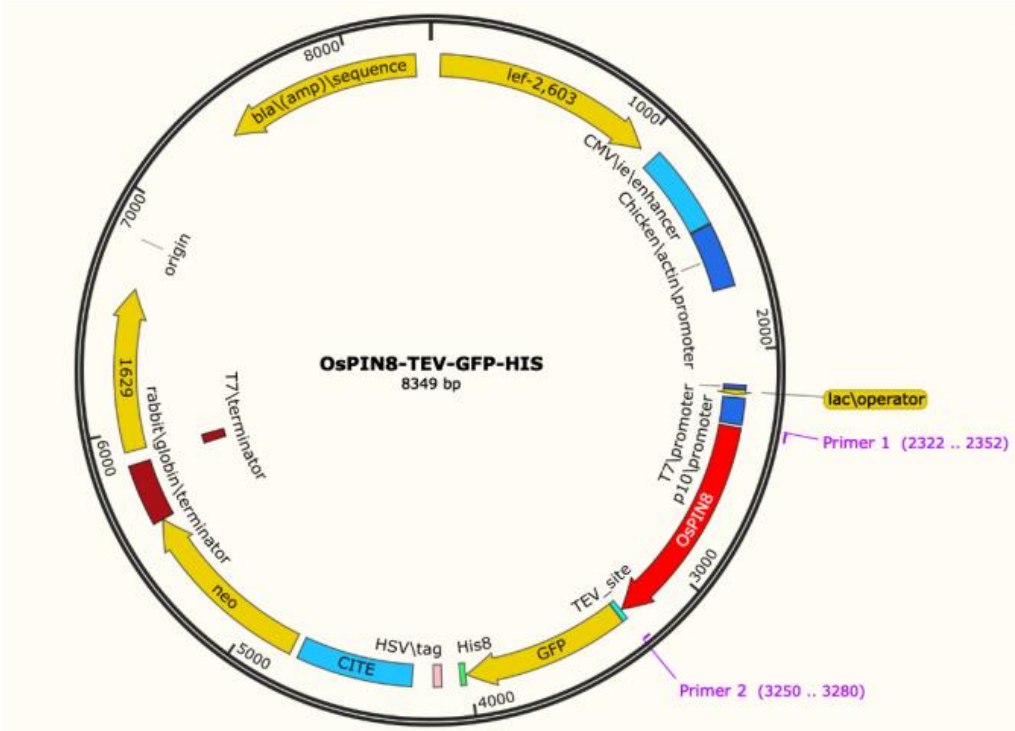

Figure 4.2 Example Plasmid Maps of C-terminal tagged OsPIN8 fusion protein

a. Plasmid map of OsPIN8-3C-FLAG-His8 fusion protein

b. Plasmid map of OsPIN8-TEV-eGFP-His8 fusion protein

4.2 OsPIN8 Purification Detergent Screening

The OsPIN8:GFP detergent screening method was the same as the one described for AtPIN5:GFP in section 3.1. The bands at 45kDa are the expected size of OsPIN8:GFP fusion protein.

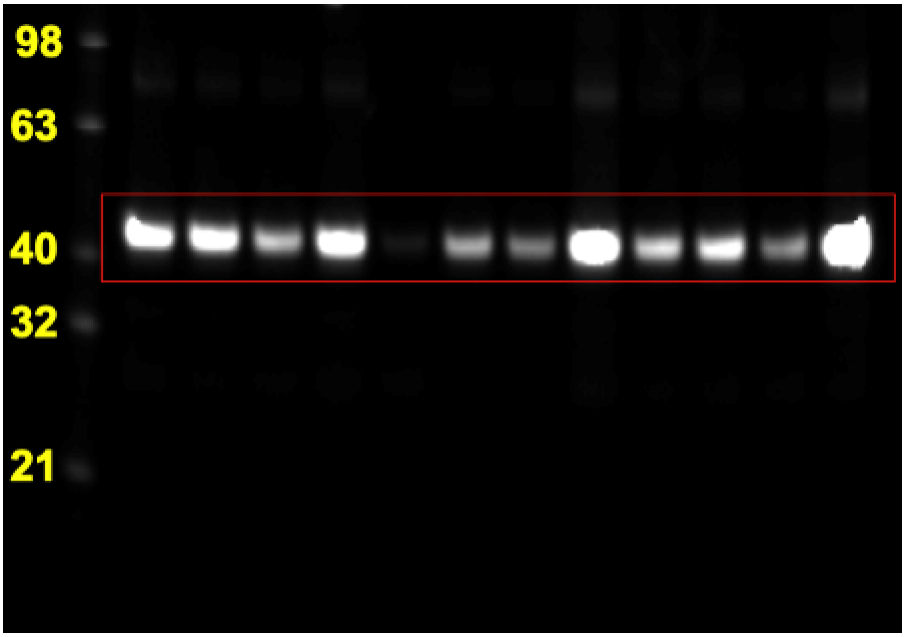

Figure 4.3 Optimizing detergents for TALON column protein purification of OsPIN8:GFP.

SDS-PAGE was run on detergent-solubilized samples and the gel visualized under UV light to monitor in-gel fluorescence from the GFP fusion protein; 1: 1%DDM solubilized sample, 2: 1%DDM/ 0.2%CHS solubilized sample, 3: 1%DM solubilized sample, 4 1%DM/0.2%CHS solubilized sample, 5: 1%OG solubilized sample, 6: 1%LMNG solubilized sample, 7: 1%OGNG/0.2%CHS solubilized sample, 8: 1%LDAO solubilized sample, 9: 1%C12E8 solubilized sample, 10: 1%C12E9 solubilized sample, 11: 1%Cymal-5 solubilized sample, 12: 1%Fos choline-12 solubilized sample. The OsPIN:GFP runs at an apparent molecular weight of 45 kDa (red box)

OsPIN8:GFP was solubilized into 12 different detergents and each was purified by TALON resin. All samples were loaded onto SDS-PAGE for in-gel fluorescent analysis (Figure 4.3), and the highest yield was obtained with Fos choline-12, although as discussed previously this is not a convenient detergent to work with. No crystal structure of a protein that was both purified and crystallized with this detergent has been reported in the Protein Data Bank.

DDM, DDM/CHS, DM/CHS and LDAO also showed relatively high solubility for OsPIN8:GFP, the rest of other detergents did not show high solubility. To confirm the solubility of OsPIN8:GFP, five detergent test samples (DDM/CHS, DM/CHS, LMNG, LDAO and C12E9) were loaded onto HPLC for HPLC-FSEC data collection. The GFP fluorescence peak is positively correlated with the OsPIN8:GFP yield, and the best selection was 1% DDM/0.2% CHS (Figure 4.3 and 4.4). Therefore, it was decided to use 1% DDM/0.2% CHS for all subsequent experiments.

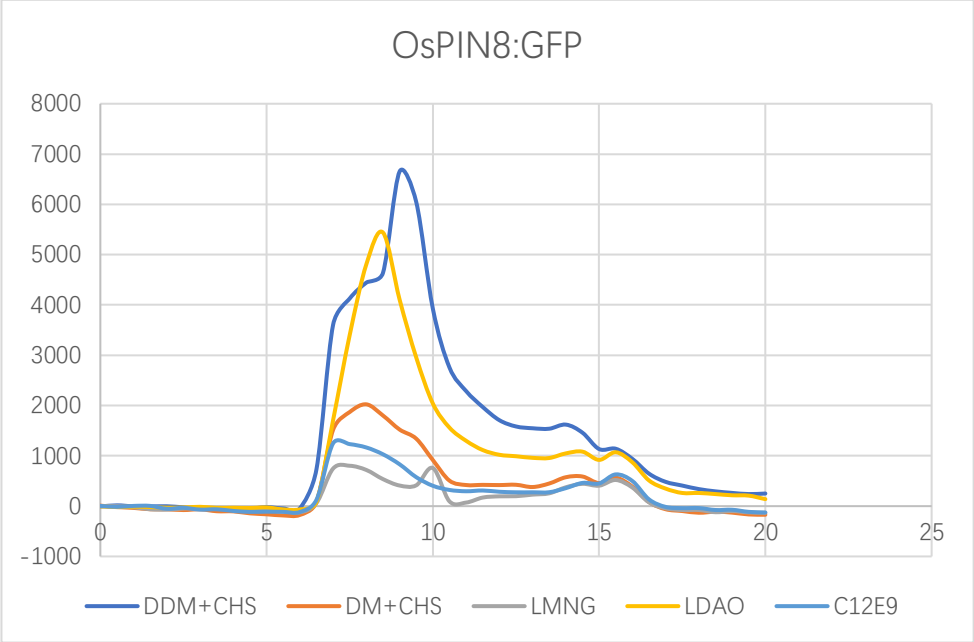

Figure 4.4 Optimizing detergent for TALON column purification of OsPIN8:GFP, HPLC-FSEC results.

OsPIN8:GFP solubilized into 5 detergents and purified by TALON resin. 10 µlof each sample were loaded into HPLC for HPLC-FSEC data collection.

4.3 OsPIN8 Lipids Screening

As for the test on AtPIN5 in section 4.1.2, OsPIN8 was solubilized into DDM/CHS. As a further optimisation test, lipid mixed with DDM combinations were tested for OsPIN8 purification optimization(Table 4.1).

Lipids	Lipids/ 10% DDM mixture, weight ratio
Cholesteryl hemisuccinate tris salt (CHS)	1:5
Soy Extract Polar Mixture (SB)	1:10
1,2-dioleoyl-sn-glycero-3-phospho-L-serine (DOPS)	1:10
1,2-dioleoyl-sn-glycero-3-phosphocholine (DOPC)	1:10
1,2-Dipalmitoyl-sn-glycero-3-phosphoglycerol (DPPG)	1:10
1,2-dioleoyl-sn-glycero-3-phosphoethanolamine (DOPE)	1:10

Table 4.1 Lipids/DDM compositions for OsPIN8 screening

Sf9 cells expressing OsPIN8:GFP were prepared using the following methods (see section 2.1.5). Cells were lysed in PBS (Table 2.2), the OsPIN8:GFP pellet was resuspended, 300 mg into 6ml PLB, and aliquoted into 6 bench-top ultracentrifuge tubes. Lipid/10% DDM stocks (Table 2.2) were added to give a final 1% DDM in all cases. Samples were incubated for 2 hours at 4℃ and centrifuged by benchtop ultracentrifugation at 200,000 RCF for 40 minutes at 4℃. Supernatant samples were collected, and 10µl of each was kept on ice for 10 minutes and another 10µl was heated at 40 C for 10 minutes before paired samples were run on SDS-PAGE, using in-gel fluorescence as a measure of protein yield and protein integrity. The results showed that 1% Soy Extract Polar Mixture (SEPM) with 10% DDM had the most promising yield (Figure 4.5).

PIN8:GFP stability was reviewed by comparing the intensity of the bands treated at 40℃ with those kept on ice. Again, DDM with soybean lipids gave the most promising results.

Because of gel tank connection problems, the middle part of protein fractions were little bit running faster.

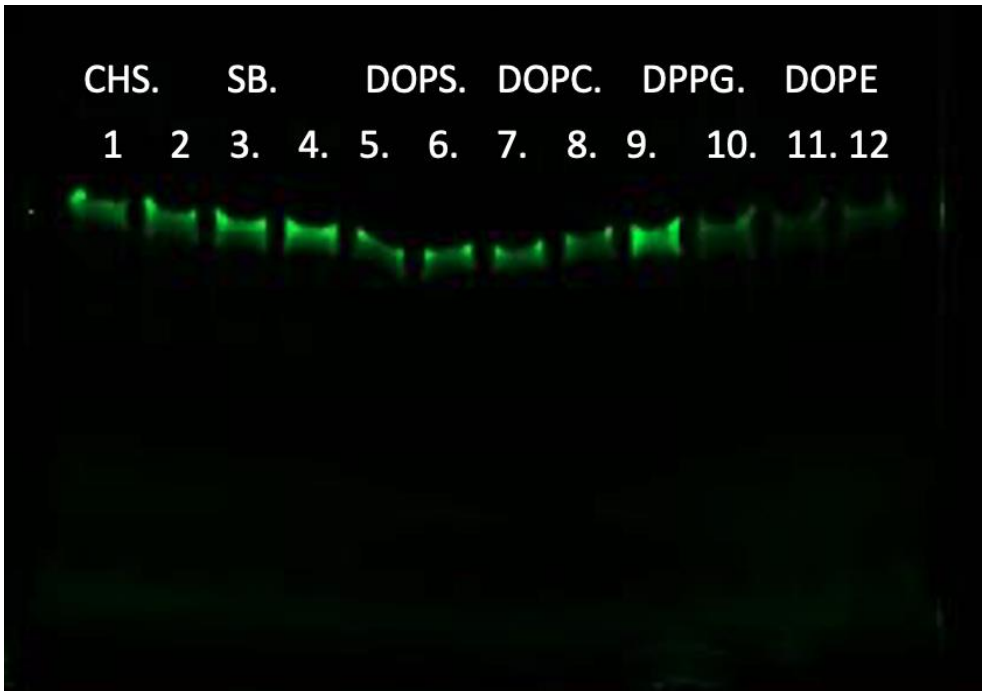

Figure 4.5 Optimizing lipid conditions for OsPIN8:GFP protein yield and stability. SDS-PAGE in-gel fluorescence.

In each DDM/Lipid condition, the left side column (odd numbers) was unheated, the right side (even numbers) protein was heated at 40℃ for 10 min before running on the gel.
Fractions: 1&2 1%DDM/0.2%CHS, 3&4 1%DDM/0.1%SB, 5&6 1%DDM/0.1%DOPS, 7&8 1%DDM/0.1%DOPC, 9&10 1%DDM/0.1%DPPG, 11&12 1%DDM/0.1DOPE

4.4 OsPIN8:GFP purification by TALON

OsPIN8:GFP cell membranes (prepared as in 2.1.5) were collected and homogenised in THB, 1g membrane with 5ml PLB and 10% DDM/ 1% SEPM added to give a final 1% DDM/ 0.1% SEPM. After incubation at 4℃ for 2 hours, samples were centrifuged in a 45Ti rotor for 60 min at 160,000 RCF and the supernatant was filtered by 0.45um PVDF filter. This was then loaded onto a glass column pre-packed with TALON resin (1 ml TALON resin for 1 L cell culture extraction). A peristaltic pump was connected from the bottom to the top of the column, flow speed at 0.5 ml/ min, and samples circulated overnight at 4℃. The column was washed by 20 column volumes PWB and eluted by 5 column volumes of PEB. Fractions were collected and analyzed by SEC using A280 and FSEC, SDS-PAGE, and in-gel fluorescence (Figure 4.6). Peak fractions of the TALON elution were combined and TEV protease added (molar ratio 1:1) for tag cleavage. After dialysis against PBS (pH=8, 0.025%DDM) overnight at 4℃, this mixture was loaded back to TALON column for reverse IMAC. Fractions of reverse IMAC flow through and elution were collected and analyzed by SDS-PAGE, in-gel fluorescence, SEC A280 and FSEC.
In SDS-PAGE Coomassie staining and in-gel fluorescence showed OsPIN8:GFP fusion protein gel bands at around 58 kDa, and from Superdex 200 increase, the OsPIN8:GFP UV A280 peak and FSEC peak were around 9 ml (Figure 4.6). After TEV protease cleavage, cleaved OsPIN8 is around 32 kDa and free GFP is around 28kDa in SDS-PAGE Coomassie staining. In the SEC profile, cleaved OsPIN8 peak shifted to 13.5ml, and the FSEC peak reflecting free GFP shifted to 15.5ml (Figure 4.7).

In the OsPIN8:GFP purification process, free GFP was observed, and the OsPIN8 also has became unstable after TEV cleavage. GFP appears to stabilize OsPIN8 fusion protein and increase its solubility. It was found that if the GFP is cleaved, the final product of OsPIN8 always had a low yield. Nevertheless, from this optimized purification protocol of OsPIN8:GFP, non-GFP tagged OsPIN8 recombinant protein was used for further studies.

a. b.

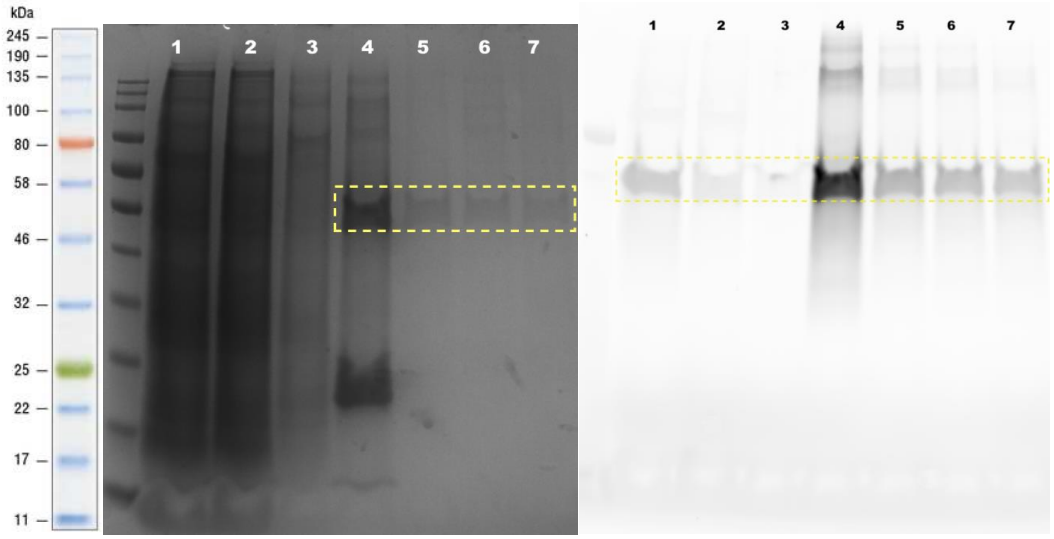

c.

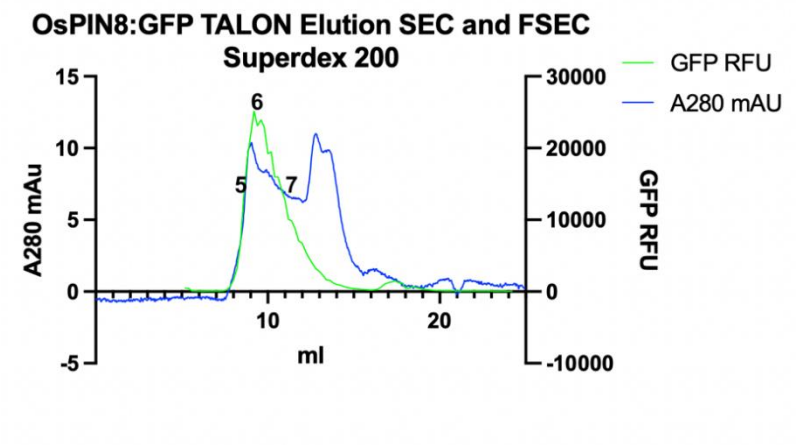

Figure 4.6 OsPIN8:GFP TALON and SEC purification process. SDS-PAGE and AKTA-FPLC profiles.

OsPIN8:GFP was purified by TALON column chromatography and the elution was loaded onto an AKTA-FPLC Superdex 200 column. Fractions from the whole process were collected and run on SDS-PAGE.

SDS-PAGE fractions: 1. OsPIN8:GFP pre-TALON column samples, 2. TALON column flow through, 3. TALON column wash through, 4. TALON column elution, 5-7. Fractions from AKTA-FPLC in figure 4.6 c.

Gel bands in yellow boxes are OsPIN8:GFP.

a. SDS-PAGE Coomassie Stain

b. SDS-PAGE in-gel fluorescence from gel in (a)

c. FPLC of TALON elution plotted for A280 SEC (blue) and FSEC (green)

a. b.

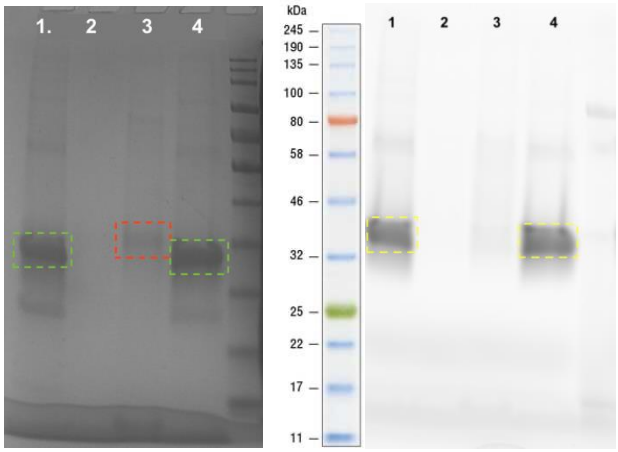

c.

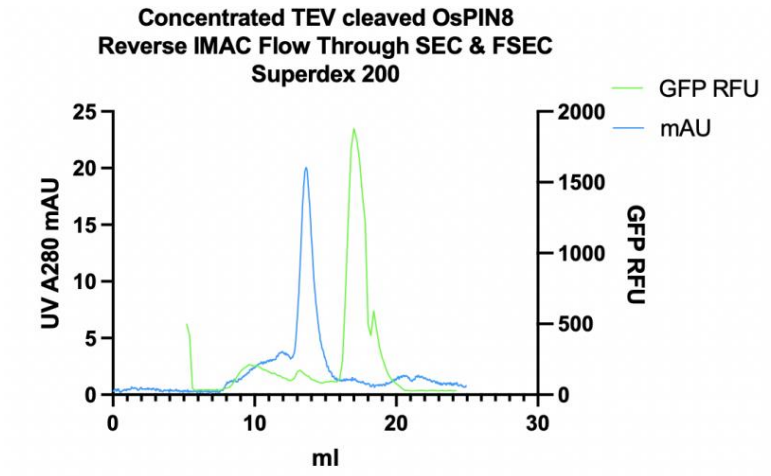

Figure 4.7 OsPIN8:GFP TALON elution followed by TEV cleavage and reverse IMAC. SDS-PAGE and AKTA-FPLC profile.

TEV protease was added to an OsPIN8:GFP TALON elution (molar ratio 1:1) for cleavage by rolling overnight at 4 C. The mix was loaded back to a fresh TALON column for reverse IMAC, and fractions of reverse IMAC flow through and elution were collected and run on SDS-PAGE, and AKTA-FPLC.

SDS-PAGE fractions: 1. OsPIN8:GFP TALON elution and TEV protease dialysis overnight, 2. Reverse IMAC flow through, 3. reverse IMAC flow through Concentrated by 100kDa concentrator, 4. IMAC column elution using HEPES elution buffer.

SDS-PAGE bands in green boxes are TEV protease, 32kDa SDS-PAGE band in red box is cleaved OsPIN8, SDS-PAGE bands in yellow boxes are cleaved free GFP with His-tag.

a. SDS-PAGE Coomassie Stain

b. SDS-PAGE in-gel fluorescence

c. FPLC elution profile of concentrated OsPIN8 reverse IMAC flow through. A280 SEC (blue) and FSEC (green)

4.5 Non-GFP tagged OsPIN8 Purification

In order to avoid the GFP effect on OsPIN8 solubility and stability after TEV cleavage, alternative OsPIN8 constructs were introduced for OsPIN8 studies. OsPIN8-3C-FLAG-His8 (in short OsPIN8-C), His8-3xFLAG-3C-OsPIN8 (in short N-OsPIN8) were expressed in Sf9 cells (Table 2.8).

4.5.1 N-OsPIN8 Buffer screening

N-OsPIN8 overexpressing Sf9 cells were lysed in PBS with 10mM NaCl. After lysis, 5M NaCl was added to give a final 150mM NaCl. N-OsPIN8 membrane was prepared (method refer to 2.1.6) and resuspended into eight different lysis buffers (1 ml each, Table 4.2) respectively, 20% DDM/10% SEPM stock was added to give a final 1% DDM/ 0.1% SEPM. Samples were incubated for 2 hours at 4 C and centrifuged by bench-top ultracentrifuge at 200,000 RCF for 45 minutes at 4 C, supernatant was collected and incubated with 50 µl TALON beads for 1 hour at 4C. The sample+TALON beads mixture was packed into mini-spin columns, washed by Washing buffer and eluted by elution buffer. Column elution samples were collected for SDS-PAGE analysis (Fig. 4.8).

Buffer base	pH	Lysis buffer	Washing buffer	Elution buffer
HEPES	7.0	50mM Buffer base, 150mM/ 500mM NaCl, Protease inhibitor, 5mM imidazole	Lysis buffer with 20mM imidazole	Lysis buffer with 250mM imidazole
HEPES	7.5			
Tris	7.5			
Phosphate	8.0			

Table 4.2 Buffers for N-OsPIN8 buffer screening

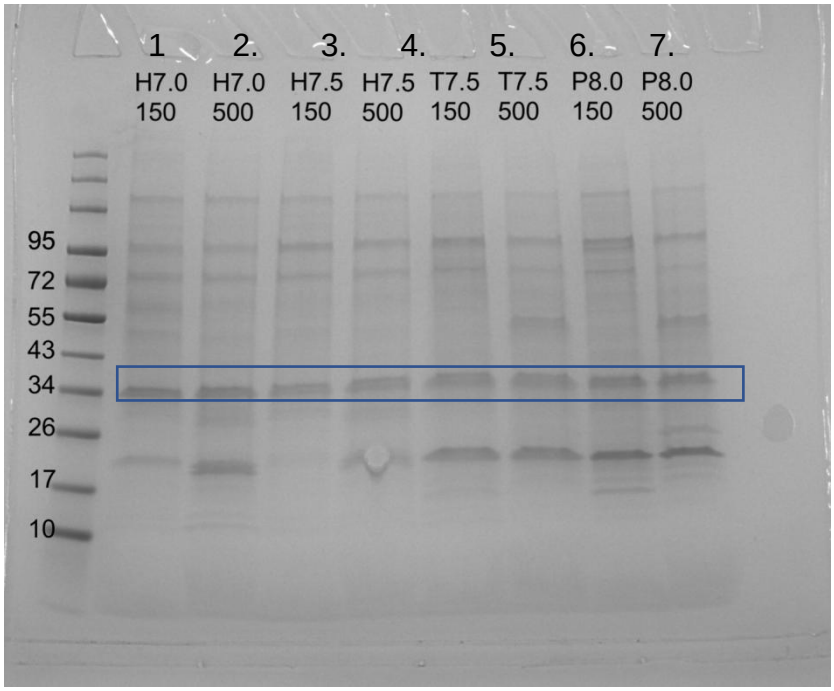

Figure 4.8 N-OsPIN8 TALON purification buffer screening SDS-PAGE

N-OsPIN8 cell membrane was resuspended into eight different buffers for TALON purification, TALON column elution samples were run SDS-PAGE. Gel bands in blue box are N-OsPIN8. SDS-PAGE fractions: 1. HEPES buffer 150mM NaCl pH 7.0, 2. HEPES buffer 500mM NaCl pH 7.0,

3. HEPES buffer 150mM NaCl pH 7.5, 4. HEPES buffer 500mM NaCl pH 7.5,

5. Tris buffer 150mM NaCl pH 7.5, 6. Tris buffer 500mM NaCl pH 7.5,

7. Phosphate buffer 150mM NaCl pH 8.0, 8. Phosphate buffer 500mM NaCl pH 8.0.

HEPES buffer with 150mM NaCl at pH 7.5 (lane 3 above) has no contaminating protein band running at around 20kDa on SDS-PAGE (Figure 4.8) and will be the buffer used for futher studies. However, the gel fractions showed many unspecific bands from TALON elution, so better methods are needed.

4.5.2 OsPIN8-C purification by TALON

OsPIN8-C overexpressed Sf9 cells were lysed in PBS with 10mM NaCl. After lysis, 5M NaCl was added to give a final 150mM NaCl. OsPIN8-C Sf9 membrane was prepared (method refer to 2.1.6) and resuspended into two different HEPES lysis buffers (1 ml each, Table 4.3, HEPES buffer) respectively, DDM/SEPM stock was added to give a final 1% DDM/ 0.1% SEPM. Samples were incubated for 2 hours at 4℃ and centrifuged by bench-top ultracentrifuge at 200,000 RCF for 45 minutes at 4℃, supernatant was collected and rolled with 50µl TALON beads for 1 hour. The mixture of sample+TALON beads was packed into mini-spin column and washed by Washing buffer 1, 2 and 3 respectively (Table 4.3) and eluted by elution buffer (Table 4.3). Column flow through, washes and elution samples were collected for SDS-PAGE and Western-Blot analysis (Figure 4.9).

Buffer base	pH	Lysis buffer	Washing buffer 1/ 2/ 3	Elution buffer
HEPES	7.5	50mM Buffer base, 150mM/ 500mM NaCl, 5% glycerol Protease inhibitor, 5mM imidazole	Lysis buffer with 10mM/ 20mM/ 30mM imidazole, 0.1%DDM	Lysis buffer with 250mM imidazole, 0.1%DDM

Table 4.3 HEPES buffer for OsPIN8-C TALON purification

a.

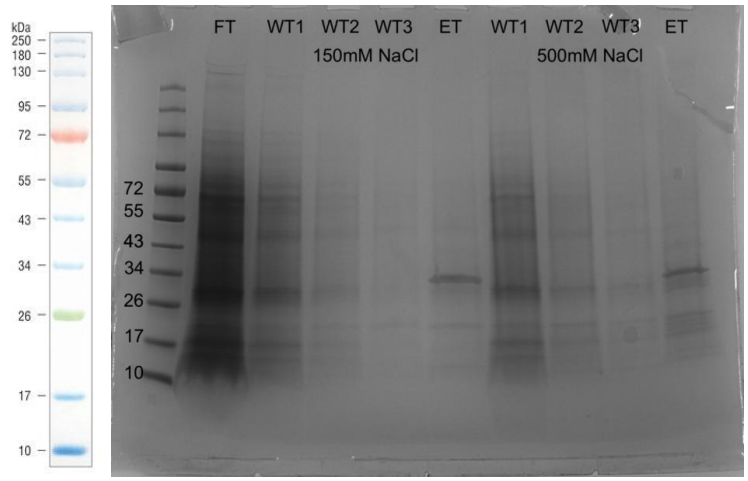

b. c.

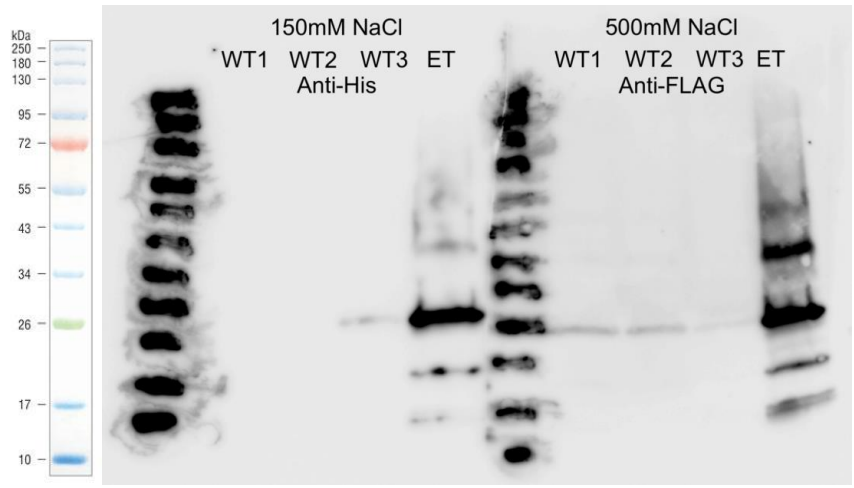

Figure 4.9 HEPES buffers screening for OsPIN8-C purification by TALON

OsPIN8-C purifications in low salt and high salt HEPES buffers were screened for TALON column purification, TALON column flow through: FT, washing through 1, 2, 3: WT1-3 and elution; ET were loaded and run SDS-PAGE, another gel with same sample loading was applied Western-Blot, low salt samples gel was blotted by Anti-PolyHistidine, high salt samples gel was blotted by Anti-FLAG.

a. SDS-PAGE Coomassie staining

b. Western-Blot Anti-PolyHistidine

c. Western-Blot Anti-FLAG

The results in Figure 4.9 showed that HEPES buffer 150mM NaCl at pH 7.5 has clearer OsPIN8-C elution and less degraded protein, therefore further OsPIN8-C studies will only use this buffer recipe.

Buffer base	pH	Lysis buffer	Washing buffer	Elution buffer	Gel-filtration buffer
HEPES	7.5	50mM Buffer base, 150mM NaCl, 5% glycerol, Protease inhibitor, 5mM imidazole	Lysis buffer with 25mM imidazole, 0.1%DDM	Lysis buffer with 250mM imidazole, 0.1%DDM	50mM Buffer base, 150mM NaCl, 5% glycerol, 0.025%DDM

Table 4.4 Optimized buffers for OsPIN8-C large scale purification

4.5.3 OsPIN8-C large scale purification by TALON and 3C cleavage

Sf9 cells expressing OsPIN8-C were lysed in 50mM HEPES with 10mM NaCl. After lysis, 5M NaCl was added to give a final 150mM NaCl. OsPIN8-C membrane was prepared (method refer to 2.1.6) and resuspended into two HEPES lysis buffers (Table 4.4), DDM/SEPM stock was added to give a final 1% DDM/ 0.1% SEPM. Sample was incubated for 2 hours at 4℃ and centrifuged by ultracentrifuge at 200,000 RCF for 1 hour at 4℃, supernatant was collected and rolled with TALON beads (1L cell culture for 1ml TALON beads) for 2 hours. The sample+beads mixture was packed into an Econo-column. Column was washed by Washing buffer and eluted by Elution buffer, with column flow through, washes and elution samples collected for SDS-PAGE (Figure 4.10a). The peak fraction elution sample was loaded into AKTA-FPLC Superdex 200 for analysis (Figure 4.10d), AKTA-FPLC fractions were collected for SDS-PAGE and Western-Blot analysis (Figure 4.10c and d). 50 µl OsPIN8-C from TALON elution was incubated with 3C protease (weight 1:1 ratio) overnight and run SDS-PAGE and Western-Blot (Figure 4.10).

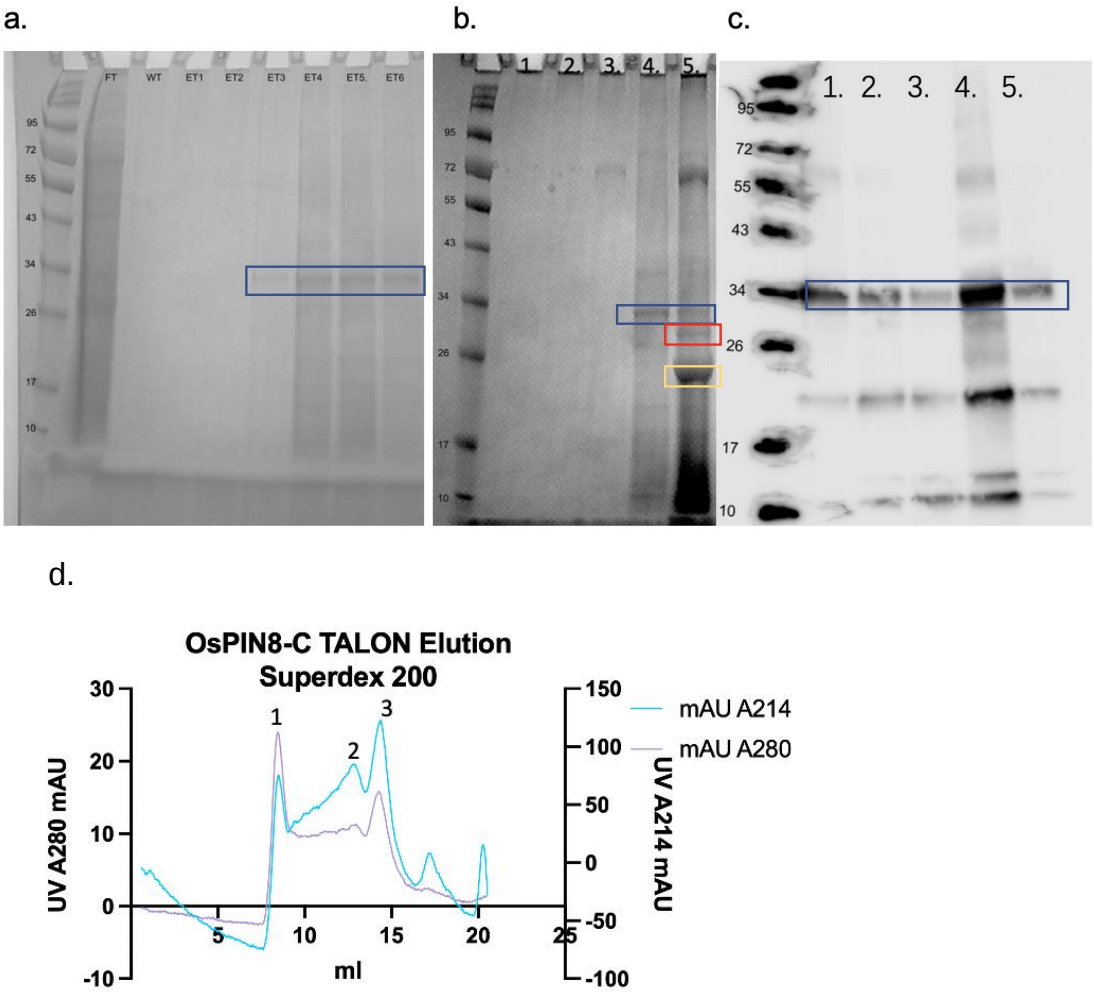

Figure 4.10 OsPIN8-C large scale purification by TALON

OsPIN8-C was purified by TALON column, the column flow through, wash and elution was loaded into SDS-PAGE. Peak fraction of TALON elution was loaded into AKTA-FPLC Superdex 200 for SEC profile collection, the SEC peak fractions and 3C OsPIN8-C mixture were run SDS-PAGE and Western-Blot.

Bands in blue boxes: OsPIN8-C, bands in red box: 3C cleaved OsPIN8, bands in yellow box: 3C protease

a. SDS-PAGE Coomassie staining, FT: TALON column flow through, WT: TALON column washing through, ET1-ET6: TALON column elution fractions 1-6.

b. SDS-PAGE Coomassie staining, 1-3: OsPIN8-C TALON elution gel-filtration peaks 1-3, 4: TALON column elution, 5: TALON column elution and 3C protease overnight incubation mixture.

c. Western-Blot of Figure 4.10b, anti PolyHistidine, 1-3: OsPIN8-C TALON elution gel-filtration peaks 1-3, 4: TALON column elution, 5: TALON column elution and 3C protease overnight incubation mixture.

d. FPLC TALON elution of OsPIN8-C UV A280 and A214 SEC

4.5.4 OsPIN8-C 3C cleavage

Results in figure 4.10 proved that OsPIN8-C can be cleaved by 3C protease. Large scale OsPIN8-C purification was repeated twice and 3C protease cleavage was applied.

OsPIN8-C was purified by TALON column and incubated with 3C protease (method refer to 4.5.3.and 2.3.2) and dialysis against gel-filtration buffer overnight, the sample mixture was loaded back to IMAC column for reverse-IMAC to remove 3C protease and un-cleaved OsPIN8-C. The TALON elution and reverse-IMAC flow through samples were run on SDS-PAGE and the concentrated reverse-IMAC flow through was loaded into AKTA-FPLC Superdex 200 for SEC analysis. Gel-filtration peaks a and b were concentrated and run on SDS-PAGE.

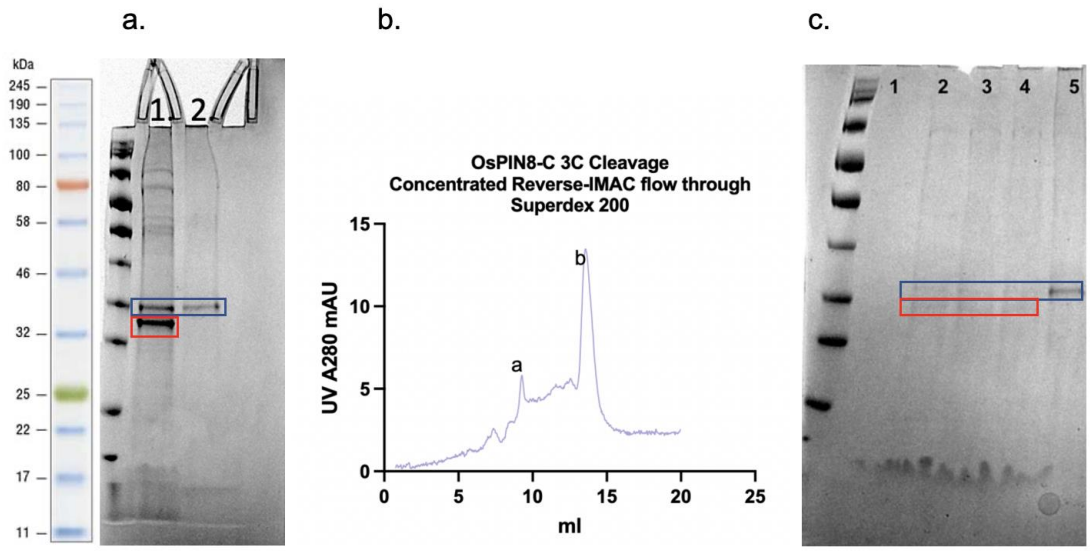

Figure 4.11 OsPIN8-C 3C cleavage and SEC profile

OsPIN8-C was purified by TALON column, mixed with 3C protease and dialysis against gel-filtration buffer overnight. Sample was loaded back to IMAC column, the reverse-IMAC flow through was collected, concentrated reverse-IMAC flowthrough was run in AKTA-FPLC Superdex 200 column, two gel-filtration peak fractions were collected and concentrated for SDS-PAGE analysis.

SDS-PAGE blue boxes, OsPIN8-C, red boxes, 3C cleaved OsPIN8.

a. SDS-PAGE Coomassie staining, 1. 3C protease cleaved OsPIN8-C reverse-IMAC flow through

b. Concentrated 3C protease cleaved OsPIN8-C reverse-IMAC flow through SEC profile

c. SDS-PAGE Coomassie staining, 1. Concentrated gel-filtration peak a, 2-4. Concentrated gel-filtration peak b, 5. OsPIN8-C purified by TALON.

The results in figure 4.11b and 4.11c showed that gel-filtration on Superdex 200 cannot separate cleaved and un-cleaved OsPIN8-C, and more 3C protease was required to make the cleavage sufficient. Meanwhile, the OsPIN8-C purification by TALON always generated some aggregation. Nickel beads will be used instead of TALON for further purifications.

4.5.5 OsPIN8-C purification by nickel beads and cleavage by 3C protease

1ml nickel beads were used for OsPIN8-C purification, the buffer was same as table 4.3+ 2mM DTT and 1mM EDTA. OsPIN8-C was purified by nickel column, incubated with 3C protease (OsPIN8-C: 3C 1:2 ratio, method refer to 4.1 and 4.2) and dialysis against gel-filtration buffer overnight, the sample mixture was loaded back to IMAC column for reverse-IMAC to remove 3C protease and un-cleaved OsPIN8-C. The nickel column flow through, wash through, elution, reverse-IMAC flow through and elution samples were run SDS-PAGE and concentrated reverse-IMAC flow through were loaded into AKTA-FPLC Superdex 200 for SEC analysis (Fig.4.12).

a. b.

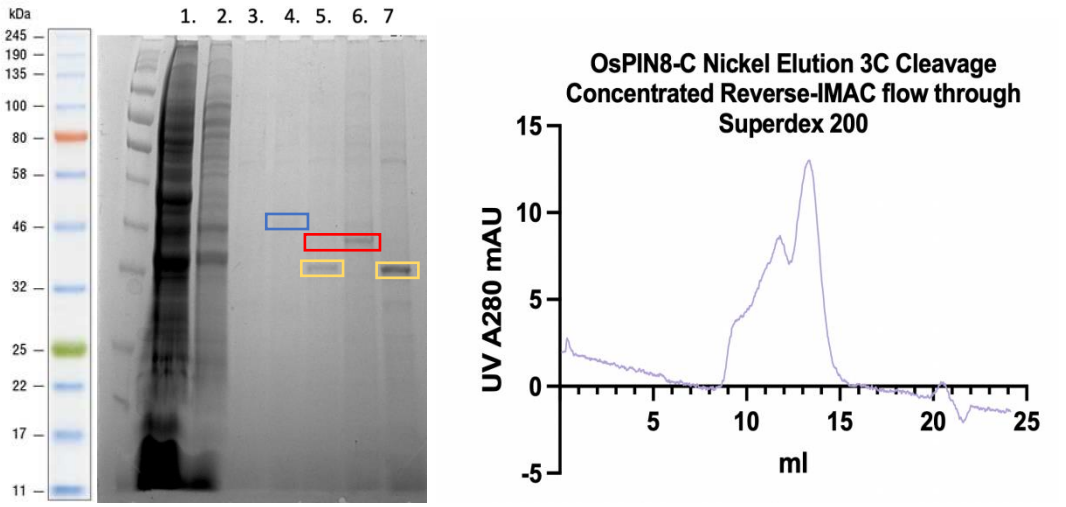

Figure 4.12 OsPIN8-C Nickel column purification and 3C cleavage

OsPIN8-C was purified by nickel IMAC, mixed with 3C protease and dialysed against gel-filtration buffer overnight. Sample was loaded back to IMAC column, the reverse-IMAC flow

through and elution were collected, and all samples were run on SDS-PAGE. Concentrated reverse-IMAC flowthrough was also run on an AKTA-FPLC Superdex 200 column.
SDS-PAGE bands: blue box: OsPIN8-C, red box: cleaved OsPIN8, yellow boxes: 3C protease
a. SDS-PAGE Coomassie staining, 1: sample before nickel column binding, 2: nickel column flow through, 3: nickel column wash through, 4: nickel column elution, 5: nickel column elution and 3C protease overnight incubation mixture, 6: concentrated 3C protease cleaved OsPIN8-C reverse-IMAC flow through, 7: reverse-IMAC elution.
b. Concentrated 3C protease cleaved OsPIN8-C reverse-IMAC flow through SEC profile

The results shown in figure 4.12 proved that OsPIN8-C can be purified by nickel beads, that 3C efficiently cleaved the affinity tag and that a sharp peak could be identified from AKTA-FPLC at 13ml. Further work would focus on separating the sharp peak at 13 ml for crystallization screening.

4.5.6 Optimized OsPIN8 purification by Nickel beads and Gel-filtration

Buffer base	pH	Lysis buffer	Washing buffer	Elution buffer	Gel-filtration buffer
HEPES	7.5	50mM Buffer base, 150mM NaCl, 5% glycerol, Protease inhibitor, 5mM imidazole, 2mM DTT, 1mM EDTA	Lysis buffer with 25mM imidazole, 2mM DTT, 0.1%DDM	Lysis buffer with 250mM imidazole, 0.1%DDM	50mM Buffer base, 150mM NaCl, 5% glycerol, 0.025%DDM

Table 4.5 Optimized buffers for OsPIN8 large scale purification

Sf9 cells expressing OsPIN8-C were lysed in 50mM HEPES buffer with 10mM NaCl (pH 7.5). After lysis, 5M NaCl was added to give a final 150mM NaCl. OsPIN8-C membrane was prepared (method refer to 2.1.6) and resuspension into two HEPES lysis buffers (Table 4.5), DDM/SEPM stock was added to give a final 1% DDM/ 0.1% SEPM. Sample was incubated for 2 hours at 4℃ and centrifuged by ultracentrifuge at 200,000 RCF for 1 hour at 4℃, supernatant was collected and rolled with nickel beads (1L cell culture for 1ml nickel beads) for 2 hours. Sample-beads mixture was packed into an Econo-column. Column was washed by Washing buffer and eluted by Elution buffer, the elution sample was incubated with 3C protease (OsPIN8-C: 3C 1:2 ratio, method refer to 4.1 and 4.2) and dialysis against gel-filtration buffer overnight, the sample mixture was loaded back to IMAC column for reverse-IMAC to remove 3C protease and un-cleaved OsPIN8-C.

800 µl concentrated reverse-IMAC flow through sample (2x 400 ul) was loaded into AKTA-FPLC Superdex 200 for analysis (Figure 4.13a and b), all AKTA-FPLC peak fractions from 13.5 ml to 15 ml (blue coloured fractions) were collected and concentrated for another gel-filtration running (Fig. 4.13c), nickel column flow through, washing through, elution, reverse-IMAC flow through, elution and reverse-SEC peak samples were collected for SDS-PAGE (Fig. 4.13d).

a.

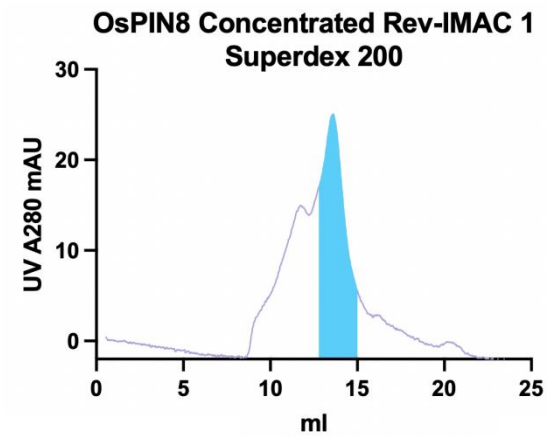

b.

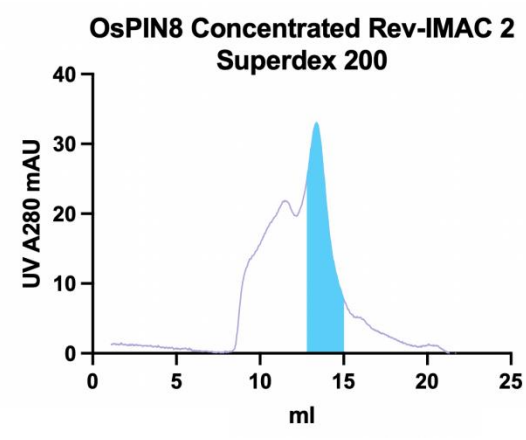

c. d.

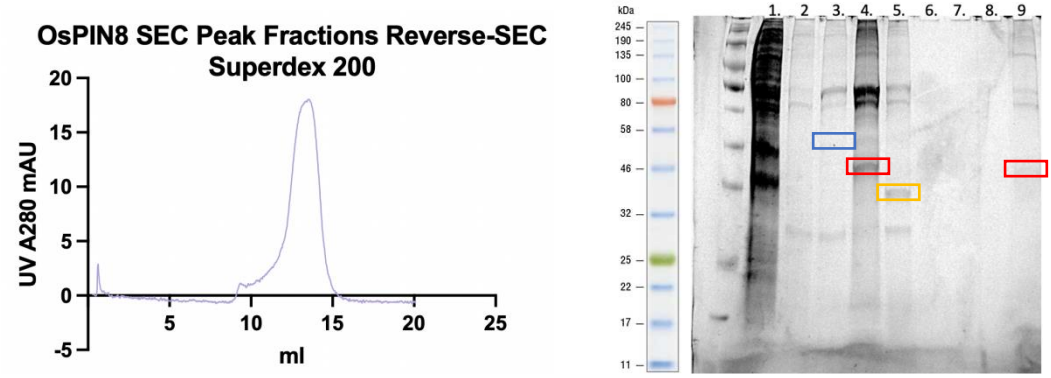

Figure 4.13 OsPIN8 optimized nickel-SEC purification

OsPIN8-C was purified by nickel beads and cleaved by 3C protease, the sample was loaded back to IMAC column and the flow through was concentrated and loaded into Superdex 200, peak fractions from 13.8ml to 15ml were concentrated and loaded into Superdex 200 again. All samples in the purification process were run SDS-PAGE
SDS-PAGE bands: blue box: OsPIN8-C, red box: cleaved OsPIN8, yellow boxes: 3C protease. SDS-PAGE fractions: 1. Nickel column flow through, 2. Nickel column washing thorough, 3. Nickel column elution, 4. Concentrated reverse-IMAC flow through, 5. Reverse-IMAC elution, 6-8 SEC peak from 5.13 a and b, 9. Concentrated SEC peak from 5.13 c.
a & b. Concentrated 3C protease cleaved OsPIN8-C reverse-IMAC flow through SEC profile
c. OsPIN8 reverse-SEC profile
d. SDS-PAGE Coomassie staining

Purified and polished OsPIN8 samples were concentrated to 5 mg/ml in 25ul, and a mosquito® crystal Nanolitre Protein Crystallization Robot was used to aliquot OsPIN8 to crystal screening plates MemGold, MemGold 2, MemMeso, MemStart+MemSys at 4℃.

In conclusion, OsPIN8-C can be purified by IMAC to get single peak in SEC and clear bands in SDS-PAGE. However, the protein is not stable enough for crystallization, and no crystal was observed in the screening.
Other short PINs were expressed and teasted in next sections for further studies.

Chapter 5 Other short PIN proteins: expression in *Saccharomyces cerevisiae* and purification

Previous AtPIN5 and OsPIN8 crystalization trails failed, and no crystallisation was observed in the screening. In addition, the melting temperature of both proteins was shown to be in the range of 20 to 25℃ (Appendix II). Therefore, a conclusion was made that both these proteins are not thermally stable for further assays. Therefore, some new short PIN proteins were expressed in *Saccharomyces cerevisiae* for further evaluation studies.

It was hypothesised that some selected short-PINs might be expressed favourably in *S cerevisiae*, allowing purification for downstream crystallography and activity assays.

5.1 Short PIN protein evaluations

There are 34 genomes available with short PIN proteins recorded in publications (Appendix III), including green algae, eudicots, monocots, and dicots. These genes were evaluated by online tools at (https://web.expasy.org/protparam/ and http://www.cbs.dtu.dk/services/TMHMM/). In particular, I studied their instability index and middle hydrophilic loop size as well as recoding the extinction coefficients.

Proteins with a high extinction coefficient, and smaller instability index can be more stable. For PIN proteins, shorter loops will be helpful for crystallization trails.

Four PIN protein genes were evaluated for expression in *S. cerevisiae*, they were *Oryza sativa* PIN5a (OsPIN5a), *Glycine max* PIN5a (GmPIN5a), *Populus trichocarpa* PIN12 (PtrPIN12) and *Amborella trichopoda* PIN5-like (AbtPIN5-like).

5.2 Four short PIN proteins expressed in *Saccharomyces cerevisiae*

Four short PIN proteins genes were synthesised as gBlocks and cDNA sequences were codon-optimized for *S. cerevisiae* expression. gBlocks were amplified by primer extension PCR with overhangs (SmaI site) for homologous recombination The SmaI-linerized vector and short-PIN PCR products were transformed into competent *S. cerevisiae* cells (Figure 5.1)(Table 2.8).
For the method refer to 2.2.1.

a.

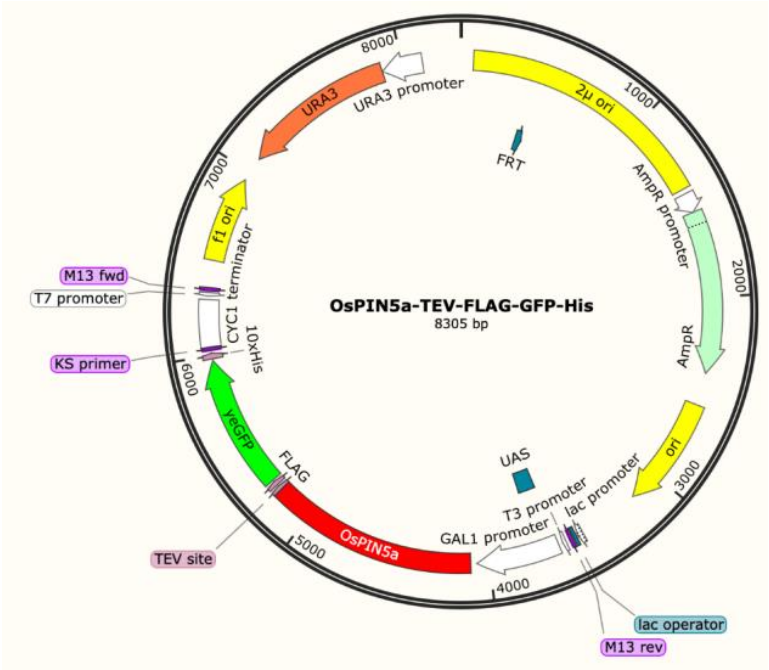

b.

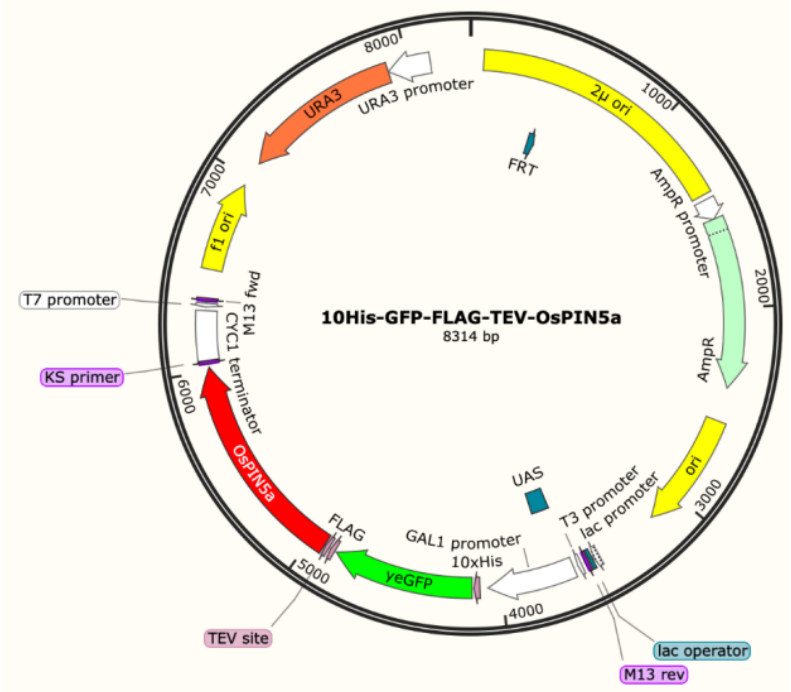

Figure 5.1 Plasmid constructs: example of OsPIN5a expression in *S. cerevisiae*

a. OsPIN5a-TEV-FLAG-yeGFP-His8 (OsPIN5a:GFP)

b. His10-yeGFP-FLAG-TEV-OsPIN5a (GFP:OsPIN5a)

GFP tags at N-terminal and C-terminals were cloned in target PINs respectively, to evaluate the protein stability of each different construct.

5.3 Four short PIN proteins: expression screening

Expression screening method - refer to chapter 2.2.2. *S. cerevisiae* cultures expressing the candidates were lysed and run on SDS-PAGE for in-gel fluorescence analysis (Fig. 5.2).

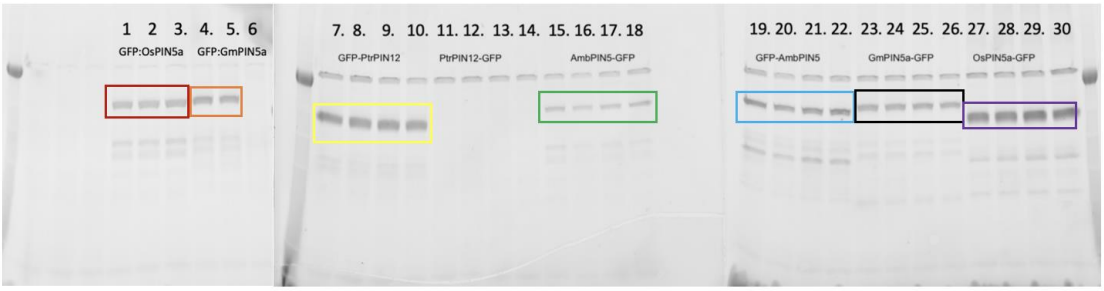

Figure 5.2 Four short PINs. N-terminal and C-terminal GFP tagged fusion protein expression screening, SDS-PAGE in-gel fluorescence.

SDS-PAGE Fractions: 1-3 red box GFP:OsPIN5a, 4-6 orange box GFP:GmPIN5a, 7-10 yellow box GFP:PtrPIN12, 11-14 PtrPIN12:GFP, 15-18 green box AmbPIN5-like:GFP, 19-22 blue box GFP:AmbPIN5, 23-26 black box GmPIN5a:GFP, 27-30 purple box OsPIN5a:GFP.

The PtrPIN12:GFP fusion protein was not found to be expressed in any of the selected *S. cerevisiae* colonies, but all the other seven expressed constructs were detected and will be used for further studies.

5.4 Short PIN proteins Detergent Screening on Nickel Column

Selecting the best detergent for protein solubilization is important for maximising the protein yield and for crystallization. To optimize the solubilization for further resin purification, solubilization of 4 short PIN proteins in 6 different detergent and lipid combinations were tested. The detergent screening process was as follows; *S cerevisiae* cell membrane was prepared (for method refer to 2.2.3) and re-suspended into Tris lysis buffer (30mg pellets/1 ml buffer), the lysate was collected and separated into 6 bench-top ultracentrifuge tubes with 6 different detergent mixes (DDM, DDM/CHS, DM, DM/CHS, CHAPS, OG) and incubated at 4℃ for two hours. Samples were centrifuged by bench-top ultracentrifuge for 30 min at 200,000x g and 4℃. The supernatant was collected and loaded on mini spin columns which were pre-packed with 0.1 ml Nickel beads. The sample flew through by spinning for 1 sec at 8,000x g. The column was washed by 2ml Tris Wash Buffer, 1ml each washing, before the sample was eluted with 0.2ml Tris Elution Buffer. 10µl of each eluate was kept on ice for 10 minutes and another 10µl was heated at 40℃ for 10 minutes were evaluated by SDS-PAGE and in-gel fluorescence (Fig. 5.3), and the elution samples with the strongest in-gel fluorescence band was run on AKTA-FPLC Superose 6 column to collect FSEC data (Fig. 5.3). It was seen that the DDM/CHS has the best solubilization for all short PINs constructs.

a1.

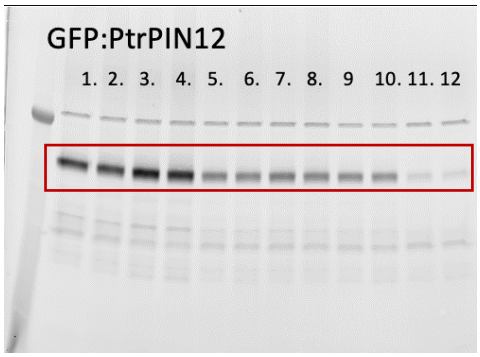

a2.

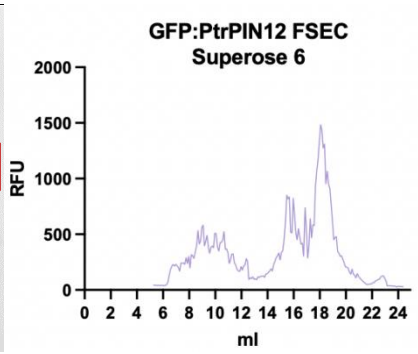

b1.

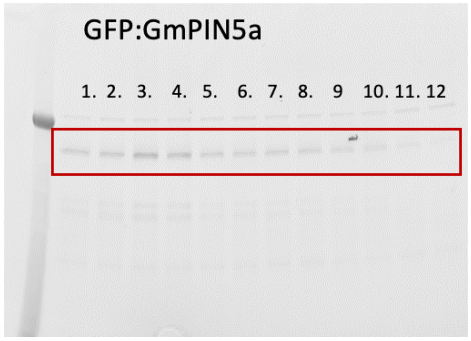

b2.

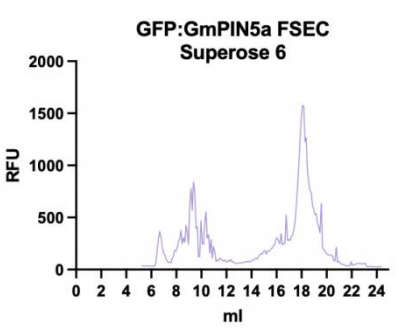

c1.

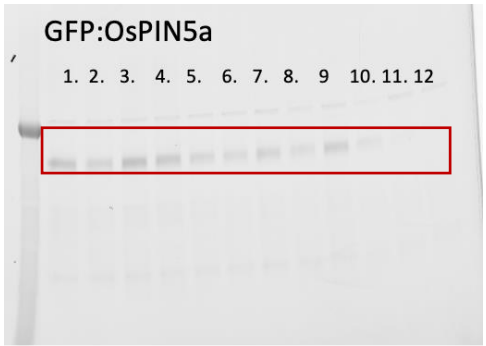

c2

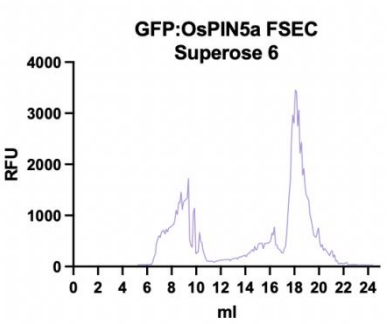

d1.

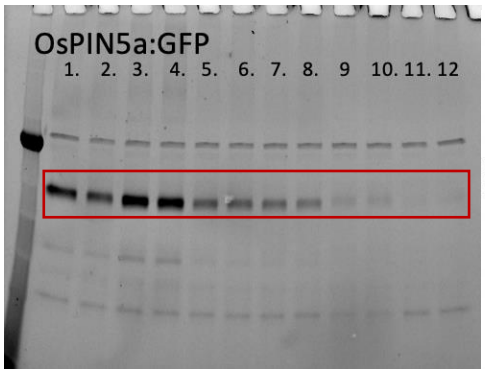

d2.

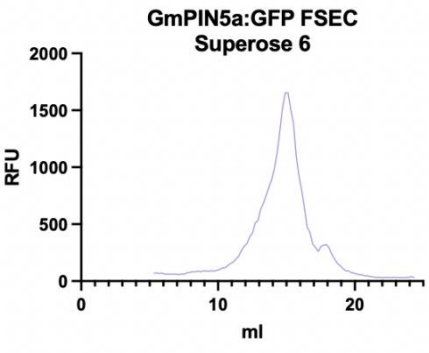

e1. e2.

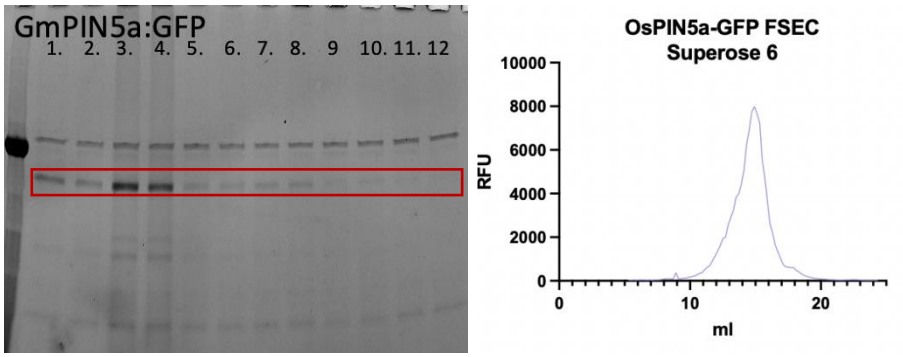

f1. f2.

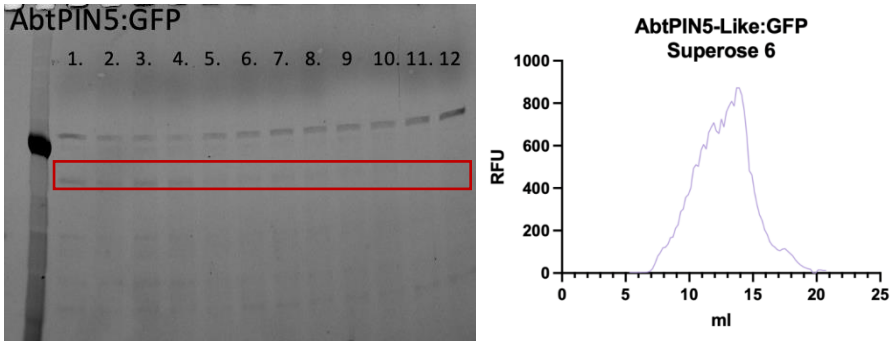

Figure 5.3 Short PIN proteins: detergent solubilization screening and FSEC profiles

Short PINs constructs were solubilized into 6 different detergents and lipids combinations for Nickel beads purification, 10 µlof each eluate was kept on ice for 10 minutes and another 10µlwas heated at 40 C for 10 minutes, all samples were analysed by SDS-PAGE in-gel fluorescence, target fusion protein bands are in red boxes.

SDS-PAGE fractions: 1.DDM 4 C, 2. DDM 40 C, 3. DDM/CHS 4 C, 4. DDM/CHS 40 C, 5. DM 4 C, 6. DM 40 C, 7. DM/CHS 4 C, 8. DM/CHS 40 C, 9. CHAPS 4 C, 10. CHAPS 40 C, 11. OG 4 C 12. OG 40 C.

DDM/CHS solubilized unheated samples were loaded into AKTA-FPLC for FSEC profile.

a1. GFP:PtrPIN12 in-gel fluorescence, a2. GFP:PtrPIN12 FSEC profile,

b1. GFP:GmPIN5a in-gel fluorescence, b2. GFP:GmPIN5a FSEC profile,

c1. GFP:OsPIN5a in-gel fluorescence, c2. GFP:OsPIN5a FSEC profile,

d1. OsPIN5a:GFP in-gel fluorescence, d2. OsPIN5a:GFP FSEC profile,

e1. GmPIN5a:GFP in-gel fluorescence, e2. GmPIN5a:GFP FSEC profile,

f1. AbtPIN5-like:GFP in-gel fluorescence, f2. AbtPIN5-like:GFP FSEC profile.

DDM/CHS shows the most promising solubilization and stability.

All the N-terminal tagged short PIN proteins have non-homogeneous FSEC profiles. C-terminal tagged AbtPIN5-like has a very low expression and broad FSEC profile, whereas good expression with good homogeneous FSEC peak is shown by constructs OsPIN5a:GFP and GmPIN5a:GFP and they will be used for further study.

5.5 OsPIN5a:GFP Purification by Nickel and M2 Anti-FLAG Beads

Buffer base	Lysis buffer	IMAC Washing buffer	IMAC Elution buffer	FLAG Washing Buffer	FLAG Elution Buffer	Gel-filtration buffer
Tris-HCl/ Tris Base 1:1 pH 7.5	50mM Buffer base, 150mM NaCl, 5% glycerol, 5mM EDTA, Protease inhibitor, 5mM imidazole	Lysis buffer with 25mM imidazole, 0.1%DDM, Protease inhibitor	Lysis buffer with 250mM imidazole, 5mM, 0.1%DDM	Lysis buffer, 0.1%DDM	Lysis buffer, 0.1%DDM, 3xFLAG peptide	50mM Buffer base, 150mM NaCl, 5% glycerol, 0.025%DDM

Table 5.1 Buffers for OsPIN5a:GFP purification

S. cerevisiae cell membranes were prepared (method refer to 2.2.3) and resuspended into Lysis buffer (15mg pellets/ ml buffer), adding 10% DDM/ 1%CHS to give a final 1%DDM/ 0.1%CHS. After incubation at 4℃ for 2 hours, samples were centrifuged in 45Ti rotor for 60 min at 200,000 RCF and the supernatant was filtered by 0.45μm PVDF filter. This was then loaded onto a glass column pre-packed with nickel resin (1 ml nickel resin for 1 L cell culture extraction). A peristaltic pump was connected from the bottom to the top of the column, flow speed at 1 ml/ min, and samples circulated overnight at 4℃. The column was washed by 20 column volumes IMAC Washing Buffer and eluted by 5 column volumes of IMAC Elution Buffer, 400μl of elution sample was loaded into AKTA-FPLC Superose 6 SEC column, FSEC profile was recorded (Fig. 5.4a). The rest of IMAC elution was loaded onto column packed 2ml M2-

Anti FLAG beads, a peristaltic pump was connected from the bottom to the top of the column, flow speed at 1 ml/ min, and samples circulated for 1 hour, The column was washed by 20 column volumes FLAG Washing Buffer and eluted by 5 column volumes of FLAG Elution Buffer, the FLAG elution was concentrated and loaded into AKTA-FPLC Superose 6 SEC column, analysed by SEC UV A280 and FSEC (Fig. 5.4b). Peak fractions of AKTA-FPLC were collected, mixed with TEV protease, incubated at 4℃ overnight.
Fractions of IMAC and FLAG column flow through, washing through, elution, SEC peak and TEV mixture were collected and analyzed by SDS-PAGE and in-gel fluorescence (Fig. 5.4c and d).

In this section, *S. cerevisiae* expressed OsPIN5a:GFP can be purified by Anti-FLAG column to get single peak in Superose 6 FSEC and strong bands in SDS-PAGE, however, an extra band at 60kDa was detected. The purified OsPIN5a:GFP fusion protein can be clevaged by TEV protease, but OsPIN5a tended to become unstable with faint band after TEV cleavge. The relatively stable fusion protein will be used for further activity assays.

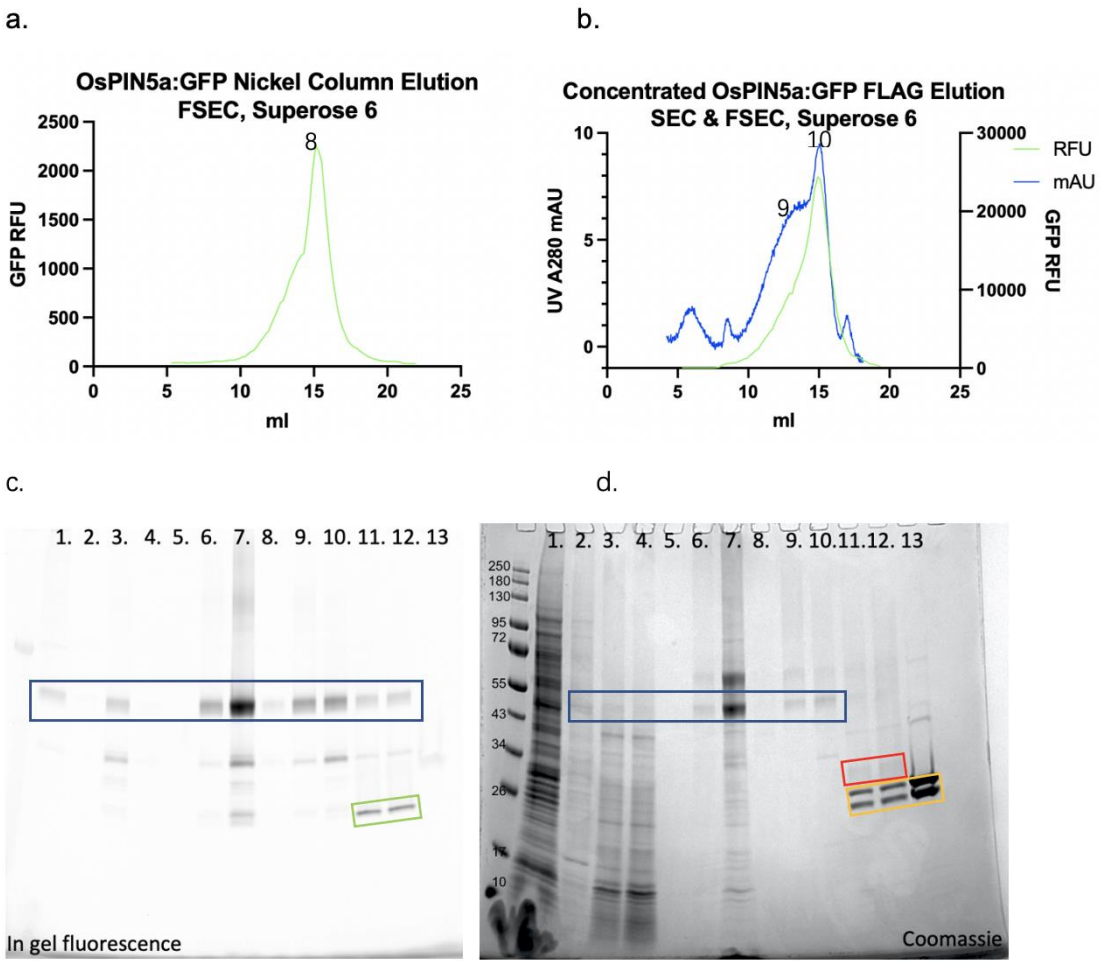

Figure 5.4 purification of OsPIN5a:GFP by Nickel-FLAG-SEC and cleavage by TEV protease

SDS-PAGE fractions: 1. Nickel column flow through, 2. Nickel column washing through, 3. Nickel column elution, 4. FLAG column flow through, 5. FLAG column washing through, 6. FLAG column elution, 7. Concentrated FLAG column elution, 8. Nickel elution FSEC peak, 9-10. FLAG elution SEC peak, 11-12. FLAG elution SEC peak fractions and TEV protease mixture, 13. TEV protease.

SDS-PAGE bands: OsPIN5a:GFP in blue boxes, TEV cleaved OsPIN5a in red box, TEV protease and GFP mixture in yellow box, TEV cleaved free GFP in green box.

a. OsPIN5a:GFP nickel elution AKTA-FPLC Superose 6 FSEC

b. OsPIN5a:GFP concentrated M2-Anti FLAG column elution AKTA-FPLC Superose 6 SEC and FSEC

c. SDS-PAGE in-gel fluorescence

d. SDS-PAGE Coomassie staining

5.6 Microscale Fluorescence Thermal Stability Assay for OsPIN5a:GFP

The CPM dye based Thermal-Shift assay is described in section 2.8.
Purified OsPIN5a:GFP was used to test the melting temperature without and with IAA, NPA, TIBA, IAA-GLU, IAA-ASP binding ligands. All data were processed with GraphPad Prism9, and a Bolzmann sigmoidal equation was fitted to raw data (Fig. 5.5)

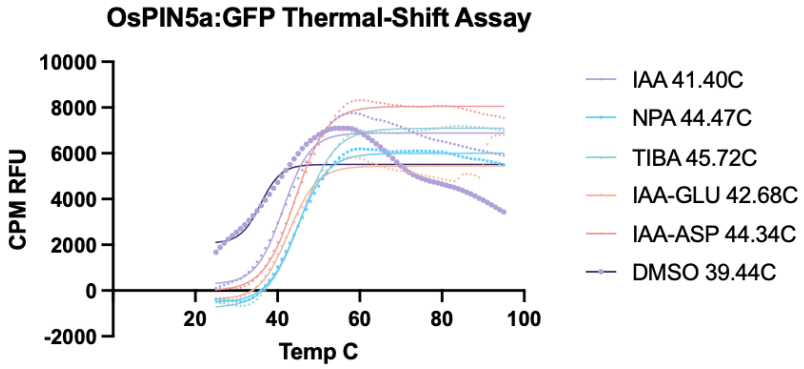

Figure 5.5 OsPIN5a:GFP Fluorescent Thermal-Shift Assay

49 µl of 10 ug/ml purified OsPIN5a:GFP was mixed with 10 µl of 0.1 mg/ml CPM dye and 1µl of 50nM target binding ligand. The sample mixture was heated in a controlled way in a qPCR plate with a ramp rate of 1 C/min from 25 C to 90 C. The excitation wavelength was set at 387 nm, while the emission wavelength was 463 nm, and CPM dye fluorescence data was collected every minute.
The melting temperatures (Tm) with different ligands were: IAA 41.40C, NPA 44.47C, TIBA 45.72C, IAA-GLU 42.68C, IAA-ASP 44.34C, DMSO control 39.44 C.

The CPM dye based Thermal-Shift assay confirmed that purified OsPIN5a was active, on the basis that when OsPIN5a bound with ligands, the thermal stability of OsPIN5a increased by around 2 to 6 ℃ compared with the DMSO control. Additionally, the assay suggested that conjugated IAA, auxin polar transport inhibitors NPA and TIBA have strong binding with OsPIN5a, stabilizing it in the temperature gradient. TIBA competes with auxin to inhibit auxin transport, NPA tends to bind with PINs and promote dimer formation of

PIN proteins to inhibit auxin transport. ER localized PIN5 might transport conjugated IAA as a storage form into the ER.

In this chapter, four short-PINs were successfully expressed in *S. cerevisiae* and purified using an Anti-FLAG column. Purified OsPIN5a:GFP gave a single peak in the SEC and FSEC. There was an improvement of protein purity after FLAG compared to only nickel (Figure 5.4d fraction 3 and 6). However, one extra band in SDS-PAGE appears at around 60kDa, which might be a yeast chaperone. Also, it seems that after TEV cleavage, the OsPIN5a tends to have faint band rather than sharp band, suggesting it might be unstable. Therefore further studies with OsPIN5a expression in insect cells and without GFP will be necessary.

Purified OsPIN5a:GFP was also tested with CPM dye based Thermal-Shift assay. A 2-6 ℃ Tm shift was observed with ligands which suggested that conjugated IAA, auxin polar transport inhibitors NPA and TIBA have activity with OsPIN5a.

Chapter 6 PIN proteins Negative Staining and Nanodisc Reconstitution

AtPIN5 and OsPIN8 crystallography trails failed, therefore, transmission electron microscopy (TEM) methods were used for alternative structural studies. Membrane protein negative staining and analysis by TEM is a quick way to visualization the size distribution and homogeneity of purified proteins. Purified protein was loaded onto the carbon film surface of TEM grids and the heavy metal salt uranyl acetate was used to stain the background and reveal protein shapes and size distributions.

It was hyprothesised that purified AtPIN5:GFP can be negatively stained and analysed by TEM. Purified PIN proteins might also be reconstituted into Saposin A protein nano-discs to help with structural studies.

6.1 AtPIN5:GFP Negative Staining

Purified AtPIN5:GFP was prepared and applied to a negative staining grid. This was inserted into a Jeol 2100Plus TEM and pictures were taken at 60k magnification. The pictures were processed by Relion software (Scheres, 2012) to generate 2D and 3D class average models (Figure 6.1).

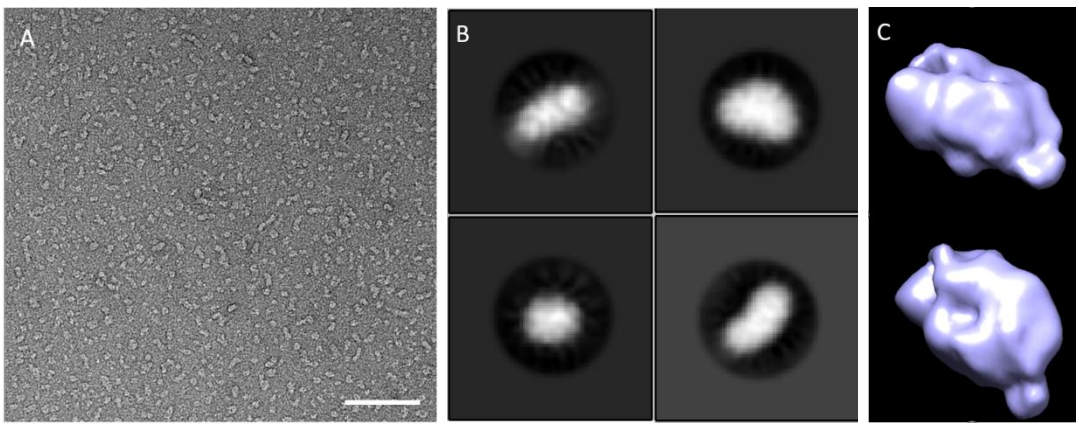

Figure 6.1 AtPIN5:GFP negative staining TEM micrographs, with 2D and 3D classifications

A. a representative electron micrograph of 0.08mg/ml AtPIN5:GFP stained with uranyl acetate. Individual side and top views of the AtPIN5:GFP can be seen. Scale bar, 200 nm.

B. Selected 2D class averages of AtPIN5:GFP; the length of each individual mask (black circle) represents 200 Å.

C. 3D classification build model of AtPIN5:GFP, filtered to 12Å. Front view and top view.

Purified AtPIN5:GFP sample was found to be monodispersed in TEM electron micrographs, however, after 2D and 3D classification using Relion, the 3D model 12Å resolution reached the limit of resolution for the negative staining TEM technique. Nevertheless, the images with symmetry are most consistent with the unit structure being a dimer. The size of AtPIN5 40kDa as a dimer with GFP fusion proteins = 140 kDa and this remains at the more challenging end for further structural resolution by TEM. Therefore, a small membrane protein nanodisc technique was introduced for PIN protein structural research, which might help stabilise the protein and allow better resolution enhancement on cryo-EM.

6.2 Saposin A protein Nanodisc purification and lipid binding

The saposin-lipoprotein nanoparticle system allows for the reconstitution of membrane proteins in a lipid environment that is stabilized by a scaffold of saposin proteins. It can also enhance resolution and simplify preparation on cryo-EM grids (Frauenfeld et al., 2016). Therefore, expression and purification of saposin A was applied.

All samples from the saposin A nonodisc purification steps were loaded into SDS-PAGE for analysis (Fig. 6.2a).

To test saposin A lipid binding, a volume of 500 µl of 1.2mg/ml purified saposin A stock was loaded onto AKTA Superdex 200 increase column for SEC profiling. Another 450 µl of 1.2mg/ml saposin A stock was left rolling with 50 µl of 200 mg/ml soybean lipids at 37℃ for 10 min after which it was loaded onto AKTA Superdex 200 increase column for SEC profile (Fig. 6.2b)

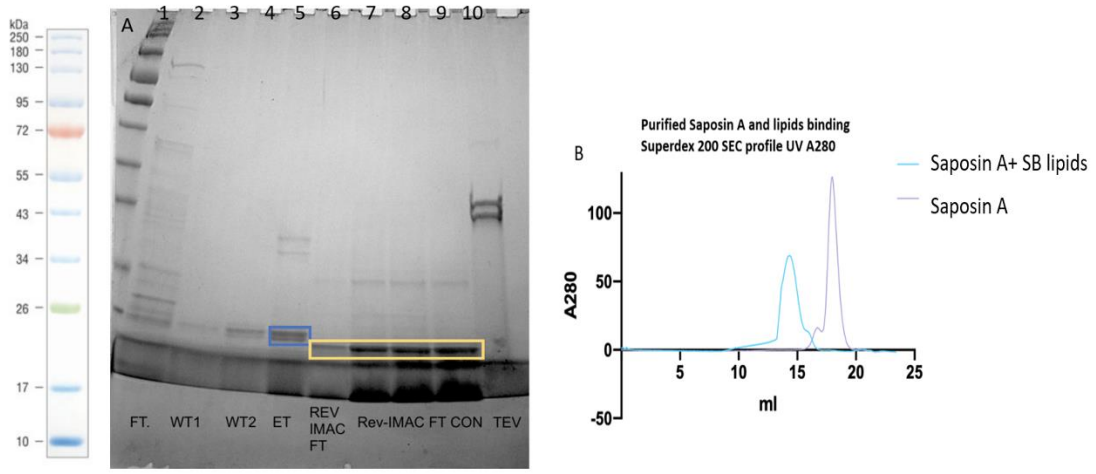

Figure 6.2 Saposin A purification and lipid binding assay

A. SDS-PAGE Coomassie staining, 1 NEB colour protein ladder, 2 Saposin A IMAC purification flow through, 3 Saposin A IMAC purification wash through 1, 4 Saposin A IMAC purification wash through 2, 5 Saposin A IMAC purification elution, 6 Saposin A reverse-IMAC flow through, 7-9 1.2mg/ml concentrated saposin A reverse-IMAC flow through, 10 TEV protease. Blue box: Saposin A with His tag before TEV cleavage 10.4kDa.

Yellow box: Saposin A after TEV cleavage 9.6kDa.

B. Purified and pooled saposin A Superdex 200 SEC profile. Blue curve: Saposin A with SB lipids binding.

Purple curve: Saposin A without lipids binding.

The SEC peak of a sample of purified saposin A was 18 ml (10kDa) and this was shifted after lipid binding to 14 ml (the elution volume of BSA; 66.5 kDa) on the Superdex 200 SEC profile. This shift was consistent with the model for saposin A activity (Flayhan et al., 2018). Four Saposin A molecules were shown to assemble into a ring like saposin A-lipid complex (Figure 6.3). With regard to these results, it was decided to reconstitute OsPIN8 and AtPIN5 proteins into these Saposin A-lipid complexes.

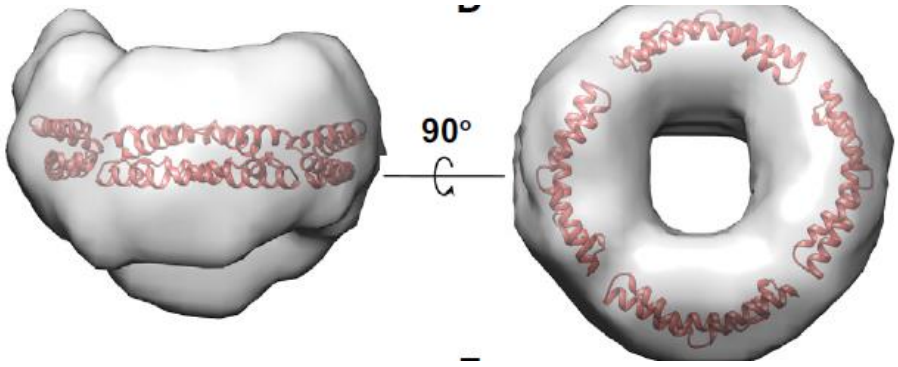

Figure 6.3 Empty saposin A-lipids complex

SapA/Lipids with four SapA molecules (PDB: 4DDJ) fitted in the shape volume (Flayhan et al., 2018).

6.3 Saposin A Nanodisc Reconstitution of OsPIN8-C

OsPIN8-C was reconstituted into Saposin A on a nickle IMAC column at 4℃ by modifying the IMAC purification method specified in section 5.1.5.2. After the OsPIN8-C-nickel beads mixture was packed into an Econo-column, the column was washed by 20 column volume HEPES Washing buffer. 80µl of a soybean lipid solution (5 mg/ml soybean lipids (Sigma-Aldrich), 50 mM HEPES, pH 7.5, 150 mM NaCl, 0.28% DDM with cOmplete EDTA-free protease inhibitor mix) was incubated for 10 min at 37℃ with 140 µl of purified Saposin A (1.2 mg/ml, 20 mM HEPES, pH 7.5, 150 mM NaCl) and HEPES buffer (50mM HEPES, 150mM NaCl, 5% glycerol, 4mM TCEP, protease inhibitors, pH=7.5) to a final volume of 2.5 ml and incubated at 37℃ for 10min. Subsequently the Saposin A lipids mixture was loaded into IMAC column, connected to a recycle pump at flow speed 1ml/ml at 4℃ for 16 hours (Fig. 6.4).

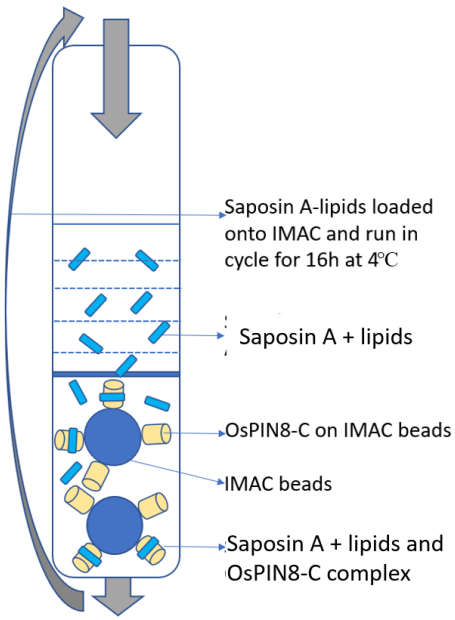

Figure 6.4 Schematic representation of OsPIN8-C reconstitution into Saposin A-Lipid complex on column

The IMAC column was washed by washing buffer and the OsPIN8-C-Saposin A-lipids complex eluted by elution buffer, the total elution sample was concentrated into 500µl and subjected to a gel filtration step on a Superose 6 10/300 GL column equilibrated with HEPES buffer without detergent (pH 7.5). Fractions of all stages were pooled and analysed by SDS-PAGE (Fig. 6.5A).

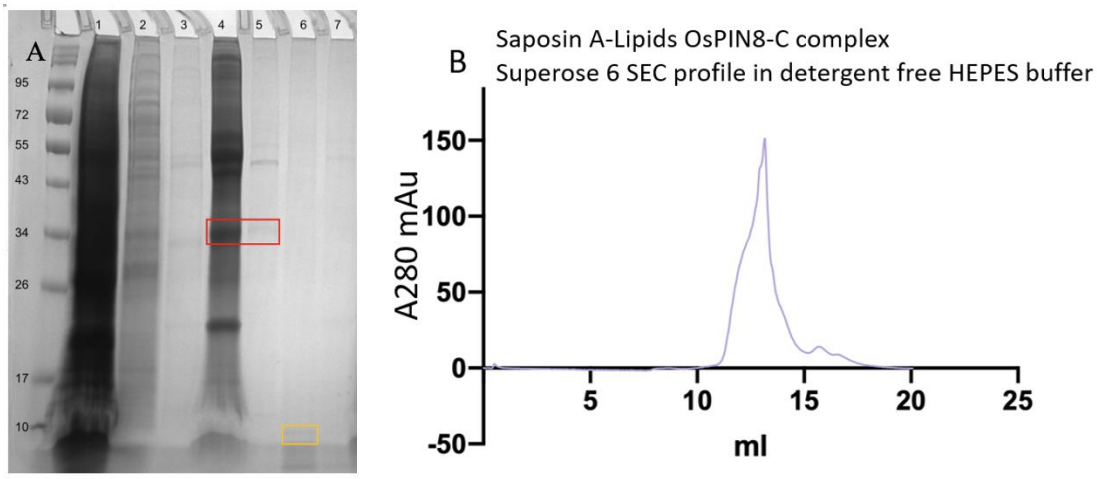

Figure 6.5 Efficiency of OsPIN8-C on-column reconstitution into Saposin A-Lipid complex

A. SDS-PAGE image of samples from OsPIN8-C IMAC purification and Saposin A on-column reconstitution .SDS-PAGE fractions: 1 Solubilized OsPIN8-C in ultracentrifugation supernatant, 2 IMAC purification flow through, 3 IMAC purification washing through, 4 Concentrated IMAC elution of reconstituted OsPIN8-C in Saposin A-lipid complex, 5 AKTA-SEC Superose 6 peak fraction, 6 Saposin A on column assembling sample flow through, 7 Saposin A on column assembling column washing collection.
Red box: OsPIN8-C. Yellow box: Saposin A.
B. Superose 6 SEC profile of the saposin A-Lipid OsPIN8-C complex in detergent free HEPES buffer. Peak fraction at 13ml.

The OsPIN8-C purified by detergent solubilisation gave a peak on Superose 6 SEC at 14ml (Figure 6.5B). After the saposin A nanodisc reconstitution the protein peak was shifted from 14ml to 13ml in detergent free buffer. This was promising. However, it was hard to identify saposin A protein as a band at 10kDa after SDS-PAGE and Coomassie staining, and OsPIN8 was not visible. Before further TEM and cryo-EM, more optimisaiton of saposin:lipid reconstitution conditions are necessary.

6.4 Saposin A Nanodisc Reconstitution on AtPIN5:GFP

For a medium-scale preparation of Saposin A-AtPIN5, 80µl of a soy bean lipid solution was incubated (5 mg/ml soybean lipids (Sigma-Aldrich) in 50 mM HEPES, pH 7.5, 150 mM NaCl, 0.28% DDM) and 100 µl of protease inhibitor stock solution (1 cOmplete EDTA-free tablet in 1 ml H2O) for 10 min at 37℃, before adding 100 µl of purified membrane protein AtPIN5:GFP (2 mg/ml, 20 mM Tris-HCl, pH 7.5, 150 mM NaCl, 5% glycerol, 0.05% DDM) and subjecting the mixture to a second incubation step at 20°C for 20min. Subsequently, 140 µl of purified saposin A (1.2 mg/ml, 20 mM HEPES, pH 7.5, 150 mM NaCl) was added and incubated the mixture for 20 min at 20℃.

Two reconstitution strategies were applied to remove detergent.

1) Bio-Beads were added at a Bio-Beads/detergent ratio of 20 (wt/wt), incubated at 20℃ for 1 hour, and 500 µl samples were collected for further analysis.

2) Another 3200 µl of 1× PBS (pH 7.5) was added and incubated with the mixture for 10 min at 20 C, after which the sample was concentrated to 500 µl and pooled for further analysis.

Three samples 1) purified AtPIN5:GFP, 2) Bio-Beads treated sample and 3) detergent free PBS diluted sample were subjected to gel filtration on a Superose 6 10/300 GL column in PBS (pH 7.5). Sample 1 was run in PBS buffer + 0.025% DDM, sample 2 and 3 were run in detergent free PBS). Fractions containing Saposin-AtPIN5:GFP were pooled and analysed by SDS-PAGE and in-gel fluorescence.

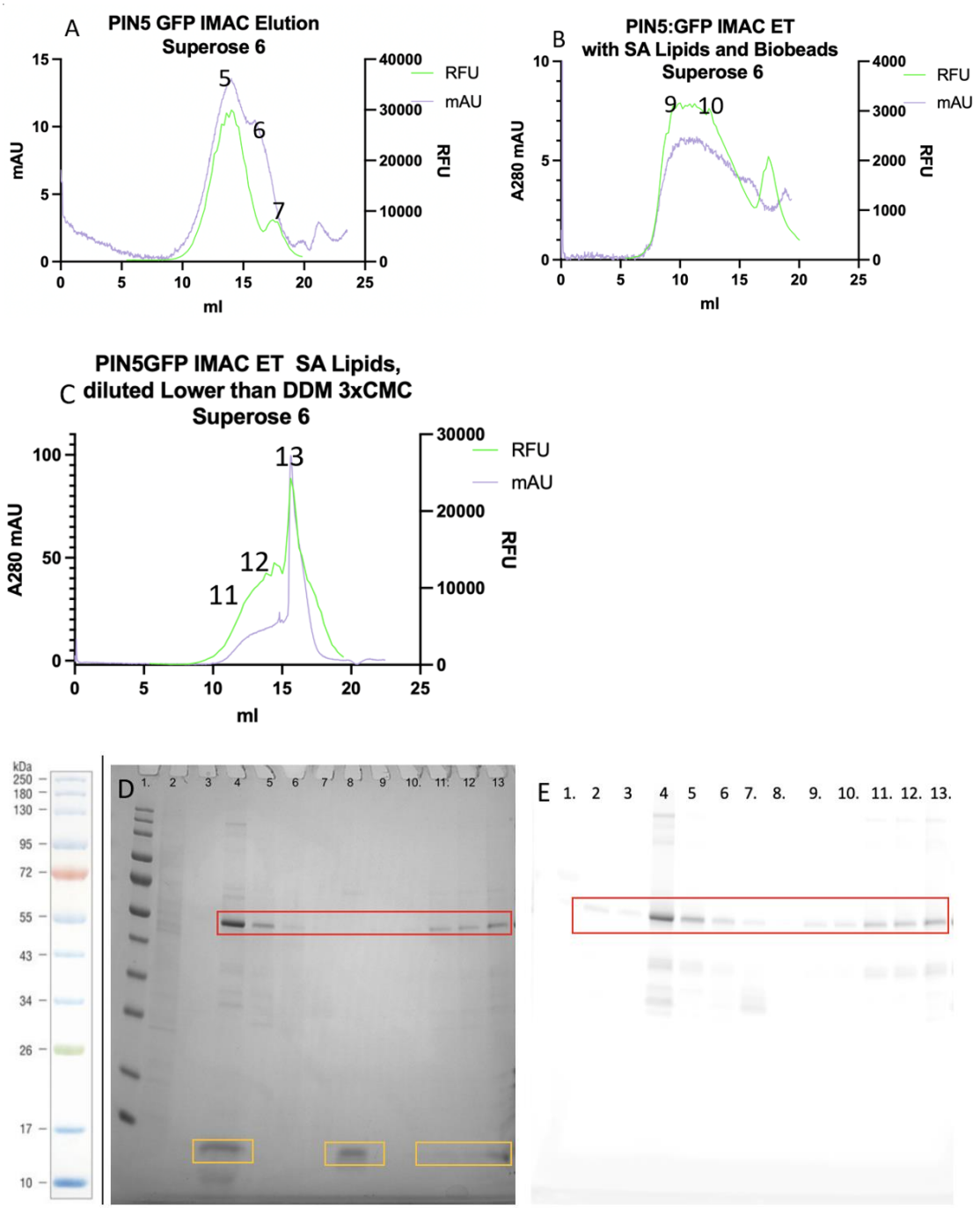

Figure 6.6 AtPIN5:GFP reconstitution into Saposin A-Lipid complex

A. Purified AtPIN5:GFP Superose 6 SEC profile in PBS buffer with 0.025% DDM, 3 fractions were loaded into SDS-PAGE.

B. Purified AtPIN5:GFP, Saposin A-lipids Bio-Beads mixture incubation sample, Superose 6 SEC profile in detergent free PBS buffer, 2 fractions were loaded into SDS-PAGE.

C. Purified AtPIN5:GFP, Saposin A-lipids diluted by detergent free PBS and concentrated sample, Superose 6 SEC profile in detergent free PBS buffer 3 fractions were loaded into SDS-PAGE.

D & E. Image of SDS-PAGE Coomassie staining and in-gel fluorescence

Fractions: 1. NEB colour protein standard, 2. AtPIN5:GFP IMAC purification washing through, 3. AtPIN5:GFP IMAC purification flow through, 4. Purified AtPIN5:GFP saposin A-lipids mixture, 5-7. SEC fractions from Figure 6.6A, 8. Saposin A-lipids stock, 9-10. SEC fractions from Figure 6.6B, 11-13. SEC fractions from Figure 6.6C.
Red boxes: AtPIN5:GFP. Yellow boxes: Saposin A nanodisc protein.

The results from Figure 6.6 C D and E showed that AtPIN5:GFP does not aggregate in detergent free PBS. Also SEC peak fractions identified saposin A protein in SDS-PAGE Coomassie staining, which suggested AtPIN5:GFP was reconstituted into the saposin A-lipids system successfully.

The negative staining protocol (section 2.9) was applied to Figure 6.6 C SEC peak fractions (Fig. 6.7), negative staining grid was inserted into TEM and the pictures were taken at 80k times zoom. Because of PBS buffer was the final buffer for AtPIN5/Saposin A-lipids complex, 2% uranyl acetate might precipitate in this salt rich buffer (PBS). Therefore, the quality of electron micrographs was not good enough for further analysis. Some more optimizations need to be applied for further negative staining and Cryo-TEM sample preparation.

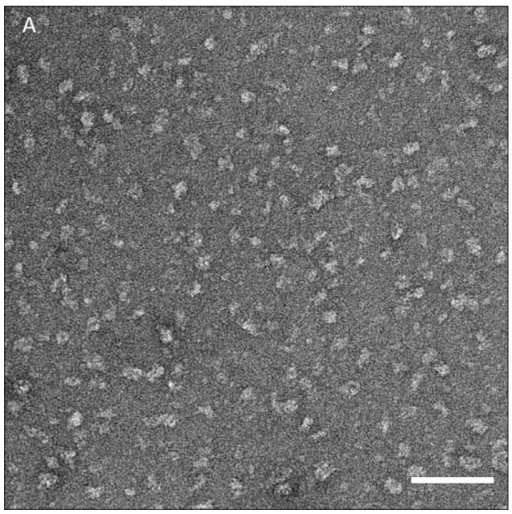

Figure 6.7 AtPIN5/Saposin A-lipids complex negative staining TEM micrographs

A representative electron micrograph of 0.05mg/ml AtPIN5:GFP stained with uranyl acetate. Individual side and top views of the disc like particles can be seen. Scale bar, 100 nm.

In this chapter, AtPIN5:GFP was successfully negative stained by uranyl acetate and analysised by TEM. Purified AtPIN5:GFP can be reconstituted into Saposin A nano-discs for further Cryo-TEM studies.

Chapter 7 General Discussion, Further Studies and Conclusion

The plant-specific proteins named PIN efflux carriers facilitate the direction of auxin flow and thus play a vital role in the establishment of local auxin maxima within plant tissues that subsequently guide plant ontogenesis. Until now, the three-dimensional structure of PINs has not been solved.

This thesis is centered on expressing and purifying a few PINs for structural studies and achieved high purity, stable homogeneous results of AtPIN5, OsPIN5a and OsPIN8.

The main difficulty which was overcome was the search of conditions which allow these extraordinary proteins to exist outside of the cell membrane for structural studies. However, this problem still needs more optimization and some extra biochemistry and biophysical assays. In addition to the conclusions in each chapter, I present here a further general discussion, and propose further studies.

7.1 PINs Expression and purification

In this thesis, AtPIN1, AtPIN1-Cut, AtPIN5, OsPIN8, were expressed in Sf9 cells, OsPIN5a, GmPIN5a, PtrPIN5, AmbPIN5-Like were expressed in yeast cells. The constructs were designed with a GFP tag in order to try and help stabilize the protein but also to help tracing and quantifying for the optimization stages in high throughput expression and purification optimization studies.

In chapter 3, the GFP tag was used to observe the distribution of AtPIN5:GFP on Sf9 cell membranes, to quantify relative protein expression levels under different medium conditions and MOI.

The GFP tag is traceable through HPLC-FSEC, FPLC-FSEC and in gel fluorescence. In Chapter 4, Chapter 5 and Chapter 6, to optimize PIN purifications, GFP tagged PINs were used for buffer and detergent/lipids screening. By measuring GFP, solubility, yield and stability were estimated under different conditions. The purification process used in-gel fluorescence for PIN:GFP fusion protein characterization, which was also faster than western-blots, because it became clear that speeding up the procedure is also critical

for protein yield and stability. The SEC UV A280 profiles were used to compare with FSEC GFP RFU profiles, which gave information of PIN dispersity before, during and after the purification processes. The FSEC and SEC profiles also suggested that PINs are naturally dimerised (Figure 6.6 A&C), which if true this native symmetry will benefit cryo-EM studies (Figure 6.1).

The yeast cell lines expressing PINs gave some good screening results to identify OsPIN5a and GmPIN5a as good candidates for further work. In further study, they will be expressed in insect cells for large scale protein production, allowing purification to be optimized to achieve better conditions for protein crystallization or Cryo-EM sample preparation.

7.2 PINs structural studies by crystallization and cryo-EM

Purified PINs (AtPIN5 and OsPIN8) were used for crystallization screening, however, after cleavage of the GFP tag, PINs tended to destabilize as shown by Figures 3.16 and 4.7. Therefore this approach was discontinued.

In Chapter 7, AtPIN5:GFP negative staining TEM photos recorded good particle distribution, and by using Relion EM image average software, a low resolution model of AtPIN5:GFP was generated. To enhance the stability and resolution of the AtPIN5:GFP 3D class average, Saposin A nanodisc protein was introduced to improve on detergent as the medium for PINs studies. OsPIN8-C and AtPIN5:GFP were reconstituted into saposin A/Lipid complexes, giving good SEC profiles in detergent free SEC buffer.

The middle hydrophilic loop of OsPIN8 is so short that it may prove inconvenient for cryo-e/m because it will not confer a sufficient geometric feature useful for 2D and 3D classifications in Relion. AtPIN5:GFP with a 5kDa middle loop may be better for TEM analysis. AtPIN1 with its 30kDa disordered middle loop could be stabilized by a nanobody to make a prefect target for Cryo-EM studies, but this will require a large and dedicated additional research programme.

A further study proposition is to scan nanobodies and antibodies for activity against PINs, to stabilize them and give them an outstanding spike in 2D and 3D classifications, which will benefit both crystallography and Cryo-EM studies

of PINs. AtPIN5:GFP Saposin A/lipid complexes need further optimization for Cryo-EM sample preparations and large quantities of purified Saposin A will be needed if it is used as a detergent free reagent to solubilize and extract PINs directly from membranes for further purification and analysis.

TEM studies normally need a reference protein model (same family protein) for particle identification. However, until now, the PINs have no crystal and cryo-EM data available, and no close homologues or other templates for model building. Some artificial intelligence (AI) methods such as Alphafold 2 are becoming available as novel tools to predict membrane protein structures, which will help as references for PINs in EM particle pick up protocols (Fig. 7.1). AlphaFold 2 has also provided some models for PIN protein structural studies, but there are some features still unknown such as how auxin bind to and is transported by PINs, how do PIN proteins work as dimers, and the mechanism of action of PIN interactions with different ligands. The AI prediction models will benefit some EM studies but can't solve all the problems, especially the mode of PIN dimer binding with auxin.

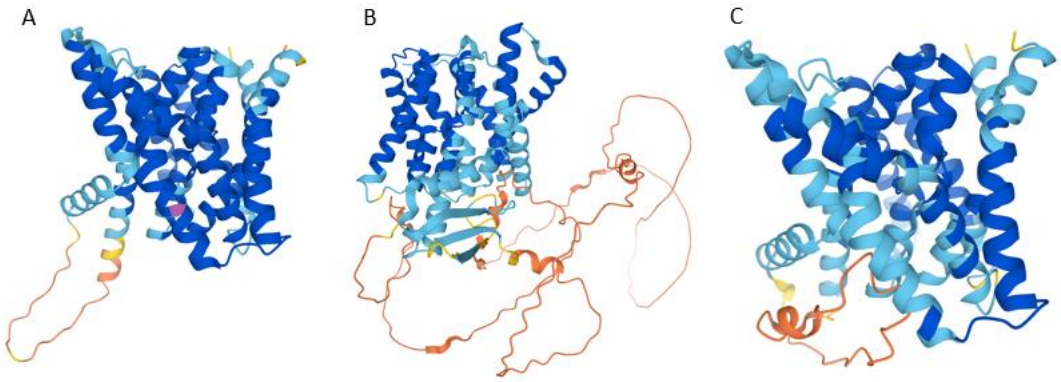

Figure 7.1Alpha Fold 2 predication of PINs monomer 3D models.

Models were generated by AlphaFold Protein Structure Database by searching protein name (Jumper et al., 2021). Blue color: high confidence of prediction, red color low confidence of prediction.

A. AtPIN5 monomer

B. GmPIN5a monomer

C. OsPIN5a monomer

7.3 PIN activity assays in vivo and in vitro

In this thesis, purified OsPIN5a was used for the CPM dye thermal-shift assay. AtPIN5 and OsPIN8 thermal-shift assays were not successful.

Many in vivo and in vitro activity assay conditions need to be further optimized, which include but are not limited to radiolabelled IAA uptake assays, patch-clamping assay on PINs expressed in Sf9 cells, purified PINs immobilized on SPR chips for kinetic auxin binding assays, and thermal-shift assays on nanoscale Differential Scanning Fluorimetry (nanoDSF).

Most of the PINs are thermally unstable at room temperature (Tm 20-30°C)(appendiex II), which means protein quality is decreasing throughout purification and preparation processes. A stable PIN protein is necessary for all biochemistry and biophysical assays. Some technology such as nanodisc systems and SMALPs may increase PIN protein stability, and will be introduced for further studies. Biotinylated Saposin A nanodiscs may also help the PIN activity assay on SPR.

7.4 Conclusion

Although PINs play very important roles in plant development, their topology has been only recently experimentally assessed and we still have to wait for Cryo-EM or crystallographic data to resolve the structure of these carriers in detail. The PIN instabilities and disordered domains made it hard to obtain ideal results. Also other approaches aimed at biochemical and structural characterization will help understanding the mechanism of action of PINs. In Chapter 1, some amino acids and motifs were identified in PINs to be essential for appropriate PIN function. Combined with Alphafold models, this level of detailed information should give a clear construct design of further PINs studies. Some of the disordered domain can be truncated, some essential areas and domains can be optimized to make the whole protein biochemically active and structurally more stable.

The PINs can also be stabilized by nanodisc lipid ceomplexes giving environments that when combined with nanobodies to stabilize the unfolded and disordered domains may allow structural determination. With AI prediction models as references to benefit cryo-EM studies, we will get closer to the real PIN structure as our final goal.

Within this framework and with the help of the results outlined in this thesis, hopefully a more comprehensive understanding of PIN structure and mechanism of action will be obtained in the future.

Chapter 8 References

ABAS, L., KOLB, M., STADLMANN, J., JANACEK, D. P., LUKIC, K., SCHWECHHEIMER, C., SAZANOV, L. A., MACH, L., FRIML, J. & HAMMES, U. Z. 2021. Naphthylphthalamic acid associates with and inhibits PIN auxin transporters. *Proceedings of the National Academy of Sciences,* 118.

ADAMOWSKI, M. & FRIML, J. 2015. PIN-dependent auxin transport: action, regulation, and evolution. *Plant Cell,* 27**,** 20-32.

BADESCU, G. O. & NAPIER, R. M. 2006. Receptors for auxin: will it all end in TIRs? *Trends in plant science,* 11**,** 217-223.

BARBEZ, E., KUBEŠ, M., ROLČÍK, J., BÉZIAT, C., PĚNČÍK, A., WANG, B., ROSQUETE, M. R., ZHU, J., DOBREV, P. I. & LEE, Y. 2012. A novel putative auxin carrier family regulates intracellular auxin homeostasis in plants. *Nature,* 485**,** 119-122.

BARBOSA, I. C., HAMMES, U. Z. & SCHWECHHEIMER, C. 2018. Activation and polarity control of PIN-FORMED auxin transporters by phosphorylation. *Trends in plant science,* 23**,** 523-538.

BENJAMINS, R., AMPUDIA, C. S. G., HOOYKAAS, P. J. & OFFRINGA, R. 2003. PINOID-mediated signaling involves calcium-binding proteins. *Plant physiology,* 132**,** 1623-1630.

BENJAMINS, R., QUINT, A., WEIJERS, D., HOOYKAAS, P. & OFFRINGA, R. 2001. The PINOID protein kinase regulates organ development in Arabidopsis by enhancing polar auxin transport. *Development,* 128**,** 4057-4067.

BENKOVÁ, E., MICHNIEWICZ, M., SAUER, M., TEICHMANN, T., SEIFERTOVÁ, D., JÜRGENS, G. & FRIML, J. 2003. Local, efflux-dependent auxin gradients as a common module for plant organ formation. *Cell,* 115**,** 591-602.

BENNETT, M. J., MARCHANT, A., GREEN, H. G., MAY, S. T., WARD, S. P., MILLNER, P. A., WALKER, A. R., SCHULZ, B. & FELDMANN, K. A. 1996. Arabidopsis AUX1 gene: a permease-like regulator of root gravitropism. *Science,* 273**,** 948-950.

BENNETT, T., BROCKINGTON, S. F., ROTHFELS, C., GRAHAM, S. W., STEVENSON, D., KUTCHAN, T., ROLF, M., THOMAS, P., WONG, G. K.-S. & LEYSER, O. 2014. Paralogous radiations of PIN proteins with multiple origins of noncanonical PIN structure. *Molecular Biology and Evolution,* 31**,** 2042-2060.

BLAKESLEE, J. J., BANDYOPADHYAY, A., LEE, O. R., MRAVEC, J., TITAPIWATANAKUN, B., SAUER, M., MAKAM, S. N., CHENG, Y., BOUCHARD, R., ADAMEC, J., GEISLER, M., NAGASHIMA, A., SAKAI, T., MARTINOIA, E., FRIML, J., PEER, W. A. & MURPHY, A. S. 2007. Interactions among PIN-FORMED and P-glycoprotein auxin transporters in Arabidopsis. *Plant Cell,* 19**,** 131-47.

BLILOU, I., XU, J., WILDWATER, M., WILLEMSEN, V., PAPONOV, I., FRIML, J., HEIDSTRA, R., AIDA, M., PALME, K. & SCHERES, B. 2005. The PIN auxin efflux facilitator network controls growth and patterning in Arabidopsis roots. *Nature,* 433**,** 39-44.

CHRISTENSEN, S. K., DAGENAIS, N., CHORY, J. & WEIGEL, D. 2000. Regulation of auxin response by the protein kinase PINOID. *Cell,* 100**,** 469-478.

CRISTINA, M. S., PETERSEN, M. & MUNDY, J. 2010. Mitogen-activated protein kinase signaling in plants. *Annual review of plant biology,* 61**,** 621-649.

DAI, Y., WANG, H., LI, B., HUANG, J., LIU, X., ZHOU, Y., MOU, Z. & LI, J. 2006. Increased expression of MAP KINASE KINASE7 causes deficiency in polar auxin transport and leads to plant architectural abnormality in Arabidopsis. *The Plant Cell,* 18**,** 308-320.

DELBARRE, A., MULLER, P., IMHOFF, V. & GUERN, J. 1996. Comparison of mechanisms controlling uptake and accumulation of 2, 4-dichlorophenoxy acetic acid, naphthalene-1-acetic acid, and indole-3-acetic acid in suspension-cultured tobacco cells. *Planta,* 198**,** 532-541.

DHARMASIRI, N., DHARMASIRI, S. & ESTELLE, M. 2005a. The F-box protein TIR1 is an auxin receptor. *Nature,* 435**,** 441-445.

DHARMASIRI, N., DHARMASIRI, S., WEIJERS, D., LECHNER, E., YAMADA, M., HOBBIE, L., EHRISMANN, J. S., JÜRGENS, G. & ESTELLE, M. 2005b. Plant development is regulated by a family of auxin receptor F box proteins. *Developmental cell,* 9**,** 109-119.

DHONUKSHE, P. 2011. PIN polarity regulation by AGC-3 kinases and ARF-GEF: a recurrent theme with context dependent modifications for plant development and response. *Plant signaling & behavior,* 6**,** 1333-1337.

DHONUKSHE, P., HUANG, F., GALVAN-AMPUDIA, C. S., MAHONEN, A. P., KLEINE-VEHN, J., XU, J., QUINT, A., PRASAD, K., FRIML, J., SCHERES, B. & OFFRINGA, R. 2015. Plasma membrane-bound AGC3 kinases phosphorylate PIN auxin carriers at TPRXS(N/S) motifs to direct apical PIN recycling. *Development,* 142**,** 2386-7.

DING, Z., WANG, B., MORENO, I., DUPLÁKOVÁ, N., SIMON, S., CARRARO, N., REEMMER, J., PĚNČÍK, A., CHEN, X. & TEJOS, R. 2012. ER-localized auxin transporter PIN8 regulates auxin homeostasis and male gametophyte development in Arabidopsis. *Nature communications,* 3**,** 1-11.

DITENGOU, F. A., GOMES, D., NZIENGUI, H., KOCHERSPERGER, P., LASOK, H., MEDEIROS, V., PAPONOV, I. A., NAGY, S. K., NADAI, T. V., MESZAROS, T., BARNABAS, B., DITENGOU, B. I., RAPP, K., QI, L., LI, X., BECKER, C., LI, C., DOCZI, R. & PALME, K. 2018. Characterization of auxin transporter PIN6 plasma membrane targeting reveals a function for PIN6 in plant bolting. *New Phytol,* 217**,** 1610-1624.

DORY, M., HATZIMASOURA, E., KALLAI, B. M., NAGY, S. K., JAGER, K., DARULA, Z., NADAI, T. V., MESZAROS, T., LOPEZ-JUEZ, E., BARNABAS, B., PALME, K., BOGRE, L., DITENGOU, F. A. & DOCZI, R. 2018. Coevolving MAPK and PID phosphosites indicate an ancient environmental control of PIN auxin transporters in land plants. *FEBS Lett,* 592**,** 89-102.

DOS SANTOS MARASCHIN, F., MEMELINK, J. & OFFRINGA, R. 2009. Auxin-induced, SCFTIR1-mediated poly-ubiquitination marks AUX/IAA proteins for degradation. *The Plant Journal,* 59**,** 100-109.

DUQUESNE, K. & STURGIS, J. N. 2010. Membrane protein solubilization. *Heterologous Expression of Membrane Proteins.* Springer.

ENDERS, T. A. & STRADER, L. C. 2015. Auxin activity: Past, present, and future. *American journal of botany,* 102**,** 180-196.

FLAYHAN, A., MERTENS, H. D., URAL-BLIMKE, Y., MOLLEDO, M. M., SVERGUN, D. I. & LÖW, C. 2018. Saposin lipid nanoparticles: a highly versatile and modular tool for membrane protein research. *Structure,* 26**,** 345-355. e5.

FRAUENFELD, J., LÖVING, R., ARMACHE, J.-P., SONNEN, A. F., GUETTOU, F., MOBERG, P., ZHU, L., JEGERSCHÖLD, C., FLAYHAN, A. & BRIGGS, J. A. 2016. A saposin-lipoprotein nanoparticle system for membrane proteins. *Nature methods,* 13**,** 345-351.

FRIML, J., BENKOVÁ, E., BLILOU, I., WISNIEWSKA, J., HAMANN, T., LJUNG, K., WOODY, S., SANDBERG, G., SCHERES, B. & JÜRGENS, G. 2002a. AtPIN4 mediates sink-driven auxin gradients and root patterning in Arabidopsis. *Cell,* 108**,** 661-673.

FRIML, J., VIETEN, A., SAUER, M., WEIJERS, D., SCHWARZ, H., HAMANN, T., OFFRINGA, R. & JÜRGENS, G. 2003. Efflux-dependent auxin gradients establish the apical–basal axis of Arabidopsis. *Nature,* 426**,** 147-153.

FRIML, J., WIŚNIEWSKA, J., BENKOVÁ, E., MENDGEN, K. & PALME, K. 2002b. Lateral relocation of auxin efflux regulator PIN3 mediates tropism in Arabidopsis. *Nature,* 415**,** 806-809.

FUCILE, G., DI BIASE, D., NAHAL, H., LA, G., KHODABANDEH, S., CHEN, Y., EASLEY, K., CHRISTENDAT, D., KELLEY, L. & PROVART, N. J. 2011. ePlant and the 3D data display initiative: integrative systems biology on the world wide web. *PLoS One,* 6**,** e15237.

GÄLWEILER, L., GUAN, C., MÜLLER, A., WISMAN, E., MENDGEN, K., YEPHREMOV, A. & PALME, K. 1998. Regulation of polar auxin transport by AtPIN1 in Arabidopsis vascular tissue. *Science,* 282**,** 2226-2230.

GANGULY, A., PARK, M., KESAWAT, M. S. & CHO, H.-T. 2014. Functional analysis of the hydrophilic loop in intracellular trafficking of Arabidopsis PIN-FORMED proteins. *The Plant Cell,* 26**,** 1570-1585.

GEISLER, M., ARYAL, B., DI DONATO, M. & HAO, P. 2017. A Critical View on ABC Transporters and Their Interacting Partners in Auxin Transport. *Plant Cell Physiol*.

GEISLER, M., WANG, B. & ZHU, J. 2014. Auxin transport during root gravitropism: transporters and techniques. *Plant Biology,* 16**,** 50-57.

GROSSMANN, K. 2007. Auxin herbicide action: lifting the veil step by step. *Plant Signaling & Behavior,* 2**,** 421-423.

HAGA, K., HAYASHI, K.-I. & SAKAI, T. 2014. PINOID AGC kinases are necessary for phytochrome-mediated enhancement of hypocotyl phototropism in Arabidopsis. *Plant physiology,* 166**,** 1535-1545.

HAJNÝ, J., PRÁT, T., RYDZA, N., RODRIGUEZ, L., TAN, S., VERSTRAETEN, I., DOMJAN, D., MAZUR, E., SMAKOWSKA-LUZAN, E. & SMET, W. 2020. Receptor kinase module targets PIN-dependent auxin transport during canalization. *Science,* 370**,** 550-557.

HUANG, F., ZAGO, M. K., ABAS, L., VAN MARION, A., GALVAN-AMPUDIA, C. S. & OFFRINGA, R. 2010. Phosphorylation of conserved PIN motifs directs Arabidopsis PIN1 polarity and auxin transport. *Plant Cell,* 22**,** 1129-42.

JIA, W., LI, B., LI, S., LIANG, Y., WU, X., MA, M., WANG, J., GAO, J., CAI, Y., ZHANG, Y., WANG, Y., LI, J. & WANG, Y. 2016. Mitogen-Activated Protein Kinase Cascade MKK7-MPK6 Plays Important Roles in Plant Development and Regulates Shoot Branching by Phosphorylating PIN1 in Arabidopsis. *PLoS Biol,* 14**,** e1002550.

JUMPER, J., EVANS, R., PRITZEL, A., GREEN, T., FIGURNOV, M., RONNEBERGER, O., TUNYASUVUNAKOOL, K., BATES, R., ŽÍDEK, A. & POTAPENKO, A. 2021. Highly accurate protein structure prediction with AlphaFold. *Nature,* 596**,** 583-589.

KAMIMOTO, Y., TERASAKA, K., HAMAMOTO, M., TAKANASHI, K., FUKUDA, S., SHITAN, N., SUGIYAMA, A., SUZUKI, H., SHIBATA, D. & WANG, B. 2012. Arabidopsis ABCB21 is a facultative auxin importer/exporter regulated by cytoplasmic auxin concentration. *Plant and Cell Physiology,* 53**,** 2090-2100.

KEPINSKI, S. & LEYSER, O. 2005. The Arabidopsis F-box protein TIR1 is an auxin receptor. *Nature,* 435**,** 446-451.

KÖGL, F., HAAGEN-SMIT, A. & ERXLEBEN, H. 1934. Über ein neues Auxin („Hetero-auxin “) aus Harn. 11. Mitteilung über pflanzliche Wachstumsstoffe.

KOMANDER, D. & RAPE, M. 2012. The ubiquitin code. *Annual review of biochemistry,* 81**,** 203-229.

KOWALCZYK, M. & SANDBERG, G. 2001. Quantitative analysis of indole-3-acetic acid metabolites in Arabidopsis. *Plant physiology,* 127**,** 1845-1853.

KRECEK, P., SKUPA, P., LIBUS, J., NARAMOTO, S., TEJOS, R., FRIML, J. & ZAZIMALOVA, E. 2009. The PIN-FORMED (PIN) protein family of auxin transporters. *Genome Biol,* 10**,** 249.

KROUK, G., LACOMBE, B., BIELACH, A., PERRINE-WALKER, F., MALINSKA, K., MOUNIER, E., HOYEROVA, K., TILLARD, P., LEON, S. & LJUNG, K. 2010. Nitrate-regulated auxin transport by NRT1. 1 defines a mechanism for nutrient sensing in plants. *Developmental cell,* 18**,** 927-937.

KUBEŠ, M., YANG, H., RICHTER, G. L., CHENG, Y., MŁODZIŃSKA, E., WANG, X., BLAKESLEE, J. J., CARRARO, N., PETRÁŠEK, J. & ZAŽÍMALOVÁ, E. 2012. The Arabidopsis concentration‐dependent influx/efflux transporter ABCB4 regulates cellular auxin levels in the root epidermis. *The Plant Journal,* 69**,** 640-654.

LEE, S., SUNDARAM, S., ARMITAGE, L., EVANS, J. P., HAWKES, T., KEPINSKI, S., FERRO, N. & NAPIER, R. M. 2014. Defining binding efficiency and specificity of auxins for SCFTIR1/AFB-Aux/IAA co-receptor complex formation. *ACS chemical biology,* 9**,** 673-682.

LUDWIG-MÜLLER, J. 2011. Auxin conjugates: their role for plant development and in the evolution of land plants. *Journal of experimental botany,* 62**,** 1757-1773.

MICHALCZUK, L. & BANDURSKI, R. S. 1982. Enzymic synthesis of 1-O-indol-3-ylacetyl-β-D-glucose and indol-3-ylacetyl-myo-inositol. *Biochemical Journal,* 207**,** 273-281.

MRAVEC, J., SKŮPA, P., BAILLY, A., HOYEROVÁ, K., KŘEČEK, P., BIELACH, A., PETRÁŠEK, J., ZHANG, J., GAYKOVA, V. & STIERHOF, Y.-D. 2009. Subcellular homeostasis of phytohormone auxin is mediated by the ER-localized PIN5 transporter. *Nature,* 459**,** 1136-1140.

MÜLLER, A., GUAN, C., GÄLWEILER, L., TÄNZLER, P., HUIJSER, P., MARCHANT, A., PARRY, G., BENNETT, M., WISMAN, E. & PALME, K. 1998. AtPIN2 defines a locus of Arabidopsis for root gravitropism control. *The EMBO journal,* 17**,** 6903-6911.

NJI, E., CHATZIKYRIAKIDOU, Y., LANDREH, M. & DREW, D. 2018. An engineered thermal-shift screen reveals specific lipid preferences of eukaryotic and prokaryotic membrane proteins. *Nature communications,* 9**,** 1-12.

NODZYNSKI, T., VANNESTE, S., ZWIEWKA, M., PERNISOVA, M., HEJATKO, J. & FRIML, J. 2016. Enquiry into the Topology of Plasma Membrane-Localized PIN Auxin Transport Components. *Mol Plant,* 9**,** 1504-1519.

OKADA, K., UEDA, J., KOMAKI, M. K., BELL, C. J. & SHIMURA, Y. 1991. Requirement of the auxin polar transport system in early stages of Arabidopsis floral bud formation. *The Plant Cell,* 3**,** 677-684.

OMASITS, U., AHRENS, C. H., MÜLLER, S. & WOLLSCHEID, B. 2014. Protter: interactive protein feature visualization and integration with experimental proteomic data. *Bioinformatics,* 30**,** 884-886.

ÖPIK, H., ROLFE, S. A. & WILLIS, A. J. 2005. *The physiology of flowering plants*, Cambridge University Press.

OSTIN, A., KOWALYCZK, M., BHALERAO, R. P. & SANDBERG, G. 1998. Metabolism of indole-3-acetic acid in Arabidopsis. *Plant physiology,* 118**,** 285-296.

PETRÁŠEK, J., MRAVEC, J., BOUCHARD, R., BLAKESLEE, J. J., ABAS, M., SEIFERTOVÁ, D., WIŚNIEWSKA, J., TADELE, Z., KUBEŠ, M. & ČOVANOVÁ, M. 2006. PIN proteins perform a rate-limiting function in cellular auxin efflux. *Science,* 312**,** 914-918.

PETRASEK, J., MRAVEC, J., BOUCHARD, R., BLAKESLEE, J. J., ABAS, M., SEIFERTOVA, D., WISNIEWSKA, J., TADELE, Z., KUBES, M., COVANOVA, M., DHONUKSHE, P., SKUPA, P., BENKOVA, E., PERRY, L., KRECEK, P., LEE, O. R., FINK, G. R., GEISLER, M., MURPHY, A. S., LUSCHNIG, C., ZAZIMALOVA, E. & FRIML, J. 2006. PIN proteins perform a rate-limiting function in cellular auxin efflux. *Science,* 312**,** 914-8.

PRAT, T., HAJNY, J., GRUNEWALD, W., VASILEVA, M., MOLNAR, G., TEJOS, R., SCHMID, M., SAUER, M. & FRIML, J. 2018. WRKY23 is a component of the transcriptional network mediating auxin feedback on PIN polarity. *PLoS Genet,* 14**,** e1007177.

REINECKE, D. M. 1999. 4-Chloroindole-3-acetic acid and plant growth. *Plant Growth Regulation,* 27**,** 3-13.

RIGÓ, G., AYAYDIN, F., TIETZ, O., ZSIGMOND, L., KOVÁCS, H., PÁY, A., SALCHERT, K., DARULA, Z., MEDZIHRADSZKY, K. F. & SZABADOS, L. 2013. Inactivation of plasma membrane–localized CDPK-RELATED KINASE5 decelerates PIN2 exocytosis and root gravitropic response in Arabidopsis. *The Plant Cell,* 25**,** 1592-1608.

RUBERY, P. H. & SHELDRAKE, A. R. 1974. Carrier-mediated auxin transport. *Planta,* 118**,** 101-121.

RUEGGER, M., DEWEY, E., GRAY, W. M., HOBBIE, L., TURNER, J. & ESTELLE, M. 1998. The TIR1 protein of Arabidopsis functions in auxin response and is related to human SKP2 and yeast grr1p. *Genes & development,* 12**,** 198-207.

SANTNER, A. A. & WATSON, J. C. 2006. The WAG1 and WAG2 protein kinases negatively regulate root waving in Arabidopsis. *The Plant Journal,* 45**,** 752-764.

SCARPELLA, E., MARCOS, D., FRIML, J. & BERLETH, T. 2006. Control of leaf vascular patterning by polar auxin transport. *Genes & development,* 20**,** 1015-1027.

SCHERES, S. H. 2012. RELION: implementation of a Bayesian approach to cryo-EM structure determination. *Journal of structural biology,* 180**,** 519-530.

SHIRAI, A., MATSUYAMA, A., YASHIRODA, Y., HASHIMOTO, A., KAWAMURA, Y., ARAI, R., KOMATSU, Y., HORINOUCHI, S. & YOSHIDA, M. 2008. Global analysis of gel mobility of proteins and its use in target identification. *Journal of Biological Chemistry,* 283**,** 10745-10752.

SIMON, S. & PETRASEK, J. 2011. Why plants need more than one type of auxin. *Plant Sci,* 180**,** 454-60.

SIMON, S., SKŮPA, P., VIAENE, T., ZWIEWKA, M., TEJOS, R., KLÍMA, P., ČARNÁ, M., ROLČÍK, J., DE RYCKE, R. & MORENO, I. 2016. PIN6 auxin transporter at endoplasmic reticulum and plasma membrane mediates auxin homeostasis and organogenesis in Arabidopsis. *New Phytologist,* 211**,** 65-74.

SINGH, K., SINGH, J., JINDAL, S., SIDHU, G., DHALIWAL, A. & GILL, K. 2018. Structural and functional evolution of an auxin efflux carrier PIN1 and its functional characterization in common wheat. *Funct Integr Genomics*.

SKAAR, J. R., PAGAN, J. K. & PAGANO, M. 2013. Mechanisms and function of substrate recruitment by F-box proteins. *Nature reviews Molecular cell biology,* 14**,** 369-381.

STEFANOWICZ, K., LANNOO, N. & VAN DAMME, E. J. 2015. Plant F-box proteins–judges between life and death. *Critical Reviews in Plant Sciences,* 34**,** 523-552.

STIGTER, D., ALONSO, D. & DILL, K. A. 1991. Protein stability: electrostatics and compact denatured states. *Proceedings of the National Academy of Sciences,* 88**,** 4176-4180.

SUGAWARA, S., HISHIYAMA, S., JIKUMARU, Y., HANADA, A., NISHIMURA, T., KOSHIBA, T., ZHAO, Y., KAMIYA, Y. & KASAHARA, H. 2009. Biochemical analyses of indole-3-acetaldoxime-dependent auxin biosynthesis in Arabidopsis. *Proceedings of the National Academy of Sciences,* 106**,** 5430-5435.

SWARUP, R. & PERET, B. 2012. AUX/LAX family of auxin influx carriers-an overview. *Front Plant Sci,* 3**,** 225.

SZTEIN, A. E., COHEN, J. D., SLOVIN, J. P. & COOKE, T. J. 1995. Auxin metabolism in representative land plants. *American journal of Botany,* 82**,** 1514-1521.

TAM, Y. Y., EPSTEIN, E. & NORMANLY, J. 2000. Characterization of auxin conjugates in Arabidopsis. Low steady-state levels of indole-3-acetyl-aspartate, indole-3-acetyl-glutamate, and indole-3-acetyl-glucose. *Plant physiology,* 123**,** 589-596.

TAN, X., CALDERON-VILLALOBOS, L. I. A., SHARON, M., ZHENG, C., ROBINSON, C. V., ESTELLE, M. & ZHENG, N. 2007. Mechanism of auxin perception by the TIR1 ubiquitin ligase. *Nature,* 446**,** 640-645.

TEALE, W. D., PAPONOV, I. A. & PALME, K. 2006. Auxin in action: signalling, transport and the control of plant growth and development. *Nature reviews Molecular cell biology,* 7**,** 847-859.

TEALE, W. D., PASTERNAK, T., DAL BOSCO, C., DOVZHENKO, A., KRATZAT, K., BILDL, W., SCHWÖRER, M., FALK, T., RUPERTI, B. & V SCHAEFER, J. 2021. Flavonol‐mediated stabilization of PIN efflux complexes regulates polar auxin transport. *The EMBO Journal,* 40**,** e104416.

TERASAKA, K., BLAKESLEE, J. J., TITAPIWATANAKUN, B., PEER, W. A., BANDYOPADHYAY, A., MAKAM, S. N., LEE, O. R., RICHARDS, E. L., MURPHY, A. S. & SATO, F. 2005. PGP4, an ATP binding cassette P-glycoprotein, catalyzes auxin transport in Arabidopsis thaliana roots. *The Plant Cell,* 17**,** 2922-2939.

TOMINAGA, M., SONOBE, S. & SHIMMEN, T. 1998. Mechanism of inhibition of cytoplasmic streaming by auxin in root hair cells of Hydrocharis. *Plant and cell physiology,* 39**,** 1342-1349.

TROMAS, A., PAQUE, S., STIERLÉ, V., QUETTIER, A.-L., MULLER, P., LECHNER, E., GENSCHIK, P. & PERROT-RECHENMANN, C. 2013. Auxin-Binding Protein 1 is a negative regulator of the SCF TIR1/AFB pathway. *Nature communications,* 4**,** 1-9.

VIETEN, A., VANNESTE, S., WISNIEWSKA, J., BENKOVA, E., BENJAMINS, R., BEECKMAN, T., LUSCHNIG, C. & FRIML, J. 2005a. Functional redundancy of PIN proteins is accompanied by auxin-dependent cross-regulation of PIN expression. *Development,* 132**,** 4521-31.

VIETEN, A., VANNESTE, S., WISNIEWSKA, J., BENKOVÁ, E., BENJAMINS, R., BEECKMAN, T., LUSCHNIG, C. & FRIML, J. 2005b. Functional redundancy of PIN proteins is accompanied by auxin-dependent cross-regulation of PIN expression.

WALZ, A., PARK, S., SLOVIN, J. P., LUDWIG-MÜLLER, J., MOMONOKI, Y. S. & COHEN, J. D. 2002. A gene encoding a protein modified by the phytohormone indoleacetic acid. *Proceedings of the National Academy of Sciences,* 99**,** 1718-1723.

WANG, B., CHU, J., YU, T., XU, Q., SUN, X., YUAN, J., XIONG, G., WANG, G., WANG, Y. & LI, J. 2015. Tryptophan-independent auxin biosynthesis contributes to early embryogenesis in Arabidopsis. *Proceedings of the National Academy of Sciences,* 112**,** 4821-4826.

WANG, J.-R., HU, H., WANG, G.-H., LI, J., CHEN, J.-Y. & WU, P. 2009. Expression of PIN genes in rice (Oryza sativa L.): tissue specificity and regulation by hormones. *Molecular Plant,* 2**,** 823-831.

WANI, S. H., KUMAR, V., SHRIRAM, V. & SAH, S. K. 2016. Phytohormones and their metabolic engineering for abiotic stress tolerance in crop plants. *The Crop Journal,* 4**,** 162-176.

WILLIGE, B. C., OGISO-TANAKA, E., ZOURELIDOU, M. & SCHWECHHEIMER, C. 2012. WAG2 represses apical hook opening downstream from gibberellin and PHYTOCHROME INTERACTING FACTOR 5. *Development,* 139**,** 4020-4028.

WISNIEWSKA, J., XU, J., SEIFERTOVA, D., BREWER, P. B., RUZICKA, K., BLILOU, I., ROUQUIE, D., BENKOVA, E., SCHERES, B. & FRIML, J. 2006. Polar PIN localization directs auxin flow in plants. *Science,* 312**,** 883.

WOLTERS, H. & JÜRGENS, G. 2009. Survival of the flexible: hormonal growth control and adaptation in plant development. *Nature Reviews Genetics,* 10**,** 305-317.

WOODWARD, A. W. & BARTEL, B. 2005. Auxin: regulation, action, and interaction. *Annals of botany,* 95**,** 707-735.

ZAŽÍMALOVÁ, E., KŘEČEK, P., SKŮPA, P., HOYEROVA, K. & PETRÁŠEK, J. 2007. Polar transport of the plant hormone auxin–the role of PIN-FORMED (PIN) proteins. *Cellular and molecular life sciences,* 64**,** 1621-1637.

ZHANG, J., NODZYNSKI, T., PENCIK, A., ROLCIK, J. & FRIML, J. 2010. PIN phosphorylation is sufficient to mediate PIN polarity and direct auxin transport. *Proc Natl Acad Sci U S A,* 107**,** 918-22.

ZHANG, J., VANNESTE, S., BREWER, P. B., MICHNIEWICZ, M., GRONES, P., KLEINE-VEHN, J., LOFKE, C., TEICHMANN, T., BIELACH, A., CANNOOT, B., HOYEROVA, K., CHEN, X., XUE, H. W., BENKOVA, E., ZAZIMALOVA, E. & FRIML, J. 2011. Inositol trisphosphate-induced Ca2+ signaling modulates auxin transport and PIN polarity. *Dev Cell,* 20**,** 855-66.

ZOURELIDOU, M., MÜLLER, I., WILLIGE, B. C., NILL, C., JIKUMARU, Y., LI, H. & SCHWECHHEIMER, C. 2009. The polarly localized D6 PROTEIN KINASE is required for efficient auxin transport in Arabidopsis thaliana. *Development,* 136**,** 627-636.

ZWIEWKA, M., BILANOVIČOVÁ, V., SEIFU, Y. W. & NODZYŃSKI, T. 2019. The nuts and bolts of PIN auxin efflux carriers. *Frontiers in plant science,* 10**,** 985.

Chapter 9 Appendix

Appendix I Superose 6 and Suprrose 200 cliberation curve

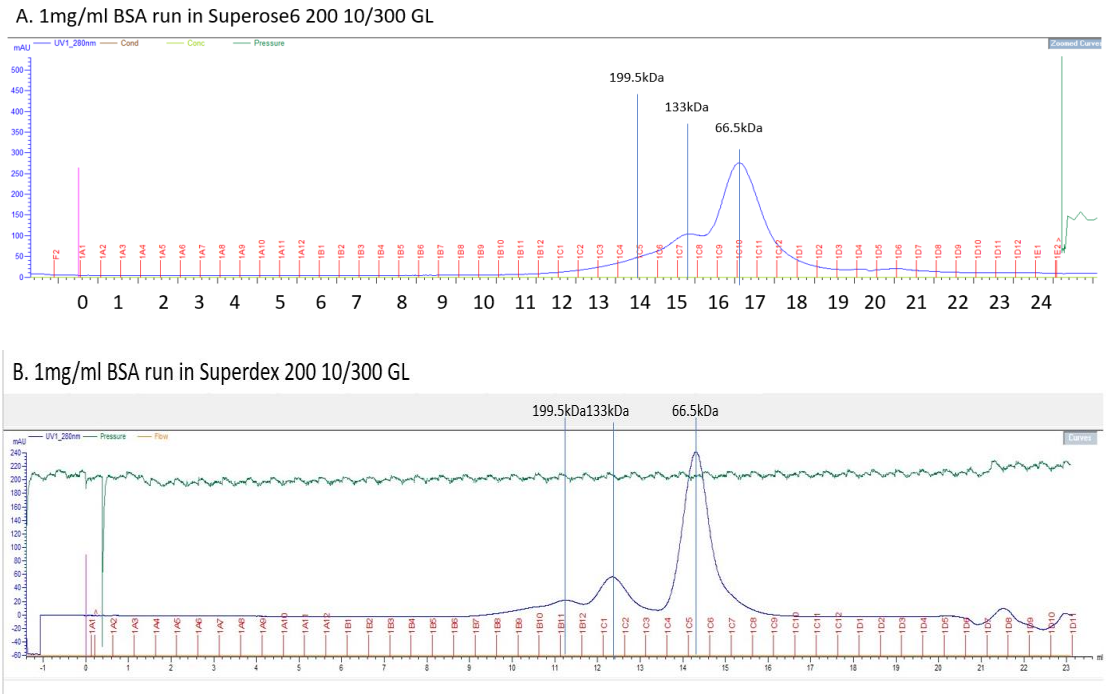

Figure 9.1 Superose 6 and Superose 200 elution calibration curve

A. BSA run in Superose 6

B. BSA run in Superdex 200

1 mg/ml BSA samples in TBS were loaded into Superose 6 and Superdex 200 SEC columns respectively at 4C, TBS (pH 7.5) was used as SEC running buffer, sample flow speed was 0.3 ml/min.

In Superose 6 SEC column elution, a BSA monomer (66.5kDa) peak was at 16.5ml, BSA dimer peak (133kDa) was at 15.2ml, BSA trimer peak (199.5kDa) was at 14ml.

In Superdex 200 SEC column elution, a BSA monomer (66.5kDa) peak was at 14.3ml, BSA dimer peak (133kDa) was at 12.4ml, BSA trimer peak (199.5kDa) was at 11.2ml.

Appendix II OsPIN8:GFP and AtPIN5:GFP GFP fluorescence melting curve.

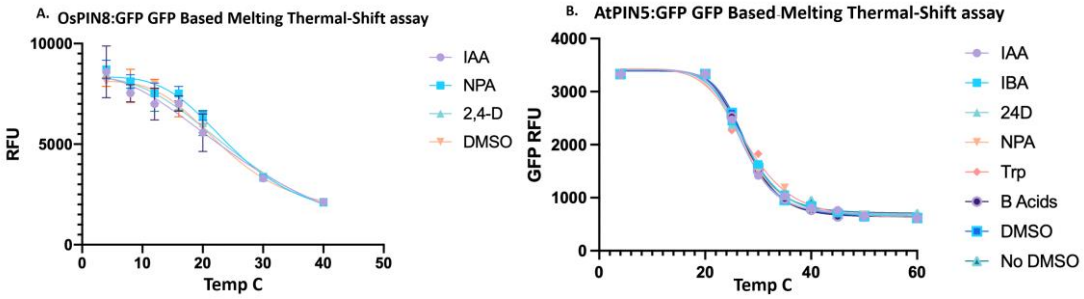

Figure 9.2 OsPIN8:GFP and AtPIN5:GFP GFP fluorescent melting curve

A OsPIN8:GFP GFP based melting curva assay, Tm is around 20C.

B AtPIN5:GFP GFP based melting curva assay, Tm is around 25C.

Unpurified AtPIN5:GFP and OsPIN8:GFP was solubilized into 1% DDM and alquotted to 100µlin PCR tubes. 1% Beta-octylmaltoside and 0.05 mM of ligands was added respectively. Samples was applied to a heating gradient from 4C to 60C, for 20min. All samples were spun down and the supernatant used for GFP RFU reading. Data were processed with GraphPad Prism (GraphPadPrism v.9.00 for MAC OS). In order to determine the inflection point of the melting curves, which was assumed to equal the melting temperature (Tm), a Bolzmann sigmoidal equation was fitted to the raw data (Figure. 9.2)(Nji et al., 2018).

Appendix III Short PINs candidates for expression

Organism	ASSIGNED NAME IF KNOW	Locus ID	Amino acids number	Extinction coefficient	Instability Index
Amborella trichopoda	N/A	scaffold00013.199	365	57785	29.49
Amborella trichopoda	N/A	scaffold00038.32	386	62255	43
Amborella trichopoda	N/A	scaffold00038.35	380	55140	33.53
Amborella trichopoda	N/A	scaffold00038.38	359	52285	31.55
Brachypodium distachyon	N/A	Bradi2g48170	362	58370	34.99
Brachypodium distachyon	N/A	Bradi2g52640	417	61100	38.36
Brachypodium distachyon	N/A	Bradi2g58917	343	87485	37.55
Brachypodium distachyon	N/A	Bradi3g41080	370	85285	35.35
Brachypodium distachyon	N/A	Bradi4g34510	365	85870	51.41
Brassica oleracea	N/A	Bo3g012090	348	63745	36.56
Brassica oleracea	N/A	Bo6g087700	285	34170	43.86
Brassica oleracea	N/A	Bo9g163100	348	63745	36.01
Brassica oleracea	N/A	Bo9g165420	341	47565	45.8
Glycine max	GmPIN5a	Glyma.09G251600.1	377	68785	30.08
Glycine max	GmPIN5b	Glyma.18G241000.1	369	68910	35.2
Glycine max	GmPIN8a	Glyma.05G109800.1	362	51130	43.86
Glycine max	GmPIN8b	Glyma.17G157300.1	363	51130	43.62
Glycine max	GmPIN8c	Glyma.09G240500.1	358	49640	42
Glycine max	GmPIN8d	Glyma.18G255800.1	359	49640	44.25

Oryza sativa	OsPIN5a	LOC_Os01g69070.1	363	63160	23.48
Oryza sativa	OsPIN5b	LOC_Os08g41720.1	357	70150	41.27
Oryza sativa	OsPIN5c	LOC_Os09g32770.1	398	59525	42.36
Physcomitrella patens	PpPIND	Phpat.014G031300	429	69245	30.91
Populus trichocarpa	PtrPIN11	Potri.013G087000.1	346	71765	36.72
Populus trichocarpa	PtrPIN12	Potri.019G052800.1	346	71765	36.19
Populus trichocarpa	PtrPIN13	Potri.004G124200.1	355	46660	35.54
Populus trichocarpa	PtrPIN14	Potri.017G078300.1	356	49515	30.78
Populus trichocarpa	PtrPIN15	Potri.014G146800.1	460	65485	32.21
Solanum tuberosum	StPIN5	PGSC0003DMP400031315	355	74620	36.26
Solanum tuberosum	StPIN8	PGSC0003DMP400002547	260	27055	34.97
Solanum tuberosum	StPIN10	PGSC0003DMP400018629	321	64775	35.41
Zea mays	ZmPIN5b	GRMZM2G148648	264	64190	30.44
Zea mays	ZmPIN5c	GRMZM2G040911	365	77140	33.71
Zea mays	ZmPIN8	GRMZM5G839411	359	56630	26.43
Klebsormidium nitens	N/A	GAQ81096.1	517	55725	33.83
Arabidopsis thaliana	AtPIN8	At5g15100	365	52035	46.1

Table 9.1 Short PIN candidates for expression.